Bactericidal Paper Containing Silver Nanoparticles for Water Treatment

by

Theresa A. Dankovich

A thesis submitted to McGill University in partial fulfillment of the requirements for the degree of

Doctor of Philosophy

Department of Chemistry
McGill University
Montreal, Quebec
Canada

 March 2012

Abstract

In the past decade, silver nanoparticles (AgNP) have gained attention due to their highly effective bactericidal properties, and have been incorporated into many consumer products. The addition of AgNPs to cellulosic materials is not novel, but the application of a bactericidal paper as a cheap water purifier is. Our main objective in this thesis is to prepare and evaluate a bactericidal paper embedded with AgNPs. The two most successful methods to form AgNPs in paper were *in situ* reductions of silver ions directly on the paper fibers, and differed by the means of reduction. The first used a commonly employed reducing agent for nanoparticle synthesis - sodium borohydride. The second was a "green" method involving the use of microwave radiation and glucose for the formation of AgNPs in paper. The nanoparticles formation was characterized by scanning and transmission electron microscopy, ultraviolet-visible spectrophotometry, and atomic absorption analysis following acid digestion of the paper. Silver nanoparticle formation in paper was dependent upon initial silver ion concentration absorbed in the paper, an excess of reducing agent, and temperature for the glucose reduction. The bactericidal effectiveness of the silver nanoparticle paper was evaluated with two types of common fecal bacteria - *Escherichia coli* and *Enterococcus faecalis*. A bacterial suspension was percolated through the silver nanoparticle paper and the effluent water was analyzed for bacteria viability through two methods, qualitatively through optical density measurements and quantitatively through enumeration of bacterial colonies on nutrient media agar plates. The AgNP sheets exhibited antibacterial properties towards suspensions of *E. coli* and *E. faecalis*, with log reduction values in the effluent of over log 8 and log 3, respectively. Additionally, silver loss from the silver nanoparticle sheets was minimal, with values under 0.1 ppm (the current U.S. Environmental Protection Agency and World Health Organization limit for silver in drinking water). The AgNP formation on model nano-crystalline cellulose films was examined and subsequently,

they were evaluated for the long term stability and aggregation behavior of AgNPs on these films. Lastly, the effects of dissolved materials present in natural water sources, including natural organic matter and salts, were examined in order to understand their impacts on the bactericidal functioning of AgNP papers.

Résumé

À cause de leur pouvoir bactéricide, les nanoparticules d'argent (NPAg) ont été incorporées dans plusieurs produits de consommation au cours de la dernière décennie. L'ajout de NPAg à des matériaux cellulosiques n'est pas un concept nouveau. Cependant, l'utilisation de ces particules pour fabriquer un papier bactéricide permettant la purification d'eau à faible coût est une idée très novatrice. L'objectif principal de cette thèse consiste à préparer et évaluer un papier bactéricide composé de nanoparticules d'argent. Deux types de réductions in situ des ions d'argent sur les fibres du papier ont été utilisés pour synthétiser et lier les NPAg au papier de manière efficace. Pour le premier type de réduction, un agent de réduction courant, le borohydrure de sodium, a été utilisé alors que pour la seconde réduction, un procédé plus vert impliquant des radiations micro-ondes et du glucose, a permis la formation de nanoparticules d'argent dans le papier. La formation de nanoparticules a été caractérisée par microscopie à transmission et balayage électronique, par spectroscopie UV-Vis et par l'analyse GF-AA suivant une digestion acide. La formation de nanoparticules d'argent a été fortement influencée par la concentration initiale d'ions d'argent adsorbés sur le papier, de la quantité en excès de l'agent réducteur et de la température de la réduction du glucose. L'efficacité bactéricide des papiers de NPAg a été évaluée pour deux types de bactéries fécales communes, soit *Escherichia coli* et *Enterococcus faecalis*. La viabilité des bactéries contenues dans l'eau effluente d'un papier NPAg, précédemment imprégné d'une suspension bactérienne, a été analysée de façon qualitative par mesure de densité optique, et de façon quantitative par comptabilisation des colonies bactériennes formées sur des plaques d'agar. Les feuilles de NPAg ont démontré des propriétés antibactériennes envers les suspensions *d'E. coli* et *d'E. faecalis*, avec des réductions logarithmiques de la valeur des effluents allant au-delà de log 8 et de log 3 respectivement. De plus, la perte d'argent des feuilles de

NPAg s’est avérée minimale avec des valeurs au-dessous de 0.1ppm, qui correspond à la limite courante d’ion dans l’eau potable fixée par le US EPA et WHO. La formation NPAg sur des films modèles de cellulose nano-cristallines a été examiné et par la suite, ils ont été évalués pour la stabilité à long terme et comportement d'agrégation de NPAg sur ces films. Enfin, les effets de matières dissoutes présentes dans les sources d'eau naturelles, y compris la matière organique naturelle et des sels, ont été examinés afin de comprendre leurs impacts sur le fonctionnement bactéricide de papiers de NPAg.

Foreword

In addition to a general introduction provided in Chapter 1, and a summary of the main conclusions given in Chapter 6, this dissertation includes four papers, each of which comprises one chapter. A re-formatted version of one paper was published in a scientific journal: three are to be submitted for publications.

Chapter 2: *Environmental Science and Technology,* **2011**, 45(5), 1992-1998.
Chapters 3, 4, and 5: the manuscripts are to be submitted.

Contributions of Authors

All papers presented in the thesis were entirely written by Theresa Dankovich. All papers were co-authored with Prof. Derek G. Gray (Department of Chemistry, McGill University), who acted as a research advisor. All of the research presented in this dissertation was planned, performed, and critically analyzed by the author. Ms. Ruoxi (Rosie) Gao helped with some experiments presented in Chapters 2, 3, and 5. Mr. Sangjin (Andrew) Bae helped with some experiments presented in Chapters 3 and 5. Both Ms. Gao and Mr. Bae were undergraduate students working under the direct supervision of the author.

Acknowledgements

I am very thankful for the opportunity to pursue my graduate studies in Montreal and at McGill. I grew up so close here, on the other side of the US/Canadian border and never thought to visit this special city. “Oh, they speak French up there!” That sentiment really did stop so many New Yorkers from traveling up north. Or maybe it was the cold, cold winter... Either way, I never considered going to school in Canada until I had a Canadian roommate in undergrad who complained that she should have gone to McGill instead of Cornell. Well, looks like someone was listenin’.

I have learned so much during my studies here at McGill. I have been fortunate to have Derek Gray as my Ph.D. advisor. His flexible attitude, childlike enthusiasm, appreciation of bizarre (and highly creative) experiments, and generosity always helped through the years. I have had many opportunities to present my research at conferences in Europe and California and well, almost everywhere in between. I really appreciated working and studying in his research group. I am also grateful to my committee members, Professors T. van de Ven and C. Barrett, for their helpful and encouraging comments and discussions.

I thank my family for always being so supportive. My mom for always pushing me to work harder and reminding me not to worry and come up with a plan whenever possible. My mom has always been a model for excelling at everything she undertakes and making it look so easy. My dad for being patient, well organized, a very early Apple computer adopter, and encouraging my interest in science from a young age. Also, for all those trips up here with the mini-van to move my stuff. My uncle Jim for actually reading my published articles and discussing science with me at family get-togethers. My little brother James (not to be confused with Jim) for always telling me about his kitchen (i.e. applied chemistry) experiments. My older brother Louis for always telling crazy tales and sharing his love for quirky research.

The students and staff in the chemistry department have really made my Ph.D. a memorable experience. First, I have to thank the members of the Gray lab through out the years: Dr. Tiffany Abitbol, Dr. Jani Salmi, Rosie Gao, Dr. Elisabeth Kloser, Dr. Annie Dorris, Dr. Emily Cranston, Dr. Erick Gonzalez, Maggie Weller, Dr. Stephanie Beck-Candanedo, Josh Lucate, Jordan Wilson, Andrew Bae, Helen Huang-Hobbs, and Dr. Nilgun Ulkem. I especially enjoyed working with the summer students, Rosie, Helen, and Andrew. It's one thing to do lab work and another to teach someone else how to do the same! Perhaps the craziest lesson of how to start a fire in the microwave was the most memorable (silver is highly conductive!). Other students at McGill who I have also discussed some research thoughts with: Dr. Renata Vynalkova, Zeinab Hosseini, Dr. Jimmy Huang, and George Rizis. I cannot forgot Colleen McNamee for always being helpful, even if only through Facebook during the MUNACA strike.

I have unexpectedly learned a lot about science and tech entrepreneurship through my research at McGill. Joining the Technology Entrepreneurship Club during my program opened my mind to the parallels between running a research lab and starting one's own business. I also met Dr. Erica Besso, who informally taught me about many of these business ideas. Though, I still waver on jumping into owning a business, it sure does sound like fun!

So many great friends I've met here! I am so thankful to have meet them all but especially Erica Gipson, Vishya Goel, Steph Palmer, Dr. Jonathan Levine, Gabe Guzman, Dr. Jan de Bakker, and Hisako Kobayashi. All the fun times hanging out in the Mile End, the many barbecues, cooking experimental dinners, brewing beer, bike trips around the city, going to shows, craft projects, traveling around Europe and to NYC, and that memorable road trip to PEI.

Lastly, I have been lucky to be part of the Sentinel Bioactive Paper Network in Canada, which has given me many opportunities to learn about deadly bacteria, all kinds of paper, seeing the country of Canada, and well, networking. I found its informal meetings great for encouraging collaborations and discussions with other students and researchers. Without this funding, only my leftovers for lunch would have been heated up in the microwave and I wouldn't have made the silver lining, ahem, the silver nanoparticle paper.

Table of Contents

List of Tables

List of Figures

List of Symbols and Abbreviations

AgNP	silver nanoparticle
ATCC	American type culture collection
CCD	charge-coupled device
CFU	colony forming units
DMF	dimethylformamide
EDX	energy-dispersive x-ray spectroscopy detector
EPA	US Environmental Protection Agency
GF-AA	graphite furnace atomic absorption
HS	hot spot
HMF	5-(hydroxymethyl)furfural
ICP-AES	inductively coupled plasma atomic emission spectrometer
IHSS	International Humic Substances Society
IGC	inverse gas chromatographic adsorption
MIC	minimal inhibitory concentration
MPN	most probable number
MW	microwave
nano-Ag	silver nanoparticle
NCC	nanocrystalline cellulose
NHS	non hot spot
NOM	natural organic matter
NP	nanoparticle
NR	not rotated
PAPTAC	Pulp and Paper Technical Association of Canada
POU	point-of-use

R	rotation
RCF	relative centrifugal force
RH	relative humidity
SEM	scanning electron microscope
SPR	surface plasmon resonance
TDS	total dissolved solids
TEM	transmission electron microscope
TOC	total organic carbon
UV	ultraviolet
Vis	visible
WHO	World Health Organization

Greek symbols:

θ	contact angle, theta

Chapter 1

Introduction

This chapter provides an introduction to the research related to bactericidal papers and water purifiers containing silver. This research project is part of the Sentinel Bioactive Paper Network, a collaborative research network focusing on the design of paper-based products that can detect, capture, and/or inactivate pathogenic bacteria and viruses in paper-based consumer applications. In particular, the goal of this project has been to develop bactericidal paper for microbiological water purification.

1.1 Bactericidal paper for water purification

1.1.1 Relevance

This research project focused on eliminating microbial contaminants from water using a thick paper containing silver nanoparticles. Some of the pathogens transmitted through untreated water can lead to severe and life-threatening diseases, such as typhoid, cholera, hepatitis, *E. coli* 0157:H7 (Figure 1.1)[1]. Potential health effects from these microorganisms are gastrointestinal illnesses, e.g. diarrhea, vomiting, cramps, and dehydration. These pathogens are directly transmitted through contaminated water or food. According to the World Health Organization, water borne diseases are responsible for the deaths of 3.5 million people every year [2].

The majority of people affected by a poor water supply and inadequate sanitation and hygiene are located in developing countries. About 783 million people do not have access to an improved water source and acquire their water from unprotected groundwater or surface water. The majority of these people live in rural settings [3]. To address these problems, there are many possible strategies, depending upon the specific contaminants in the local region's water supply. An ideal solution for some places could be to build more wastewater treatment plants and to extend the network of water pipes to reach all communities, but the capital and time investment needed to achieve this goal may be too difficult. A more immediate approach would be to treat drinking water at households, also called point-of-use (POU) water purification.

This thesis documents the design of a simple, lightweight, and portable paper for disinfecting water. Silver nanoparticles, a potent biocide, have been incorporated into thick, porous papers. Only very small quantities of silver are required due to the use of nanoparticles, which have a highly toxic effect specific towards microorganisms at low concentrations. This bactericidal paper has the potential to be a very convenient and

affordable method for sustainable water disinfection. It could be used to purify water in emergency and disaster relief situations or as temporary relief for communities with inadequate water sources.

FIGURE 1.1. Transmission pathways for and examples of water-related pathogens from WHO [1].

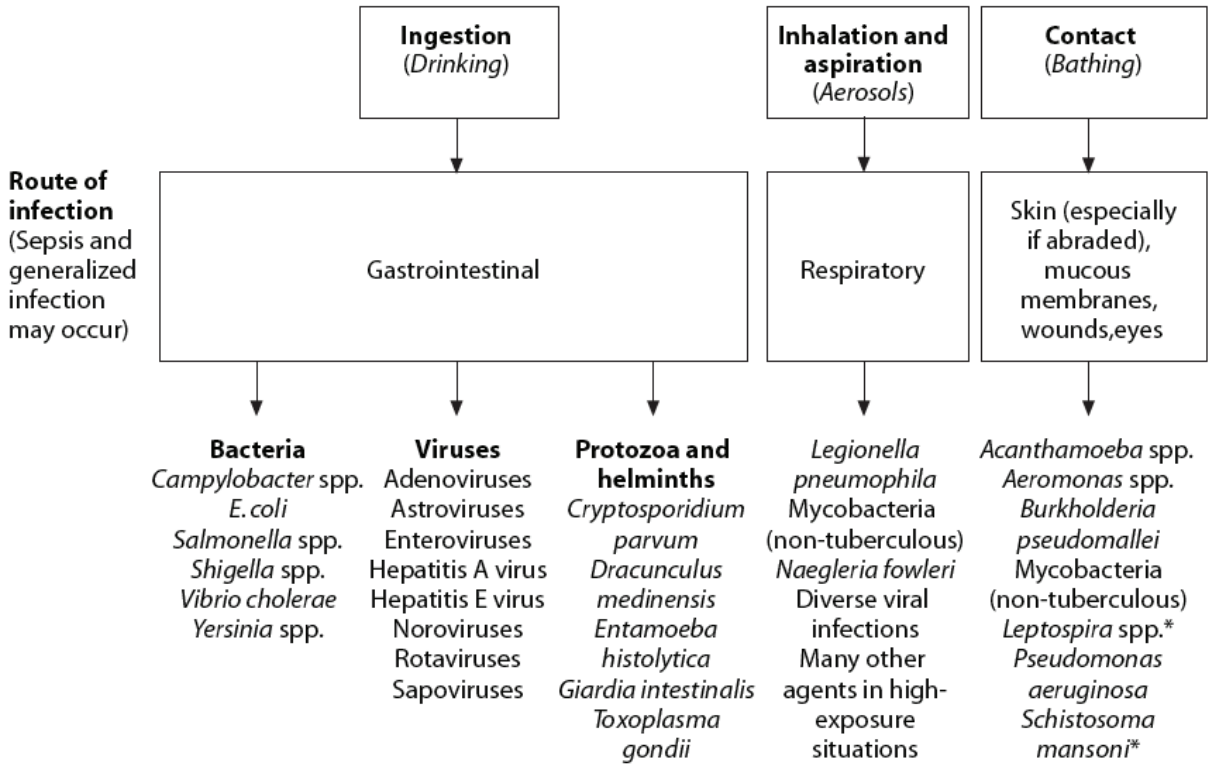

* Primarily from contact with highly contaminated surface waters.

1.2 Silver nanoparticles for antibacterial applications

1.2.1 Silver ions

Silver has been used for disease prevention for many centuries. The earliest example is the storage of potable water in silver vessels in ancient times throughout Rome, Greece, Egypt, and Phoenicia [4]. In the late1800s, the Swiss botanist, Carl von Naegeli, discovered the “oligodynamic effect,” which is the observation that a low concentration of metal ions are biocidal to many different types of microorganisms [5].

The silver ion is the most bactericidal of all the metals, followed by mercury, lead and copper [5]. Several researchers have reported that the necessary concentration for antibacterial effectiveness of silver ions is only 0.3 to 2.0 ppm [6-10]. Table 1.1 lists a survey of the literature of the diversity of microorganisms inactivated by silver ions and/or nanoparticles. In medical treatment, silver salts are used to control certain types of infections, although somewhat less frequently since the advent of modern antibacterial pharmaceuticals. Silver nitrate drops are placed in newborns' eyes at birth for the prevention of contracting gonorrhea from the mother [4]. To prevent infections in burn wounds, silver sulfadiazine topical creams are applied to damaged skin [11]. Copper-silver ionization systems for water disinfection are used to eliminate the spread of *Legionella* in healthcare facilities [12, 13].

TABLE 1.1. Survey of literature on microorganisms inactivated by silver ions and/or nanoparticles.

Microbe Type	Microbe Name	Form of Ag	Reference
Bacteria			
	Bacillus anthracis	Ag Zn zeolite	[162]
	Bacillus cereus	Ag Zn zeolite AgBR NP polymer composite	[162] [152]
	Bacillus subtilis	AgNPs Ag Zn zeolite Fe_3O_4@AgNPs AgNP polymer films	[96, 155] [162] [151] [154]
	Enterococcus faecalis	Ag^+ ions, AgNPs	[153]
	Vancomycin-R E. faecium	Ag^+ ions, AgNPs	[23, 153]
	Escherichia coli	Ag^+ ions AgNPs Ag - activated carbon fibers AgNP - granular activated carbon Fe_3O_4@AgNPs AgNP rice paper plant stem AgNP ceramic beads AgBR NP polymer composite Ag^+ ions in ceramics Polyethersulfone membranes with AgNPs in multilayers	[6, 10, 26, 153] [17, 23, 96, 155, 156] [145, 161] [90] [151] [59] [146] [152] [141] [98]
	Escherichia coli GFP	AgNPs	[20]
	Escherichia coli O157:H8	AgNPs	[21]
	Ampicillin-R E. coli	AgNPs	[156]
	Klebsiella pneumoniae	AgNPs	[157]

	ESBL-R K. pneumoniae	Ag^+ ions, AgNPs	[23, 153]
	Legionella	Cu and Ag ionization	[12, 13]
	Listeria monocytogenes	AgNPs on paper, silicone	[160]
	Micrococcus lylae	AgNP TiO_2	[159]
	Nitrifying bacteria	Ag^+ ions, AgNPs, AgCl colloids	[7]
	Providencia stuartii	Ag^+ ions	[6]
	Proteus mirabilis	Ag^+ ions	[6]
	Pseudomonas aeruginosa	Ag^+ ions AgNPs AgNP polymer films AgNP ceramic beads AgBR NP polymer composite	[6] [17, 23, 153] [150, 154] [146] [152]
	Salmonella typhi	AgNPs	[17, 156]
	Serratia	Ag^+ ions	[6]
	Sphingomonas	Ag ceramic beads	[158]
	Staphylcoccus albus	Ag^+ ions	[6]
	Staphylcoccus aureus	Ag^+ ions AgNPs AgNP polymer films AgNP ceramic beads	[6, 26, 153] [21, 23, 155-157] [150, 154] [146]
	Methicillin-R. S. aureus	Ag+ ions, AgNPs AgBR NP polymer composite	[23, 153] [152]
	Staphylcoccus epidermis	Fe_3O_4@AgNPs AgNP polymer films	[151] [150]
	MR S. epidermidis	AgNPs	[23]
	Streptococcus group D	Ag^+ ions	[6]
	Streptococcus mitis	Ag^+ ions, Ag Zn zeolite	[6] [149]
	Streptococcus mutans	Ag^+ ions, Ag Zn zeolite	[6] [149]
	Streptococcus pyogenes	Ag^+ ions	[6]
	Streptococcus salivarius	Ag^+ ions	[6]
	Vibrio cholera	Ag^+ ions AgNPs	[148] [17]
Fungi			
	Aspergillus niger	AgNP hydrogel AgNP ceramic beads	[147] [146]
	Bovine mastits	AgNPs	[21]
	Candida albicans	AgNP hydrogel, AgNP rice paper plant stem, AgNP ceramic beads	[147] [59] [146]
	Pichia pastoris	Ag - activated carbon fibers	[145]
	Saccharomyces cerevisiae	Ag - activated carbon fibers	[145]
Protozoa			
	Hartmannella vermiformis	Cu and Ag ionization	[143]
	Naegleria fowleri	Cu and Ag ionization	[144]
	Tetreahymena pyriformis	Cu and Ag ionization	[143]

Viruses			
	HIV-1	AgNPs	[142]
	Murine Norovirus	AgNPs in ceramics	[97]
	Reovirus	Ag^+ ions in ceramics	[141]
	SARS Coronavirus	Ag/Al_2O_3 wafers	[140]

*R = resistant, and ESBL = extended spectrum beta-lactamase

1.2.2 Silver nanoparticles

Silver nanoparticles are crystalline particles of Ag_0 metal with at least one dimension between 1 to 100 nm. AgNPs can have spherical, prism, cubic, or rod shaped morphologies. In comparison with silver ions, the nanoparticles have longer lasting biocidal properties, are less prone to complexation and precipitation into forms unavailable to bacteria, and are easier to incorporate into matrix materials, such as papers, fibers, polymers, and ceramics. The nanoparticles act as a controllable reservoir for silver ion release over time, which lends to the material's reusability. Due to the nanometer-sized diameters of the nanoparticles, the surface area is much greater than the bulk metal, and is more bio-active as a result.

Applications of silver nanoparticles are currently of intense interest in nanotechnology. Due to their biocidal properties, the Woodrow Wilson Database lists over 300 commercial products that contain them, as of March 2011 [14]. These products include textiles, cosmetics, health supplements, filters, detergents, and others [14, 15]. Some indication of the biocidal materials containing nano-silver is given in Table 1.1.

1.2.3 Antibacterial mechanism of silver

Silver ions and nanoparticles show a wide spectrum biocidal activity (Table 1.1). In diagnostic laboratories, researchers use the procedure of minimum inhibitory concentration (MIC) to determine microbial resistance to various antibiotic medications. The MIC is defined as the lowest concentration of an antimicrobial that will inhibit the visible growth of a microorganism after overnight incubation in a specified culture media [16]. Silver ions and silver nanoparticles in suspension have similar MIC values,

however generally the MIC for silver ions is somewhat lower (Figure 1.2). The MIC literature values for AgNPs in suspension are in the ppm range but vary due to experimental differences in the AgNP diameters, bacteria concentration, exposure time, and nutrient media. In general, silver nanoparticles have been observed to have the largest antibacterial effects with the smallest particle sizes, with average diameters under 10 nm being most effective [17]. The higher proportion of surface atoms in smaller particle sizes results in greater reactivity and biocidal activity [17, 18].

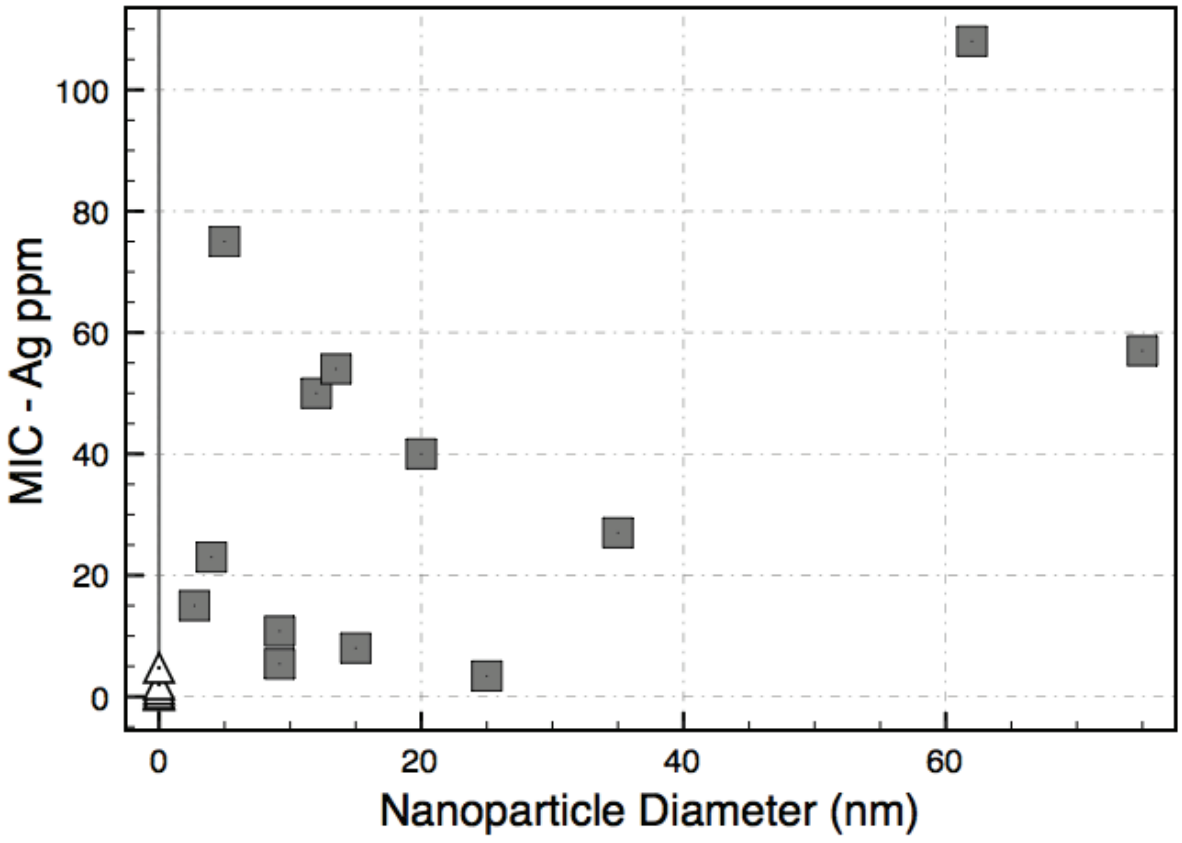

FIGURE 1.2. Scatterplot of MIC values of AgNPs in ppm with comparison to the NP diameters from selected literature (gray squares). MIC values for Ag ions from silver nitrate are represented by the white triangles, which are included as a reference. Studies referenced: [6, 7, 10, 17, 19-25]

The bactericidal activity of silver nanoparticles has been largely attributed to the release of silver ions from the AgNP surface [22, 26]. Silver ions have been shown to

bind preferentially on thiol groups in membrane proteins, and to cause DNA aggregation [26]. Silver ions have been shown to inhibit enzymes in nitrifying bacteria [27], block DNA transcription, interrupt bacterial respiration and ATP synthesis [28]. Treatment with silver nanoparticles caused pitted membranes, increased membrane permeability, and cytoplasm leakage in *E. coli* [17, 24]. Researchers have demonstrated that AgNPs in growing cultures of wild type *E. coli* led to the production of superoxide radicals, which aided silver ion penetration into the cell membrane [29].

Silver ions, nanoparticles, and other compounds have shown great success in many antimicrobial applications, but are not without some problems. Some bacteria have evolved resistance to many antibiotics, including silver. Resistance refers to the ability of bacteria to reproduce in high concentrations of a disinfectant or antibiotic [30]. Silver-resistant bacteria were first isolated from environments contaminated with silver, such as polluted soil near silver mine drainage areas, skin burn wound regions, watersheds near photographic industry effluents, etc. [8, 31-33]. Genes encoding silver resistance in bacteria are carried on plasmids, which have been found in *Pseudomonas stutzeri* that were isolated from a silver mine [34] and *E. coli* [35]. Differing mechanisms explain silver resistance in bacteria, which include either cell wall impermeability to metal ions or metal accumulation within the cells [32, 36].

1.3 Formation of silver nanoparticles in paper/cellulose

As a porous substrate for nanoparticle formation, paper offers many advantages over other polymeric materials. Cellulose, the primary component in paper, is the most abundant natural polymer, and is renewable and biodegradable. Cellulose materials serve as a good material for embedding metal nanoparticles due to their ability for metal ion absorption. Metal cations have an affinity for anionic carboxylic acid groups in paper, which are introduced into the pulp during isolation and purification. Several

researchers have formed silver nanoparticles on cellulose surfaces for a variety of applications including bandages [37], clothing [38-42], food packaging [15, 43], conductive materials [44], catalytic materials [44], substrates for surface enhanced raman spectroscopy [45, 46], etc. All sorts of different cellulosic substrates have been used including filter paper [47, 48], textiles [38-42], microcrystalline cellulose [49], bacterial cellulose [37, 50-52], cellulosic gels [53], nanocrystalline cellulose [54-57], lint free paper wipes [58], etc.

1.3.1 Chemical reduction of silver salts

There are several chemical methods to form metal nanoparticles on cellulosic surfaces, which vary greatly in complexity, from simple *in situ* reduction to surface modification to increase reactive groups. The most commonly used method involves an *in situ* chemical reduction of metal ions sorbed to the cellulose surface. Reducing agents employed include: sodium borohydride [37, 47, 49, 53, 58, 59], ascorbic acid [51], butylamine [38], triethanolamine, potassium phosphate [49], Tollen's reagent [44], and various plant extracts [39, 41]. Different chemical reductants result in different particle sizes, but generally sodium borohydride as the reducing agent gives the smallest and most uniform nanoparticles that fall within the range of 1-10 nm in diameter [37, 47, 49, 53, 58, 59]. A nonconventional biological reduction method involves certain silver-resistant microorganisms as the reducing agent, such as fungi, *Fusarium oxysporum* [40].

Some researchers have investigated ways to incorporate higher amounts of silver nanoparticles into cellulosic materials. Generally, this involves an extra step of surface modification through chemical grafting of various functional groups or physical modification of nano-porous or nano-fibrous forms of cellulose. Surface modification also may reduce nanoparticle aggregation by anchoring nanoparticle formation to specific functional groups. Various surface modifications of cellulose include:

oxidization [44, 60], amine grafting [61], grafting with a chelating monomer [62], polyacrylic grafting [48], and multilayering of polyelectrolytes [52]. To increase the surface area on cellulosic fibers and therefore increase possible crystallization nuclei sites for nanoparticle formation, researchers have explored AgNP synthesis on the following: bacterial cellulose [37, 50-52], cellulose acetate nano-fibrils [63], electrospun cellulose acetate [64, 65], nanocrystalline cellulose [54-57], and nano-porous cellulose gels [53].

1.3.2 Physical methods for nanoparticle synthesis

In addition to the chemical reduction of silver salts to form silver nanoparticles, several researchers have used physical methods [42, 49, 53, 60, 66]. Similar to chemical reduction, the procedure for nanoparticle synthesis also involves the absorption of silver ions on cellulose fibers followed by irradiation or a thermal treatment. Examples of physical methods to form silver nanoparticles include: autoclave [42], microwave [67-69], thermal [49, 53, 60], ultrasound [66], and UV light [43, 52, 64]. Physical methods are often used to avoid toxic chemical reducing agents. Sometimes physical and chemical reduction methods are used together.

1.3.3 Cellulose substrates

In this research project, we have studied two different models of pure cellulosic materials: blotting paper and nanocrystalline cellulose (NCC) (I) films. Blotting papers are pure cellulose papers with no additives and are thick sheets of paper (0.5 mm). They are highly absorbent and porous. The high water absorbency facilitates the uptake of silver salt solutions for *in situ* reduction. The porosity of the blotter paper allows microorganisms to come into contact with the biocide during water purification. It is thicker and more porous than typical laboratory filter papers.

Nanocrystalline cellulose (I) films are formed by casting from an aqueous suspension of NCC and stabilized by gentle heating. Since these macroscopic films are essentially pure cellulose (I), this facilitates surface studies on flat materials more closely resembling the form of cellulose found in natural cellulose fibers [70]. The motivation for studying thin nanocrystalline cellulose (I) films embedded with silver nanoparticles is to analyze the stability of AgNPs in a model solid system that avoids porosity and surface roughness. The limitations of this model film include the inability to be used in a filtration flow experiment and the overall brittleness of the material.

1.4 Microbiological water purification

1.4.1 Water quality

Most surface waters are not safe for human consumption. To protect public health, it is essential to treat drinking water. Many different types of contaminants may be present in untreated water, such as pathogenic microorganisms, synthetic chemicals from petroleum and pharmaceuticals, heavy metals, pesticides, and radioactive chemicals. A survey of physical, chemical and biological characteristics of common water sources and treated drinking water has been compiled by the US EPA (Table 1.2). At a minimum, drinking water treatment should include disinfection prior to consumption. Specific procedures are in place to monitor and assess the water quality. Water quality assessments can be divided into two main categories: physical/chemical and microbiological.

Table 1.2. Physical, chemical, and biological characteristics of various waters, taken from [71].

	Water Source			Selected Drinking Water Quality Objectives	
Characteristics	Typical Surface Water	Typical Ground-water	Domestic wastewater (U.S.)	Raw water source	Drinking water
Physical					
Turbidity, NTU	--	--	--	--	< 1
Solids, total, g/m^3	--	--	700	--	500
Suspended, g/m^3	> 50	--	200	--	--
Settleable, mL/L	--	--	10	--	--
Volatile, g/m^3	--	--	300	--	--
Filtrable (dissolved), g/m^3	< 100	> 100	500	--	--
Color, units	--	--	--	< 150	< 15
Odor, number	--	--	Stale	--	< 3
Temperature, °C	0.5-30	2.7-25	2012-10-25	< 20	--
Chemical: Inorganic Matter					
Alkalinity, eq/m^3	< 2	> 2	> 2	--	--
Hardness, eq/m^3	< 2	> 2	--	--	--
Chlorides, g/m^3	50	200	> 100	250	250
Calcium, g/m^3	20	150	--	--	--
Heavy metals, g/m^3	--	0.5	--	--	--
Nitrogen, g/m^3	< 10	<10	40	--	--
Organic, g/m^3	5	--	15	--	--
Ammonia, g/m^3	--	--	25	--	--
Nitrate, g/m^3	< 5	5	0.5-30	--	10
Phosphorus, total, g/m^3	--	--	12	--	--
Sulfate, g/m^3	--	--	--	--	250
pH, unitless	--	6.5-8	6.5-8.5	--	6.0-8.5
Chemical: Organic Matter					
Total organic carbon (TOC), g/m^3	< 5	--	150	--	--
Fats, oil, greases, g/m^3	--	--	100	--	--
Pesticides, g/m^3	< 0.1	--	100	--	--
Phenols, g/m^3	< 0.001	--	--	--	0.2
Surfactants, g/m^3	< 0.5	< 0.5	--	--	0.5
Chemical: Gases					
Oxygen, g/m^3	7.5	~7.5	< 1.0	> 4.0	> 4.0
Biological					
Bacteria, MPN/100 mL	< 2000	< 100	10^8-10^9	< 5000	< 1.0
Viruses, pfu/100 mL	<10	< 1	10^2-10^4	--	--

1.4.1.1 Freshwater chemical composition and terminology

The chemical composition of freshwater can be quite variable, but only a very small number of compounds exist in concentrations higher than 0.01 mM. Generally, in water quality literature, the chemical composition is classified into “dissolved solids” and “particulate matter.” The term “total dissolved solids” (TDS) is a measure of suspended forms of all inorganic and organic substances, and refers to the suspended matter that passes through a 0.45-μm filter. Common dissolved solids include: inorganic ions (Ca^{2+}, Na^{+}, Mg^{2+}, HCO_3^{-}, SO_4^{2-}, Cl^{-}), proteins, polysaccharides, and humics. “Particulate matter” includes: clays, silicates, iron oxides, organism debris, larger humics, and organo-mineral particles [72].

In addition to the usual physicochemical descriptors (e.g., turbidity, pH), some more specialized terms are used to describe water quality. Total organic carbon (TOC) refers to the weight of elemental carbon in per unit volume of water, excluding the inorganic content from dissolved carbon dioxide. The main constituents of TOC are decaying natural organic matter (NOM) and synthetic compounds. NOM includes humic acids, fulvic acids, and amines, but often is simplified to humic acids, which is the largest component. Both humic and fulvic acids are extracted from soil humus, and only fulvic acid is soluble below pH 2. Fulvic acids are generally lower molecular weight compounds with higher oxygen and lower carbon contents than humic acids [73]. Synthetic organic substances found in water include detergents, pesticides, chlorinated organics [74]. TDS is closely related to the water hardness, which is the sum of the molar concentrations of divalent cations [74]. Specific test water compositions have been established for simulating freshwater conditions in laboratory tests, such as for assessing microbiological water purification [75]. These water compositions vary the TOC, pH, turbidity, and TDS to portray public tap water with low levels of dissolved matter to stressed “challenge” waters with high levels of TOC, turbidity, and TDS [75].

Silver contamination can sometimes be found in natural water sources. Typically, the silver concentration found in surface water is between 0.2 and 2.0 ppb, but can be as much as one hundred times higher in waters that originate near silver-bearing ores, or that are contaminated due to proximity to industries using silver [76].

1.4.1.2 Microorganisms in freshwater

Many different types of microorganisms live in freshwater including bacteria, cyanobacteria, protozoa, algae, and rotifers. The majority of microorganisms perform diverse ecological niche roles and are harmless to human health. However, there are a number of microorganisms which contaminate or pollute the freshwater, and if present in high enough levels, can cause disease. Examples of waterborne pathogenic microorganisms are listed in Figure 1.1. In most cases, the transmission of pathogenic microorganisms into freshwaters occurs through fecal matter contamination from warm-blooded animals.

1.4.1.3 Indicator organisms for water quality

Microbiological tests for water contamination analyze for the presence and enumeration of indicator organisms, not actual pathogenic organisms. Generally, the presence of coliform bacteria, which are present in the gut and feces of warm-blooded animals, are representative of the degree of water pollution and the sanitary quality [77]. The detection of indicator organisms is generally less expensive, more practical, and easier to enumerate than the detection of specific pathogenic organisms. Most frequently examined coliform bacteria are *Escherichia coli,* fecal streptococci and enterococci. Additionally, water pollution of bathing places may include skin and upper respiratory tract bacteria, such as *Staphylococcus* and *Pseudomonas aeruginosa*. Examples of high levels of microbial indicators found in various water sources are included in Table 1.3. While indicator organisms are useful in predicting the risk of

exposure to pathogenic microorganisms, no single procedure can isolate all the microorganisms in contaminated water. Certain pathogenic microorganisms may be more resistant to changing environmental conditions than the indicators, and the bacterial indicators may not adequately reflect the likelihood of viral, fungal or parasitic infection [77].

The most common and oldest method for microbial detection is culturing samples on nutrient agar plates or in nutrient broth media. This assay method is considered the most relevant and interpretable from a public health standpoint. Enumeration of bacteria from culture plates is expressed by the number of visible colonies on the agar plate, called the colony forming units (CFU) [77]. Emerging assays for indicator organisms include applying monoclonal antibodies, chromogenic stains, and gene sequencing [78]. Monoclonal antibodies detect bacteria by binding to specific surface structures on the cell surface. Chromogenic stains, such as the LIVE/DEAD® cell viability assay [79], provide rapid and easy detection of bacteria based on chromogenic color or fluorescence changes with respect to their viability. Gene sequencing uses molecular biology techniques, such as the polymerase chain reaction, for the detection of specific strains of organisms [78].

TABLE 1.3. Examples of high concentrations (colony forming units (CFU) per liter) of enteric pathogen faecal indicators detected in different types of source water (from the WHO [80]).

Pathogen or indicator group	Lakes and reservoirs	Impacted rivers and streams	Wilderness rivers and streams	Groundwater
Campylobacter	20–500	90–2500	0–1100	0–10
Salmonella	—	3–58 000 (3–1000)[a]	1–4	—
E. coli (generic)	10 000–1 000 000	30 000–1 000 000	6000–30 000	0–1000
Viruses	1–10	30–60	0–3	0–2
Cryptosporidium	4–290	2–480	2–240	0–1
Giardia	2–30	1–470	1–2	0–1

[a] Lower range is a more recent measurement.

1.4.2 Point-of-use water purification

Point-of-use water purification has been shown to improve water quality and reduce the spread of waterborne diseases [81, 82]. Mostly, POU water purification focuses on the disinfection of drinking water due to the acute health concerns, i.e. diarrheal diseases, from microbiological contaminants. A POU device should be easy to use and distribute, affordable, and sustainable. The capacity should be appropriate for daily household water use, around 50 liters per day, which will cover basic sanitation, drinking, and hygiene needs [83].

Examples of existing POU technologies include: chemical disinfection, filtration through ceramic, polymeric membranes, or granular materials, disinfection by exposure to sunlight or UV light, thermal treatment, coagulation, and various combination approaches. No single technology has been able to successfully reduce all waterborne pathogens [1, 82]. Different technologies can have vastly differing abilities to reduce pathogens, as shown in Table 1.4, where higher log reduction values correspond to a higher efficiency at removing pathogens [82]. The log reduction value is the difference of the log of the pretreatment CFU and of the post-treatment CFU, as enumerated through culturing methods. Additionally, the effectiveness of water treatment in the field is often impaired due to improper instruction or handling, which results in lower than expected pathogen removal.

TABLE 1.4. Estimates of baseline* and maximum** effectiveness of POU technologies against microbes [82].

Microbiological Assessment							
EPA requirements		6.0		4.0		3.0	
Filter/Method	Bacterial Log Reduction		Virus Log Reduction		Protozoa Log Reduction		Diarrheal Reduction (%)
	Baseline	Max	Baseline	Max	Baseline	Max	
Porous ceramic filtration	2	6	0.5	4	3	6	63
Free Chlorine (Bleach)	3	6+	3	6+	3	6+	37
Solar Disinfection	3	5.5+	2	4+	1	3+	31
Coagulation/Chlorination	7	9	2-4.5	6	3	5	31
Biosand Filter	1	3	0.5	3	1	3+	47

* Baseline refers to expected performance in actual field practice with unskilled users.

** Maximum refers to optimized performance with skilled operators.

1.4.3 Silver use in water disinfection

Silver ions and nanoparticles have been used previously in drinking water disinfection. One of the first uses of silver in water purification is in the Katadyn silver technology, which was commercialized by Alexander Krause in 1928. The Katadyn water purifier combines three technologies: a silver impregnated ceramic disc, a glass fiber filter, and a carbon granulate filter [84]. Other applications range from POU devices [84-93], reverse osmosis membrane filters [94-98], and point-of-entry filters in hospital systems [12, 13]. In POU filter media, silver nanoparticles have been added to polyurethane foams [85], activated carbon media [90], activated alumina media [91], and ceramic filters [86, 87, 92, 93]. Recent POU proposals include a sachet filled with activated carbon coated with AgNPs [89], and cotton fabric coated with Ag nanowires and carbon nanotubes with a current applied [88]. These POU treatments have largely been demonstrated in laboratory settings to inactivate bacteria, such as *E. coli,* [85, 87, 88, 90, 91], and viruses, such as noroviruses [97]. The Ag coated ceramic pot filters have performed well in field studies by reducing the bacteria count after purifying environmental water samples [86, 92, 93] and reducing the occurrences of diarrheal

disease [99]. Silver nanoparticles have been proposed to prevent the growth of biofilms, highly organized microbial communities, on reverse osmosis and microfiltration membranes, such as polysulfone polymer membranes [95] and polyethersulfone membranes with polyelectrolyte multilayer coatings [98]. To control the spread of nosocomial Legionnaire's disease in hospitals, copper-silver ionization disinfection has been successfully implemented in many healthcare facilities since the 1980s [12, 13].

1.5 Environmental interactions with silver nanoparticles

1.5.1 Release of silver from nanomaterials

In the past five years, the addition of AgNPs to consumer products has increased nearly tenfold [14]. Many of these products are textiles and apparel, cosmetics, food packaging, medical devices, etc., which come into contact with aqueous solutions that can oxidize the nanoparticles and release either silver ions and/or nanoparticles into the environment [100-103]. This silver release can negatively impact the antibacterial purpose of the product as well as possibly can cause a detrimental effect on various environmental ecosystems, such as wastewater treatment, aquatic life, leachate into soil, etc. [7, 104, 105]. Studying the behavior of nanoparticles in suspension can assist in predicting the transport, fate, and toxic effects of AgNPs beyond their originally intended functions.

Several researchers have analyzed for silver release from consumer products, notably socks [100, 101], textiles [102, 103], paints [106], and filter media containing silver nanoparticles [87, 95]. During washing or filtering, AgNPs encounter aqueous solutions containing surfactants, and oxidizing agents over a range of pH values. Considerable variations in silver release were observed, from non-detectable to a few ppm, with distilled water having the least effect and detergents the greatest release [87, 100, 101]. These differences may also be due to the variations in how nano-silver is

embedded into the materials or the particular chemical composition of the matrix material.

1.5.2 Stability of AgNPs in aqueous systems

The stability of silver nanoparticles in aqueous suspensions has been more thoroughly studied than AgNP stability in composite materials [18, 107-110]. Researchers have examined the silver ion release and aggregation behavior of AgNPs in a variety of suspensions typical of environmental and biological compositions [107, 110-115]. Some of the environmental variables in natural water sources are listed in Table 1.2, and are simulated in laboratories by “synthetic” test waters by varying the chemical characteristics such as TOC, TDS, and pH [75]. Biological media compositions generally consist of some variety of protein digest, salt, and nucleic acid extract. Slow dissolution of AgNPs has been observed in test solutions with dissolved oxygen, and the dissolution reaction kinetics increases with stronger oxidizers and low pH [115]. Aggregation is dependent upon the concentration of particles, surface charge groups, and the ionic strength of the suspension [104, 116]. In environmental test waters, the ionic strength from hard water can contribute to particle aggregation, but conversely natural organic matter can stabilize the AgNPs in suspension [113]. Similarly, in biological media, AgNPs aggregate with a high electrolyte content, but the presence of proteins can stabilize the nanoparticles [107, 111]. The overall persistence and activity of AgNPs in environmental and biological suspensions is largely dependent upon the solution chemistry.

1.5.3 Environmental toxicology of AgNPs

Silver ions pose a risk for aquatic microorganisms in laboratory testing [117], and by extension, silver nanoparticles could be harmful to the health of many ecosystems. The transport, fate, and toxicity of silver nanoparticles in aquatic environments is an

emerging area of environmental chemistry research. The transport of silver nanoparticles has been investigated by passage of AgNPs through various porous media columns, which simulate soils. Transport of AgNPs in groundwater can be aided by the surface coatings on nanoparticles [118]. Studying AgNPs in environmental test solutions has contributed to the understanding of their chemical fate in terms of dissolution, aggregation, deposition, and transformation processes. The environmental corrosion of AgNPs could lead to an increase or decrease in the environmental toxicity by either releasing potent silver ions or by becoming less bioavailable through binding to complexing agents, such as thiosulfate compounds [27]. For example, in sewage treatment plants, nano-sized silver sulfide particles have been detected, where the silver is assumed to originate from AgNP products [119]. Higher rates of aggregation will lead to particle deposition into the sediments [104]. The release of silver nanoparticles as composite colloids bound to organic binders was observed in weathering of exterior paints containing AgNPs [106]. Toxicity and bioaccumulation of silver ions, nanoparticles, and compounds are not well understood. There have been some reports of fish toxicity from AgNPs in fathead minnows and zebra fish embryos [120, 121]. Other studies have shown considerable variation in toxicity and bioaccumulation in many species of plants and algae, with the main conclusion being that the toxicity results from silver nitrate more so than from other forms of silver compounds [27]. Certain bacteria, specifically *Pseudomonas maltophilia*, located near silver mine drainage areas have even shown silver resistance and bioaccumulation [31]. Currently there is insufficient toxicity and exposure data necessary to fill the knowledge gap for the ‘‘source to pathway to receptor to impact’’ framework necessary for proper risk assessment of silver nanoparticles [122].

1.5.4 Effects of silver on human health

Silver has very low toxicity in humans and is non-carcinogenic [123]. Most people retain 0-10% of the silver they are exposed to, and like many heavy metals, silver is mostly excreted through the skin and hair [5, 124]. High exposure to silver ions

can result in the metal binding strongly to sulfrydryl, amino, imidazole, carboxylate or phosphate groups on protein complexes throughout the body. Excessive long term accumulation of silver has led to some people developing argyria, which is a bluish-gray discoloration of the skin due to insoluble silver deposits (Figure 1.3) [125]. These high concentrations of silver exposure are very rare, and occur mostly with colloidal silver supplements or in occupational exposure [124].

FIGURE 1.3. Clinical appearance of argyrosis [125].

More recently, researchers have begun investigating the *in vitro* toxicity of AgNPs on various human cell lines [111, 126-131]. With higher concentrations of AgNPs than recommended for bactericidal applications, oxidative stress has been observed to cause cytotoxicity and apoptosis in human cells [127]. In contrast, at lower concentrations, AgNPs have shown therapeutic benefits, such as anti-inflammatory effects [131]. On-going research will eventually clarify the dose-response curve for silver ions and nanoparticles for human exposure.

1.5.5 Guidelines for silver in water

The current US EPA guidelines specify the maximal level for silver in drinking water as 100 ppb. This non-enforceable guideline is part of the National Secondary Drinking Water Regulation, which regulates contaminants that cause cosmetic or aesthetic effects in drinking water [132]. For silver, this guideline is based on the idea that if a person lives 70 years, the limit would be half the maximum daily intake needed to accumulate enough silver to develop argyria [133]. For the protection of aquatic microorganisms, the dissolved silver criterion in moderately hard freshwater is 3.2 ppb, and in seawater, it is 1.9 ppb [134]. Generally, the presence of water hardness decreases the environmental toxicity of metal ions due to metal ion competition for binding sites on cell surfaces [27].

1.6 Thesis overview

Much progress has been made towards incorporating silver nanoparticles into cellulose materials having potential applications as antibacterial products. Here we investigate the well-dispersed and uniform incorporation of silver nanoparticles on thick blotter papers and model nanocrystalline cellulose (I) films. These forms of cellulose were chosen to represent a practical filter and a model cellulose surface, respectively.

The work described here begins by looking at the preparation and characterization of blotter papers containing silver nanoparticles through a couple of different synthetic methods, in Chapter 2, by a sodium borohydride reduction, and in Chapter 3, by a microwave-assisted reduction. The AgNP papers are examined by UV-Vis spectroscopy, electron microscopy, bactericidal activity in a model filter setup, and measurement of silver leaching. The aim is to show that bactericidal paper containing silver nanoparticles can be used in a microbiological water purification application. The bactericidal tests demonstrated that AgNP paper was an effective water purifier for the inactivation of water pathogen indicator bacteria including: *Escherichia coli* and

Enterococci faecalis. Chapter 4 examines the formation of AgNPs on NCC films and describes the monitoring of the long term stability and aggregation behavior of silver nanoparticles on these films. Chapter 5 describes some of the potential effects of dissolved materials present in natural water sources and biomedical environments, including dissolved proteins, salts and fulvic acid, on the bactericidal functioning of AgNP papers. Chapters 4 and 5 are relevant to the lifespan and reusability of AgNP-containing products. The final chapter summarizes the conclusions from this research project and discusses possible directions for further research.

1.7 References

1. World Health Organization, ed. *Guidelines for drinking-water quality, 4th edition*. 2011. 123.
2. C. Mathers, D.M. Fat, and J.T. Boerma, *The global burden of disease: 2004 update*. 2008, Geneva, Switzerland: WHO Press. 11.
3. UNICEF, *Progress on sanitation and drinking-water: 2010 update*. World Health Organization/UNICEF Joint Monitoring Programme for Water Supply and Sanitation, 2010.
4. R. Davies and S. Etris, *The development and functions of silver in water purification and disease control.* Catalysis Today, 1997. **36**(1): p. 107-114.
5. A.B.G. Lansdown, *Silver in healthcare: its antimicrobial efficacy and safety in use*. Issues in toxicology, 2010, Cambridge: Royal Society of Chemsitry.
6. T.J. Berger, J.A. Spadaro, S.E. Chapin, and R.O. Becker, *Electrically generated silver ions - quantitative effects on bacterial and mammalian cells.* Antimicrob Agents Ch, 1976. **9**(2): p. 357-358.
7. O. Choi, K. Deng, N. Kim, L. Rossjr, R. Surampalli, and Z. Hu, *The inhibitory effects of silver nanoparticles, silver ions, and silver chloride colloids on microbial growth.* Water Research, 2008. **42**(12): p. 3066-3074.
8. W. Ghandour, J.A. Hubbard, J. Deistung, M.N. Hughes, and R.K. Poole, *The uptake of silver ions by Escherichia coli K12: toxic effects and interaction with copper ions.* Appl Microbiol Biot, 1988. **28**(6): p. 559-565.
9. C. Gunawan, W.Y. Teoh, C.P. Marquis, J. Lifia, and R. Amal, *Reversible antimicrobial photoswitching in nanosilver.* Small, 2009. **5**(3): p. 341-344.
10. G.J. Zhao and S.E. Stevens, *Multiple parameters for the comprehensive evaluation of the susceptibility of Escherichia coli to the silver ion.* Biometals, 1998. **11**(1): p. 27-32.
11. S. Hoffmann, *Silver sulfadiazine: an antibacterial agent for topical use in burns.* Scandinavian Journal of Plastic and Reconstructive Surgery and Hand Surgery, 1984. **18**(1): p. 119-126.

12. R. Vonberg, D. Sohr, J. Bruderek, and P. Gastmeier, *Impact of a silver layer on the membrane of tap water filters on the microbiological quality of filtered water.* BMC Infectious Diseases, 2008. **8**: p. 5.
13. J.E. Stout and V.L. Yu, *Experiences of the first 16 hospitals using copper-silver ionization for Legionella control: Implications for the evaluation of other disinfection modalities.* Infection Control and Hospital Epidemiology, 2003: p. 563-568.
14. Project on Emerging Nanotechnologies. 2011. Cited on November 11, 2011. Available from: http://www.nanotechproject.org/inventories/consumer/analysis_draft/.
15. E. Fauss, *The silver nanotechnology commercial inventory.* Project on Emerging Nanotechtnologies, 2008: p. 21.
16. J.M. Andrews, *Determination of minimum inhibitory concentrations.* Journal of Antimicrobial Chemotherapy, 2001. **48**(Suppl 1): p. 5.
17. J.R. Morones, J.L. Elechiguerra, A. Camacho-Bragado, K. Holt, J.B. Kouri, J.T. Ramírez, and M.J. Yacaman, *The bactericidal effect of silver nanoparticles.* Nanotechnology, 2005. **16**(10): p. 2346-2353.
18. J. Liu, D.A. Sonshine, S. Shervani, and R.H. Hurt, *Controlled release of biologically active silver from nanosilver surfaces.* ACS Nano, 2010. **4**(11): p. 6903-6913.
19. C. Baker, A. Pradhan, L. Pakstis, D. Pochan, and S. Shah, *Synthesis and antibacterial properties of silver nanoparticles.* Journal of Nanoscience and Nanotechnology, 2005. **5**(2): p. 244-249.
20. S.K. Gogoi, P. Gopinath, A. Paul, A. Ramesh, S.S. Ghosh, and A. Chattopadhyay, *Green fluorescent protein-expressing Escherichia coli as a model system for investigating the antimicrobial activities of silver nanoparticles.* Langmuir, 2006. **22**(22): p. 9322-9328.
21. J. Kim, E. Kuk, K. Yu, J. Kim, S. Park, H. Lee, S. Kim, Y. Park, Y. Park, and C. Hwang, *Antimicrobial effects of silver nanoparticles.* Nanomedicine: Nanotechnology, Biology and Medicine, 2007. **3**(1): p. 95-101.

22. C.-N. Lok, C.-M. Ho, R. Chen, Q.-Y. He, W.-Y. Yu, H. Sun, P.K.-H. Tam, J.-F. Chiu, and C.-M. Che, *Silver nanoparticles: partial oxidation and antibacterial activities.* J Biol Inorg Chem, 2007. **12**(4): p. 527-534.
23. A. Panacek, L. Kvitek, R. Prucek, M. Kolar, R. Vecerova, N. Pizurova, V.K. Sharma, T. Nevecna, and R. Zboril, *Silver Colloid Nanoparticles: Synthesis, characterization, and their antibacterial activity.* J Phys Chem B, 2006. **110**: p. suppl info.
24. I. Sondi and B. Salopek-Sondi, *Silver nanoparticles as antimicrobial agent: a case study on E. coli as a model for Gram-negative bacteria.* Journal of Colloid and Interface Science, 2004. **275**(1): p. 177-182.
25. P. Li, J. Li, C. Wu, and Q. Wu, *Synergistic antibacterial effects of beta-lactam antibiotic combined with silver nanoparticles.* Nanotechnology, 2005. **16**(9): p. 1912-1917.
26. Q.L. Feng, J. Wu, G.Q. Chen, F.Z. Cui, T.N. Kim, and J.O. Kim, *A mechanistic study of the antibacterial effect of silver ions on Escherichia coli and Staphylococcus aureus.* J Biomed Mater Res, 2000. **52**(4): p. 662-668.
27. H.T. Ratte, *Bioaccumulation and toxicity of silver compounds: A review.* Environmental toxicology and chemistry, 1999. **18**(1): p. 89-108.
28. R. Kumar, S. Howdle, and H. Munstedt, *Polyamide/silver antimicrobials: Effect of filler types on the silver ion release.* J Biomed Mater Res B, 2005. **75B**(2): p. 311-319.
29. E. Hwang, J. Lee, Y. Chae, Y. Kim, B. Kim, B. Sang, and M. Gu, *Analysis of the toxic mode of action of silver nanoparticles using stress-specific bioluminescent bacteria.* Small, 2008. **4**(6): p. 746-750.
30. N. Silverstry-Rodriguez, E.E. Sicairos-Ruelas, C.P. Gerba, and K.R. Bright, *Silver as a disinfectant.* Rev Environ Contam Toxicol, 2007. **191**: p. 23-45.
31. R.C. Charley and A.T. Bull, *Bioaccumulation of silver by a multispecies community of bacteria.* Arch Microbiol, 1979. **123**(3): p. 239-244.
32. S. Silver, *Bacterial silver resistance: molecular biology and uses and misuses of silver compounds.* Fems Microbiology Reviews, 2003. **27**(2-3): p. 341-353.

33. T. Pumpel and F. Schinner, *Silver tolerance and silver accumulation of microorganisms from soil materials of a silver mine.* Appl Microbiol Biot, 1986. **24**: p. 244-247.
34. C. Haefeli, C. Franklin, and K. Hardy, *Plasmid-determined silver resistance in Pseudomonas stutzeri isolated from a silver mine.* J Bact, 1984. **158**: p. 389-392.
35. A.O. Summers, G.A. Jacoby, M.N. Swartz, G. Mchugh, and L. Sutton, *Metal cation and oxyanion resistances in plasmids of gram-negative bacteria*, in *Microbiology*, D. Schlessinger, Editor 1978, American Society for Microbiology. p. 128-131.
36. J.T. Trevors, Oddie, K.M., Belliveau, B.H., *Metal resistance in bacteria.* Fems Microbiology Reviews, 1985. **32**: p. 39-54.
37. T. Maneerung, S. Tokura, and R. Rujiravanit, *Impregnation of silver nanoparticles into bacterial cellulose for antimicrobial wound dressing.* Carb Polym, 2008. **72**(1): p. 43-51.
38. H.Y. Lee, H.K. Park, Y.M. Lee, K. Kim, and S.B. Park, *A practical procedure for producing silver nanocoated fabric and its antibacterial evaluation for biomedical applications.* Chem. Commun., 2007. (28): p. 2959-2961.
39. S. Ravindra, Y.M. Mohan, N.N. Reddy, and K.M. Raju, *Fabrication of antibacterial cotton fibres loaded with silver nanoparticles via a green approach.* Colloids and Surfaces A: Physicochemical and Engineering Aspects, 2010. **367**(1-3): p. 31-40.
40. N. Duran, P. Marcato, G. De Souza, O. Alves, and E. Esposito, *Antibacterial effect of silver nanoparticles produced by fungal process on textile fabrics and their effluent treatment.* Journal of Biomedical Nanotechnology, 2007. **3**(2): p. 203-208.
41. M. Sathishkumar, K. Sneha, and Y.-S. Yun, *Immobilization of silver nanoparticles synthesized using Curcuma longa tuber powder and extract on cotton cloth for bactericidal activity.* Bioresource Technology, 2010. **101**(20): p. 7958-7965.
42. N. Vigneshwaran, A.A. Kathe, P.V. Varadarajan, and R.H. Balasubramanya, *Functional finishing of cotton fabrics using silver nanoparticles.* J Nanoscience Nanotechnol, 2007. **7**: p. 1893-1897.

43. A. Fernández, E. Soriano, G. López-Carballo, P. Picouet, E. Lloret, R. Gavara, and P. Hernández-Muñoz, *Preservation of aseptic conditions in absorbent pads by using silver nanotechnology.* Food Research International, 2009. **42**(8): p. 1105-1112.
44. M. Wu, S. Kuga, and Y. Huang, *Quasi-one-dimensional arrangement of silver nanoparticles templated by cellulose microfibrils.* Langmuir, 2008. **24**(18): p. 10494-10497.
45. M. Fleischmann, P.J. Hendra, and A.J. Mcquillan, *Raman spectra of pyridine adsorbed at a silver electrode.* Chem Phys Lett, 1974. **26**: p. 163-166.
46. Y.H. Ngo, D. Li, G.P. Simon, and G. Garnier, *Paper surfaces functionalized by nanoparticles.* Advances in Colloid and Interface Science, 2011. **163**(1): p. 23-38.
47. J.H. He, T. Kunitake, and A. Nakao, *Facile in situ synthesis of noble metal nanoparticles in porous cellulose fibers.* Chem Mater, 2003. **15**(23): p. 4401-4406.
48. F. Tang, L. Zhang, Z. Zhang, Z. Cheng, and X. Zhu, *Cellulose filter paper with antibacterial activity from surface-initiated ATRP.* Journal of Macromolecular Science Part A-Pure and Applied Chemistry, 2009. **46**(10): p. 989-996.
49. N. Kotelnikova, V. Demidov, G. Wegener, and E. Windeisen, *Mechanisms of diffusion-reduction interaction of microcrystalline cellulose and silver ions.* Russian Journal of General Chemistry, 2003. **73**(3): p. 427-433.
50. H. Barud, C. Barrios, T. Regiani, R. Marques, M. Verelst, J. Dexpert-Ghys, Y. Messaddeq, and S. Ribeiro, *Self-supported silver nanoparticles containing bacterial cellulose membranes.* Materials Science & Engineering C-Biomimetic and Supramolecular Systems, 2008. **28**(4): p. 515-518.
51. L.C. de Santa Maria, A.L.C. Santos, P.C. Oliveira, H.S. Barud, Y. Messaddeq, and S.J.L. Ribeiro, *Synthesis and characterization of silver nanoparticles impregnated into bacterial cellulose.* Materials Letters, 2009. **63**(9-10): p. 797-799.
52. R.J.B. Pinto, P.A.A.P Marques, C.P. Neto, T. Trindade, S. Daina, and P. Sadocco, *Antibacterial activity of nanocomposites of silver and bacterial or vegetable cellulosic fibers.* Acta Biomaterialia, 2009. **5**(6): p. 2279-2289.

53. J. Cai, S. Kimura, M. Wada, and S. Kuga, *Nanoporous cellulose as metal nanoparticles support.* Biomacromolecules, 2009. **10**(1): p. 87-94.
54. Y. Shin, I.-T. Bae, B.W. Arey, and G.J. Exarhos, *Facile stabilization of gold-silver alloy nanoparticles on cellulose nanocrystal.* J Phys Chem C, 2008. **112**(13): p. 4844-4848.
55. N. Drogat, R. Granet, V. Sol, A. Memmi, N. Saad, C. Koerkamp, P. Bressollier, and P. Krausz, *Antimicrobial silver nanoparticles generated on cellulose nanocrystals.* Journal of Nanoparticle Research, 2011. **13**(4): p. 1557-1562.
56. H. Liu, D. Wang, Z. Song, and S. Shang, *Preparation of silver nanoparticles on cellulose nanocrystals and the application in electrochemical detection of DNA hybridization.* Cellulose, 2011. **18**(1): p. 67-74.
57. E. Fortunati, I. Armentano, Q. Zhou, A. Iannoni, E. Saino, L. Visai, L.A. Berglund, and J.M. Kenny, *Multifunctional bionanocomposite films of poly(lactic acid), cellulose nanocrystals and silver nanoparticles.* Carbohydrate Polymers, 2011. **87**(2): p. 1596-1605.
58. C. Zhu, J. Xue, and J.H. He, *Controlled in-situ synthesis of silver nanoparticles in natural cellulose fibers toward highly efficient antimicrobial materials.* Journal of Nanoscience and Nanotechnology, 2009. **9**(5): p. 3067-3074.
59. F. Zeng, C. Hou, S. Wu, X. Liu, Z. Tong, and S. Yu, *Silver nanoparticles directly formed on natural macroporous matrix and their anti-microbial activities.* Nanotechnology, 2007. **18**(5): p. 055605.
60. S. Ifuku, M. Tsuji, M. Morimoto, H. Saimoto, and H. Yano, *Synthesis of silver nanoparticles templated by TEMPO-mediated oxidized bacterial cellulose nanofibers.* Biomacromolecules, 2009. **10**(9): p. 2714-2717.
61. A.M. Ferraria, S. Boufi, N. Battaglini, A.M. Botelho Do Rego, and M. Reivilar, *Hybrid systems of silver nanoparticles generated on cellulose surfaces.* Langmuir, 2010. **26**(3): p. 1996-2001.
62. C. Chen and C. Chiang, *Preparation of cotton fibers with antibacterial silver nanoparticles.* Materials Letters, 2008. **62**(21-22): p. 3607-3609.

63. N.D. Luong, Y. Lee, and J.-D. Nam, *Highly-loaded silver nanoparticles in ultrafine cellulose acetate nanofibrillar aerogel.* Eur. Polym. J., 2008. **44**(10): p. 3116-3121.
64. W.K. Son, J.H. Youk, and W.H. Park, *Antimicrobial cellulose acetate nanofibers containing silver nanoparticles.* Carb Polym, 2006. **65**: p. 430-434.
65. N.L. Lala, R. Ramaseshan, L. Bojun, S. Sundarrajan, R.S. Barhate, L. Ying-Jun, and S. Ramakrishna, *Fabrication of nanofibers with antimicrobial functionality used as filters: Protection against bacterial contaminants.* Biotechnol Bioeng, 2007. **97**(6): p. 1357-1365.
66. R. Gottesman, S. Shukla, N. Perkas, L.A. Solovyov, Y. Nitzan, and A. Gedanken, *Sonochemical coating of paper by microbiocidal silver nanoparticles.* Langmuir, 2011. **27**(2): p. 720-726.
67. A.R. Silva and G. Unali, *Controlled silver delivery by silver-cellulose nanocomposites prepared by a one-pot green synthesis assisted by microwaves.* Nanotechnology, 2011. **22**(31): p. 315605.
68. S.-M. Li, N. Jia, J.-F. Zhu, M.-G. Ma, F. Xu, B. Wang, and R.-C. Sun, *Rapid microwave-assisted preparation and characterization of cellulose silver nanocomposites.* Carbohydrate Polymers, 2011. **83**(2): p. 422-429.
69. S.-M. Li, N. Jia, M.-G. Ma, Z. Zhang, Q.-H. Liu, and R.-C. Sun, *Cellulose silver nanocomposites: Microwave-assisted synthesis, characterization, their thermal stability, and antimicrobial property.* Carbohydrate Polymers, 2011. **86**(2): p. 441-447.
70. T.A. Dankovich and D.G. Gray, *Contact angle measurements on smooth nanocrystalline cellulose (I) thin films.* J Adhes Sci Technol, 2011. **25**(6): p. 699-708.
71. U.S. Environmental Protection Agency: Office Of Water, *National interim primary drinking water regulations*. 1977, Washington, D.C.: US EPA. 59566-59589.
72. J. Buffle and R.R. De Vitre, *Chemical and biological regulation of aquatic systems*. 1994, Boca Raton, Florida: CRC Press.
73. F.J. Stevenson, *Humus chemistry: genesis, composition, reactions.*, 1982, New York: Wiley.

74. G. Tchobanoglous, *Water quality: characteristics, modeling, modification*. 1985, Reading, Mass.: Addison-Wesley.
75. U.S. Environmental Protection Agency: Office of Pesticide Programs, ed. *Guide standard and protocol for testing microbiological water purifiers*. 1987, US EPA: Washington, D.C.
76. U.S. Public Health Service, *Report for agency for toxic substances and disease registry*, 1990: Atlanta, Georgia.
77. L.S. Clesceri, A.E. Greenberg, and A.D. Eaton, eds. *Standard methods for the examination of water and wastewater*. 20th ed., American Water Works Association, Water Pollution Control Federation, Water Environment Federation, 1998, American Public Health Association: Washington, D.C.
78. N.J. Ashbolt, W.O.K. Grabow, and M. Snozzi, *Indicators of microbial water quality*, in *Water quality: Guidelines, standards and health*, World Health Organization, 2001, WHO: Geneva, Switzerland. p. 289-316.
79. Live/Dead®. Available from: http://www.invitrogen.com/site/us/en/home/brands/Molecular-Probes/Key-Molecular-Probes-Products/LIVE-DEAD-Viability-Brand-Page.html.
80. World Health Organization, ed. *Guidelines for drinking-water quality*. 2006. 137.
81. T. Clasen, S. Nadakatti, and S. Menon, *Microbiological performance of a water treatment unit designed for household use in developing countries.* Trop Med Int Health, 2006. **11**(9): p. 1399-405.
82. M.D. Sobsey, C.E. Stauber, L.M. Casanova, J.M. Brown, and M.A. Elliott, *Point of use household drinking water filtration: A practical, effective solution for providing sustained access to safe drinking water in the developing world.* Environ Sci Technol, 2008. **42**(12): p. 4261-4267.
83. World Health Organization and Engineering and Development Center Water, *Technical notes on drinking-water, sanitation, and hygiene in emergencies: How much water is needed in emergencies.* 2011: p. 1-4.
84. G. Sykes, *Disinfection and sterilization: Theory and practice*. Spon's General and Industrial Chemistry Series, 1958, London: E. & F.N. Spon.

85. P. Jain and T. Pradeep, *Potential of silver nanoparticle-coated polyurethane foam as an antibacterial water filter.* Biotechnol Bioeng, 2005. **90**(1): p. 59-63.
86. E.N. Kallman, V.A. Oyanedel-Craver, and J.A. Smith, *Ceramic filters impregnated with silver nanoparticles for point-of-use water treatment in rural Guatemala.* J Environ Eng-Asce, 2011. **137**(6): p. 407-415.
87. V.A. Oyanedel-Craver and J.A. Smith, *Sustainable colloidal-silver-impregnated ceramic filter for point-of-use water treatment.* Environ Sci Technol, 2008. **42**(3): p. 927-933.
88. D.T. Schoen, A.P. Schoen, L. Hu, H.S. Kim, S.C. Heilshorn, and Y. Cui, *High speed water sterilization using one-dimensional nanostructures.* Nano Lett., 2010. **10**(9): p. 3628-3632.
89. L. Dicks, M. Botes, D. Du Plessis, E. Cloete, M. De Kwaadstenient, and N. Dlamini. *Water filter assembly and filter element.* 2011. WO/2011/107847. World Intellectual Property Organization.
90. R. Bandyopadhyaya, M. Sivaiah, and P. Shankar, *Silver-embedded granular activated carbon as an antibacterial medium for water purification.* J. Chem. Technol. Biotechnol., 2008. **83**(8): p. 1177-1180.
91. Q. Chang, H. He, and Z. Ma, *Efficient disinfection of Escherichia coli in water by silver loaded alumina.* Journal of Inorganic Biochemistry, 2008. **102**(9): p. 1736-1742.
92. D.S. Lantagne, *Investigation of the Potters for Peace colloidal silver-impregnated ceramic filter: Intrinsic effectiveness and field performance in rural Nicaragua.* Report prepared for USAID, Washington, DC, 2001.
93. D.S. Lantagne, M. Klarman, A. Mayer, K. Preston, J. Napotnik, and K. Jellison, *Effect of production variables on microbiological removal in locally-produced ceramic filters for household water treatment.* Int J Environ Health Res, 2010. **20**(3): p. 171-187.
94. W. Chou, D. Yu, and M. Yang, *The preparation and characterization of silver-loading cellulose acetate hollow fiber membrane for water treatment.* Polymers for Advanced Technologies, 2005. **16**(8): p. 600-607.

95. K. Zodrow, L. Brunet, S. Mahendra, D. Li, A. Zhang, Q. Li, and P.J.J. Alvarez, *Polysulfone ultrafiltration membranes impregnated with silver nanoparticles show improved biofouling resistance and virus removal.* Water Research, 2009. **43**(3): p. 715-723.
96. K.Y. Yoon, J.H. Byeon, C.W. Park, and J. Hwang, *Antimicrobial effect of silver particles on bacterial contamination of activated carbon fibers.* Environ Sci Technol, 2008. **42**(4): p. 1251-1255.
97. B. De Gusseme, L. Sintubin, L. Baert, E. Thibo, T. Hennebel, G. Vermeulen, M. Uyttendaele, W. Verstraete, and N. Boon, *Biogenic silver for disinfection of water contaminated with viruses.* Applied and Environmental Microbiology, 2010. **76**(4): p. 1082-1087.
98. F. Diagne, R. Malaisamy, V. Boddie, R.D. Holbrook, B. Eribo, and K.L. Jones, *Polyelectrolyte and silver nanoparticle modification of microfiltration membranes to mitigate organic and bacterial fouling.* Environ Sci Technol, 2012, **46**(7): p. 4025–4033.
99. T.F. Clasen, J. Brown, S. Collin, O. Suntura, and S. Cairncross, *Reducing diarrhea through the use of household-based ceramic water filters: a randomized, controlled trial in rural Bolivia.* The American Journal of Tropical Medicine and Hygiene, 2004. **70**(6): p. 651.
100. T. Benn, B. Cavanagh, K. Hristovski, J. Psoner, and P. Westerhoff, *Release of nanosilver from consumer products used in the home.* Journal of Environmental Quality, 2010. **39**(6): p. 1875-1882.
101. T. Benn and P. Westerhoff, *Nanoparticle silver released into water from commercially available sock fabrics.* Environ Sci Technol, 2008. **42**(11): p. 4133-4139.
102. L. Geranio, M. Heuberger, and B. Nowack, *The behavior of silver nanotextiles during washing.* Environ Sci Technol, 2009. **43**(17): p. 6458-6462.
103. C.A. Impellitteri, T.M. Tolaymat, and K.G. Scheckel, *The speciation of silver nanoparticles in antimicrobial fabric before and after exposure to a hypochlorite/ detergent solution.* Journal of Environment Quality, 2009. **38**(4): p. 1528.

104. S.N. Luoma, *Silver Nanotechnologies and the environment: old problems or new challenges?* 2008: p. 72.
105. N. Kumar, V. Shah, and V.K. Walker, *Perturbation of an arctic soil microbial community by metal nanoparticles.* Journal of Hazardous Materials, 2011. **190**(1-3): p. 816-822.
106. R. Kaegi, B. Sinnet, S. Zuleeg, H. Hagendorfer, E. Mueller, R. Vonbank, M. Boller, and M. Burkhardt, *Release of silver nanoparticles from outdoor facades.* Environmental Pollution, 2010. **158**(9): p. 2900-2905.
107. R.C. Murdock, L. Braydich-Stolle, A.M. Schrand, J.J. Schlager, and S.M. Hussain, *Characterization of nanomaterial dispersion in solution prior to in vitro exposure using dynamic light scattering technique.* Toxicological Sciences, 2008. **101**(2): p. 239-253.
108. X. Jin, M. Li, J. Wang, C. Marambio-Jones, F. Oeng, X. Huang, R. Damoiseaux, and E.M.V. Hoek, *High-throughput screening of silver nanoparticle stability and bacterial inactivation in aquatic media: Influence of specific ions.* Environ Sci Technol, 2010. **44**(19): p. 7321–7328.
109. A.M. El Badawy, T.P. Luxton, R.G. Silva, K.G. Scheckel, M.T. Suidan, and T.M. Tolaymat, *Impact of environmental conditions (pH, ionic strength, and electrolyte type) on the surface charge and aggregation of silver nanoparticles suspensions.* Environ Sci Technol, 2010. **44**(4): p. 1260-1266.
110. J.M. Zook, R.I. Maccuspie, L.E. Locascio, M.D. Halter, and J.T. Elliott, *Stable nanoparticle aggregates/agglomerates of different sizes and the effect of their size on hemolytic cytotoxicity.* Nanotoxicology, 2011. **5**(4): p. 517-530.
111. S. Kittler, C. Greulich, J.S. Gebauer, J. Diendorf, L. Treuel, L. Ruiz, J.M. Gonzalez-Calbet, M. Vallet-Regi, R. Zellner, M. Köller, and M. Epple, *The influence of proteins on the dispersability and cell-biological activity of silver nanoparticles.* J. Mater. Chem., 2010. **20**(3): p. 512.
112. R.I. MacCuspie, *Colloidal stability of silver nanoparticles in biologically relevant conditions.* Journal of Nanoparticle Research, 2011. **13**(7): p. 2893-2908.
113. R.I. MacCuspie, K. Rogers, M. Patra, Z. Suo, A.J. Allen, M.N. Martin, and V.A. Hackley, *Challenges for physical characterization of silver nanoparticles under*

pristine and environmentally relevant conditions. J. Environ. Monit., 2011. **13**(5): p. 1212.

114. J. Fabrega, S.R. Fawcett, J.C. Renshaw, and J.R. Lead, *Silver nanoparticle impact on bacterial growth: Effect of pH, concentration, and organic matter.* Environ Sci Technol, 2009. **43**(19): p. 7285-7290.
115. J. Liu and R.H. Hurt, *Ion release kinetics and particle persistence in aqueous nano-silver colloids.* Environ Sci Technol, 2010. **44**(6): p. 2169-2175.
116. J. Fabrega, S.N. Luoma, C.R. Tyler, T.S. Galloway, and J.R. Lead, *Silver nanoparticles: Behaviour and effects in the aquatic environment.* Environment International, 2011. **37**(2): p. 517-531.
117. R. Eisler and U.S. National Biological Service, *Silver hazards to fish, wildlife, and invertebrates: A synoptic review.* 1996: U.S. Dept. of the Interior, National Biological Service.
118. Y. Tian, B. Gao, C. Silvera-Batista, and K.J. Ziegler, *Transport of engineered nanoparticles in saturated porous media.* Journal of Nanoparticle Research, 2010. **12**(7): p. 2371-2380.
119. B. Kim, C.-S. Park, M. Murayama, and M.F. Hochella, *Discovery and characterization of silver sulfide nanoparticles in final sewage sludge products.* Environ Sci Technol, 2010. **44**(19): p. 7509–7514
120. G. Laban, L.F. Nies, R.F. Turco, J.W. Bickham, and M.S. Sepúlveda, *The effects of silver nanoparticles on fathead minnow (Pimephales promelas) embryos.* Ecotoxicology, 2010. **19**(1): p. 185-195.
121. K.J. Lee, P.D. Nallathamby, L.M. Browning, C.J. Osgood, and X.-H.N. Xu, *In vivo imaging of transport and biocompatibility of single silver nanoparticles in early development of zebrafish embryos.* ACS Nano, 2007. **1**(2): p. 133-143.
122. R. Owen and R. Handy, *Formulating the problems for environmental risk assessment of nanomaterials.* Environ Sci Technol, 2007. **41**(16): p. 5582-5588.
123. U.S. Environmental Protection Agency: Office of Health and Environmental Assessment. *Silver (CASRN 7440-22-4)*. cited 2011 November 18. Available from: http://www.epa.gov/iris/subst/0099.htm.

124. P. Drake and K. Hazelwood, *Exposure-related health effects of silver and silver compounds: A review.* Annals of Occupational Hygiene, 2005. **49**(7): p. 575-585.
125. N. Tomi, B. Kranke, and W. Aberer, *A silver man.* Lancet, 2004. **363**(9408): p. 532-532.
126. L. Braydich-Stolle, S. Hussain, J. Schlager, and M. Hofmann, *In vitro cytotoxicity of nanoparticles in mammalian germline stem cells.* Toxicological Sciences, 2005. **88**(2): p. 412-419.
127. S. Arora, J. Jain, J. Rajwade, and K. Paknikar, *Cellular responses induced by silver nanoparticles: In vitro studies.* Toxicology letters, 2008. **179**(2): p. 93-100.
128. N. Ayala-Núñez, H. Lara Villegas, L. Carmen Ixtepan Turrent, and C. Rodríguez Padilla, *Silver nanoparticles toxicity and bactericidal effect against methicillin-resistant Staphylococcus aureus: Nanoscale does matter.* Nanobiotechnol, 2009. **5**(1-4): p. 2-9.
129. A. Burd, C.H. Kwok, S.C. Hung, H.S. Chan, H. Gu, W.K. Lam, and L. Huang, *A comparative study of the cytotoxicity of silver-based dressings in monolayer cell, tissue explant, and animal models.* Wound Repair Regen, 2007. **15**(1): p. 94-104.
130. W. Lu, D. Senapati, S. Wang, O. Tovmachenko, A.K. Singh, H. Yu, and P.C. Ray, *Effect of surface coating on the toxicity of silver nanomaterials on human skin keratinocytes.* Chemical Physics Letters, 2010. **487**(1-3): p. 92-96.
131. J. Tian, K.K.Y. Wong, C.-M. Ho, C.-N. Lok, W.-Y. Yu, C.-M. Che, J.-F. Chiu, and P.K.H. Tam, *Topical delivery of silver nanoparticles promotes wound healing.* ChemMedChem, 2007. **2**(1): p. 129-136.
132. U.S. Environmental Protection Agency, *National secondary drinking water regulations*, 2002: Washington, DC.
133. World Health Organization, ed. *Guidelines for drinking-water quality, Fourth Edition*. 2011. 415.
134. U.S. Environmental Protection Agency: Office Of Water, ed. *National recommended water quality criteria*. 2009. 1-22.
135. J. Han, L. Chen, S.M. Duan, Q.X. Yang, M. Yang, C. Gao, B.Y. Zhang, H. He, and X.P. Dong, *Efficient and quick inactivation of SARS coronavirus and other*

microbes exposed to the surfaces of some metal catalysts. Biomed Environ Sci, 2005. **18**(3): p. 176-180.

136. L. Yang, X. Ning, Q. Xiao, K. Chen, and H. Zhou, *Development and characterization of porous silver-incorporated hydroxyapatite ceramic for separation and elimination of microorganisms.* J. Biomed. Mater. Res., 2007. **81B**(1): p. 50-56.
137. J. Elechiguerra, J.L. Burt, J.R. Morones, A. Camacho-Bragado, X. Gao, H.H. Lara, and M.J. Yacaman, *Interaction of silver nanoparticles with HIV-1.* J Nanobiotechnol, 2005. **3**: p. 6.
138. U. Rohr, S. Weber, F. Selenka, and M. Wilhelm, *Impact of silver and copper on the survival of amoebae and ciliated protozoa in vitro.* Int J Environ Health Res, 2000. **203**(1): p. 87-89.
139. J.M. Cassells, M.T. Yahya, C.P. Gerba, and J.B. Rose, *Efficacy of a combined system of copper and silver and free chlorine for inactivation of Naegleria fowleri amoebas in water.* Water Science and Technology, 1995. **31**(5-6): p. 119-122.
140. H. Le Pape, F. Solano-Serena, P. Contini, C. Devillers, A. Maftah, and P. Leprat, *Evaluation of the anti-microbial properties of an activated carbon fibre supporting silver using a dynamic method.* Carbon, 2002. **40**(15): p. 2947-2954.
141. S. Loher, O.D. Schneider, T. Maienfisch, S. Bokorny, and W.J. Stark, *Micro−organism−triggered release of silver nanoparticles from biodegradable oxide carriers allows preparation of self−sterilizing polymer surfaces.* Small, 2008. **4**(6): p. 824-832.
142. W.-F. Lee and Y.-C. Huang, *Swelling and antibacterial properties for the superabsorbent hydrogels containing silver nanoparticles.* J. Appl. Polym. Sci., 2007. **106**(3): p. 1992-1999.
143. P. Dibrov, J. Dzioba, K.K. Gosink, and C.C. Hase, *Chemiosmotic mechanism of antimicrobial activity of Ag^+ in Vibrio cholerae.* Antimicrob Agents Ch, 2002. **46**(8): p. 2668-2670.

144. M. Hotta, H. Nakajima, K. Yamamoto, and M. Aono, *Antibacterial temporary filling materials: The effect of adding various ratios of Ag-Zn-zeolite.* J Oral Rehabil, 1998. **25**(7): p. 485-9.

145. V. Zaporojtchenko, R. Podschun, U. Schuermann, A. Kulkarni, and F. Faupel, *Physico-chemical and antimicrobial properties of co-sputtered Ag-Au/PTFE nanocomposite coatings.* Nanotechnology, 2006. **17**(19): p. 4904-4908.

146. P. Gong, H. Li, X. He, K. Wang, J. Hu, W. Tan, S. Zhang, and X. Yang, *Preparation and antibacterial activity of Fe_3O_4@Ag nanoparticles.* Nanotechnology, 2007. **18**(28).

147. V. Sambhy, M. Macbride, B. Peterson, and A. Sen, *Silver bromide nanoparticle/ polymer composites: Dual action tunable antimicrobial materials.* Journal of the American Chemical Society, 2006. **128**(30): p. 9798-9808.

148. L. Kvitek, A. Panacek, J. Soukupova, M. Kolar, R. Vecerova, R. Prucek, M. Holecova, and R. Zboril, *Effect of surfactants and polymers on stability and antibacterial activity of silver nanoparticles (NPs).* J Phys Chem C, 2008. **112**(15): p. 5825-5834.

149. O. Eksik, A. Erciyes, and Y. Yagci, *In situ synthesis of oil based polymer composites containing silver nanoparticles.* Journal of Macromolecular Science Part A-Pure and Applied Chemistry, 2008. **45**(9): p. 698-704.

150. J. Ruparelia, A. Chatterjee, S. Duttagupta, and S. Mukherji, *Strain specificity in antimicrobial activity of silver and copper nanoparticles.* Acta Biomaterialia, 2008. **4**(3): p. 707-716.

151. S. Shrivastava, T. Bera, A. Roy, G. Singh, P. Ramachandrarao, and D. Dash, *Characterization of enhanced antibacterial effects of novel silver nanoparticles.* Nanotechnology, 2007. **18**(22): p. 225103.

152. N. Vigneshwaran, A. Kathe, P. Varadarajan, R. Nachane, and R. Balasubramanya, *Silver-protein (core-shell) nanoparticle production using spent mushroom substrate.* Langmuir, 2007. **23**(13): p. 7113-7117.

153. D. Han, M. Lee, M. Lee, M. Uzawa, and J. Park, *The use of silver-coated ceramic beads for sterilization of Sphingomonas sp in drinking mineral water.* World J Microbiol Biotechnol, 2005. **21**(6-7): p. 921-924.

154. L. Zhang, J. Yu, H. Yip, Q. Li, K. Kwong, A. Xu, and P. Wong, *Ambient light reduction strategy to synthesize silver nanoparticles and silver-coated TiO_2 with enhanced photocatalytic and bactericidal activities.* Langmuir, 2003. **19**(24): p. 10372-10380.

155. H. Jiang, S. Manolache, A.C.L. Wong, and F.S. Denes, *Plasma-enhanced deposition of silver nanoparticles onto polymer and metal surfaces for the generation of antimicrobial characteristics.* J. Appl. Polym. Sci., 2004. **93**(3): p. 1411-1422.

156. H. Le Pape, F. Solano-Serena, P. Contini, C. Devillers, A. Maftah, and P. Leprat, *Involvement of reactive oxygen species in the bactericidal activity of activated carbon fibre supporting silver bactericidal activity of ACF(Ag) mediated by ROS.* Journal of Inorganic Biochemistry, 2004. **98**(6): p. 1054-1060.

157. B. Galeano, E. Korff, and W.L. Nicholson, *Inactivation of vegetative cells, but not spores, of Bacillus anthracis, B. cereus, and B. subtilis on stainless steel surfaces coated with an antimicrobial silver- and zinc-containing zeolite formulation.* Applied and Environmental Microbiology, 2003. **69**(7): p. 4329-4331.

Chapter 2

Bactericidal paper impregnated with silver nanoparticles for point-of-use water treatment

This chapter demonstrates the synthesis of blotter papers containing silver nanoparticles and examines the bactericidal effects in a model filter setup. This basic knowledge is elaborated on in the subsequent chapters of this thesis. The work has been published, and is reproduced with permission from:

Dankovich, T.A.; Gray, D.G. *Environmental Science and Technology,* **2011**, 45(5), 1992-1998.

2.1 Abstract

There is an urgent need for cheap point-of-use methods to purify drinking water. We describe a method to deactivate pathogenic bacteria by percolation through a paper sheet containing silver nanoparticles. The silver nanoparticles are deposited by the in-situ reduction of silver nitrate on the cellulose fibers of an absorbent blotting paper sheet. The aim is to achieve inactivation of bacteria during percolation through the sheet, rather than removal of bacteria from the effluent by filtration (Figure 2.1). The silver-nanoparticle containing (AgNP) papers were tested for performance in the laboratory with respect to bacteria inactivation and silver leaching as suspensions of bacteria percolated through the paper. The AgNP sheets exhibited antibacterial properties towards suspensions of *Escherichia coli* and *Enterococcus faecalis*, with log reduction values in the effluent of over log 6 and log 3, respectively. The silver loss from the AgNP sheets was minimal, with values under 0.1 ppm (the current US EPA and WHO limit for silver in drinking water). These results show promise that percolation of bacterially contaminated water through paper embedded with silver nanoparticles could be an effective emergency water treatment.

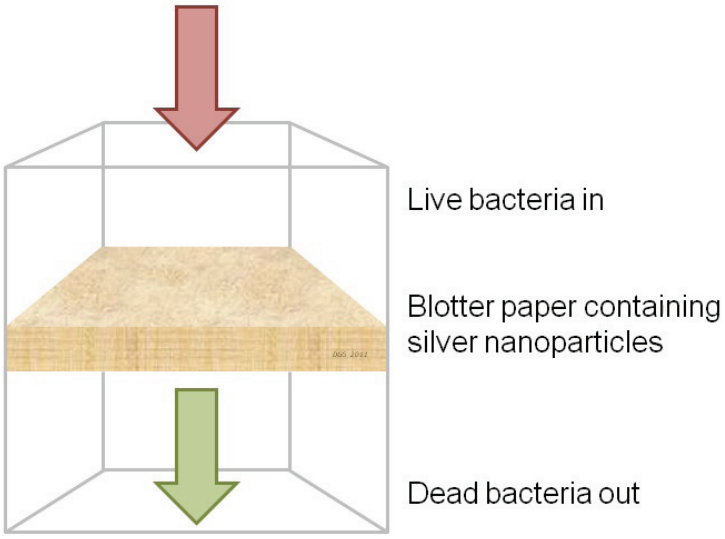

FIGURE 2.1. Schematic of bacteria percolation and inactivation through the silver nanoparticle paper.

2.2 Introduction

At least one billion people worldwide do not have access to clean, potable water sources, according to the WHO [1]. The greatest water-borne threat to human health is bacterial contamination of drinking water sources, leading to outbreaks of diseases such as giardiasis, cholera, cryptosporidiosis, gastroenteritis, etc. [2]. Recently, considerable interest has arisen in the use of nanotechnology for water purification [3]. In particular, functional nanomaterials can be used for small-scale or point-of-use systems for water systems that are not connected to a central network and for emergency response following disasters. Such systems should be cheap, highly portable, nontoxic, easy to use and distribute, and require low energy input.

Our approach uses silver nanoparticles embedded in blotter papers to purify drinking water contaminated with pathogenic bacteria. Silver nanoparticles have been incorporated into a range of cellulosic materials, such as bacterial cellulose, filter paper, cotton fabric and cellulose gels [4-10]. Silver and some other metals have been used for centuries to store potable water, and the antibacterial properties of trace quantities of

these metal are well-known [11]. The surface area of AgNPs is much greater than the bulk metal, and is more bio-active as a result [12]. Silver nanoparticles have been used previously in water filtration applications, generally to prevent bacterial fouling of membrane filters [13-15]. Point-of-use filtration applications include nanosilver in polyurethane foams [16] and ceramic filters [17].

As a bactericide, we use silver nanoparticles produced by in situ reduction of silver nitrate solution in the sheet. To test for the bactericidal effectiveness of the AgNP papers, we passed model bacterial suspensions through an AgNP paper sheet, and analyzed the effluent water for viable bacteria. In our case, we use relatively thick (0.5 mm) sheets of an absorbent porous blotter paper. The porosity of the base paper allows microorganisms to come into contact with the biocide, but attachment to the fiber surfaces limits the levels of silver in the effluent water. The primary purification mechanism is not the removal of bacteria from the effluent by filtration, but rather the deactivation of bacteria as they percolate through the AgNP paper structure. Consequently, the filter effluent contains dead bacteria. The large pore size in the filter paper allows for reasonably rapid flow by gravity, without the need for pressure or suction. As far as we know, this is the first attempt to prepare and test AgNP paper as a point-of-use water purifier.

2.3 Materials and methods

2.3.1 Materials

We used absorbent blotting papers made from bleached softwood kraft pulp. The blotters (made by Domtar Inc. and kindly supplied by FP Innovations, Pointe-Claire, QC) are used for drying laboratory handsheets during pulp testing. The sheet thickness and grammage for the blotting paper sheets are 0.5 mm and 250 g/m^2, respectively, and the sheets are free from sizing agents, fluorescent agents and chemical additives.

Silver nitrate ($AgNO_3$), sodium borohydride ($NaBH_4$), 30% hydrogen peroxide (H_2O_2), concentrated nitric acid (HNO_3), poly(L-lysine (0.01% solution), trisodium citrate ($Na_3C_6H_5O_7$), and ethanol were purchased from Sigma Aldrich and used as received. Nutrient broth components (Luria Bertani, Lauryl sulfate, BBL Brain Heart Infusion) and Endo and Difco mE agars were from the same source. Water treated with a Barnstead Nanopure system was used throughout.

2.3.2 Preparation of silver nanoparticle (AgNP) paper

We immersed blotting paper sheets (6.5 cm by 6.5 cm) in 20 mL of silver nitrate solutions at concentrations from 0 to 100 mM for 30 minutes. We removed the sheets from the silver nitrate solution and rinsed them with ethanol to remove excess silver nitrate that was not adsorbed to the cellulose surface. To form AgNPs, the paper was then placed in aqueous $NaBH_4$ solutions (ranging from 1:1 to 10:1 molar ratio, $NaBH_4$: $AgNO_3$) for 15 minutes. Following this, the paper was soaked in water for 60 minutes, and the excess water was removed by drying the sheet in an oven at 60°C for 2-3 hours. (This approach was based on methods reported in references [5] and [7]). For some experiments, the blotting paper was soaked overnight in a concentrated AgNP suspension, which was prepared separately. The concentrated AgNP suspension was a mixture of 0.95 mM trisodium citrate, 0.23 mM silver nitrate, and 0.23 mM sodium borohydride.

2.3.3 Characterization

The presence of AgNPs in the blotting paper was established by measuring the reflectance spectra of the AgNP papers with a diffuse reflectance attachment (Labosphere, DRA-CA-30) on a UV-Vis spectrophotometer (Varian TCA-Cary 300) at wavelengths of 300 to 800 nm. The reflectance was measured relative to a poly(tetrafluoroethylene) powder standard. Silver nanoparticles have a characteristic

surface plasmon resonance peak around 400 nm [18]. The shape and distribution of the silver nanoparticles in the sheet were examined by electron microscopy. Individual paper fibers containing silver nanoparticles were deposited on carbon coated copper grids that had been treated with poly(L-lysine), and imaged with a Philips CM200 200 kV transmission electron microscope (TEM). Nanoparticle diameters were measured for greater than 100 particles per sample, with standard deviation values reported. Imaging and analysis of the AgNP paper was performed with a field emission scanning electron microscopy (Hitachi S-4700 FE-SEM) attached to an energy-dispersive X-ray spectroscopy detector (EDX).

To quantify the amount of silver in the AgNP papers, we performed an acid digestion of the paper and analysed the amount of dissolved silver with an inductively coupled plasma atomic emission spectrometer (ICP-AES). Briefly, approximately 100 mg of dried paper was reacted with 5 mL 70% nitric acid in 5 mL water, then boiled until the paper disintegrated. After a few minutes of cooling, ~5 mL of hydrogen peroxide (30%) was added and the suspension was re-boiled. After cooling, the suspension was filtered through a glass paper filter and the effluent was diluted to 100 mL with water. The silver content of the effluent was measured with ICP-AES (Iris, Thermo Jarrell Ash), with ten replicates per sample, and standard deviations were reported.

2.3.4 Bactericidal testing

The bactericidal activity of the AgNP paper was tested against a nonpathogenic strain of *Escherichia coli* (ATCC #11229), a Gram-negative bacteria, and against *Enterococci faecalis* (ATCC #47077), a Gram-positive bacteria. We chose these organisms because of their roles as indicators for fecal contamination in drinking water. As controls, we tested an untreated paper sheet and a paper sheet soaked with a 20 mL solution of 5 mM silver nitrate, but left unreduced, to contain silver ions instead of silver nanoparticles. To prepare bacterial cultures, we added bacteria to 100 mL of an

autoclaved nutrient broth and agitated the suspension on a shaker water bath (Polyscience) at 37°C overnight at 160 rpm. Bacteria were harvested during the mid-exponential period, where the absorbance of the culture was approximately 1.0, measured at a wavelength of 600 nm by UV-Vis spectrophotometry. The bacteria were separated from the nutrient broth by centrifuging for 10 minutes at 3100 rpm (relative centrifugal force (RCF) of 1228 x g), and then resuspended in water and diluted to an initial absorption value of approximately 0.1, which corresponded to approximately 10^8 colony-forming units (CFU)/mL. This suspension (100 mL), a model for contaminated water, was passed through a sheet of AgNP paper, which was laid flat on a large, plastic grid with vertical walls to support the uniform 1-D flow. The effluent water was tested for live bacteria by two different methods, as follows. The effluent bacteria were removed from the effluent water by centrifugation, at the same conditions as earlier detailed, which separated the excess silver leachate in the effluent water from the bacteria. The effluent bacteria were re-grown with fresh nutrient broth and bacteria suspensions were analyzed for absorption values once every hour for 4 hours to qualitatively monitor growth kinetics. Additionally, the effluent bacteria were plated on nutrient agar plates (endo and mE for *E. coli* and *E. faecalis*, respectively). The nutrient agar plates were incubated overnight at 37°C for 24 hours and the colonies were counted. Ten replicates were performed per paper. Standard deviation values were reported.

2.3.5 Analysis for silver in effluent

The effluent after passing through the AgNP paper was analyzed for silver content by graphite furnace atomic absorption spectrometry (GF-AA, Perkin Elmer AAnalyst 100). The effluent was centrifuged for 10 minutes at 3100 rpm with a RCF of 1228 x g, to separate the bacteria from the supernatant. Both the supernatant and bacterial pellet were analyzed for silver. The bacterial pellet was digested by heating in

2 mL of nitric acid (70%) at 40-50°C for 30 minutes, allowing to cool, and heating with an additional 1 mL of hydrogen peroxide (30%) at 30°C for 30 minutes. The solution from the bacteria digestion was diluted with water, and analyzed by GF-AA. Ten replicates were performed per paper, and the standard deviations were reported.

The silver loss from the AgNP papers in 100 mL effluent was determined from the GF-AA values for silver concentration in the effluent water. This value was expressed as a percentage of the total silver mass contained in the papers, as determined by ICP-AES measurements.

2.3.6 Observations of bacteria morphology

Samples of bacteria were imaged by TEM (FEI Tecnai 12 120 kV TEM) before and after percolation through the AgNP paper. The samples were fixed in glutaraldehyde overnight, and were dehydrated with increasing ethanol/water mixtures to 100% ethanol. Following dehydration, the samples were cured with epoxy and sectioned with a ultramicrotome into 100 nm thick slices. The bacteria slices were deposited on carbon coated copper grids.

2.4 Results and discussion

2.4.1 Paper characterization

The silver nanoparticles were readily formed by the *in situ* reduction of silver nitrate solution absorbed in the blotting paper. An excess of sodium borohydride reductant (10:1 ratio of sodium borohydride to silver nitrate) gave more uniform and smaller nanoparticles, and resulted in deposition in the sheet rather than in the bath (8, 10). The sheets changed color from white to yellow or brown with increasing precursor silver ion concentrations; a sheet soaked in pre-formed silver nanoparticle suspensions displayed a gray color (Figure 2.2). These color changes are due to the surface

plasmon resonance of silver nanoparticles. UV-Vis reflectance spectroscopy (Figure 2.3) showed a peak at 419 nm, which falls at the long wavelength end of the characteristic surface plasmon resonance range (390-420 nm) for spherical silver nanoparticles [18]. The wider peak at 419 nm for the AgNPs from blotting paper also is indicative of a wider size distribution than for AgNPs formed in solution.

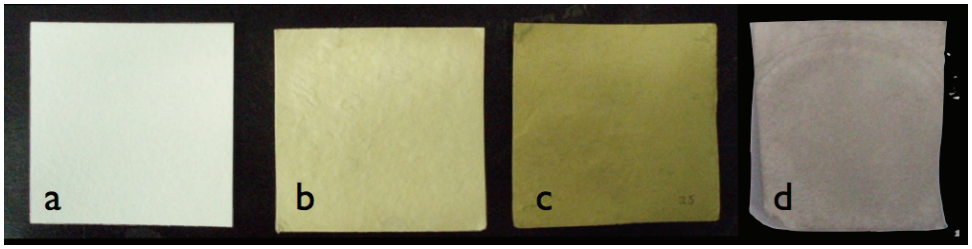

FIGURE 2.2. Blotter papers (a) untreated, and with silver nanoparticles (b) 0.2 mg Ag/ g paper. (c) 5.8 mg Ag/ g paper, and (d) sheet soaked in preformed nanoparticle suspension, 0.06 mg Ag/ g paper (each sheet is 6.5 x 6.5 cm).

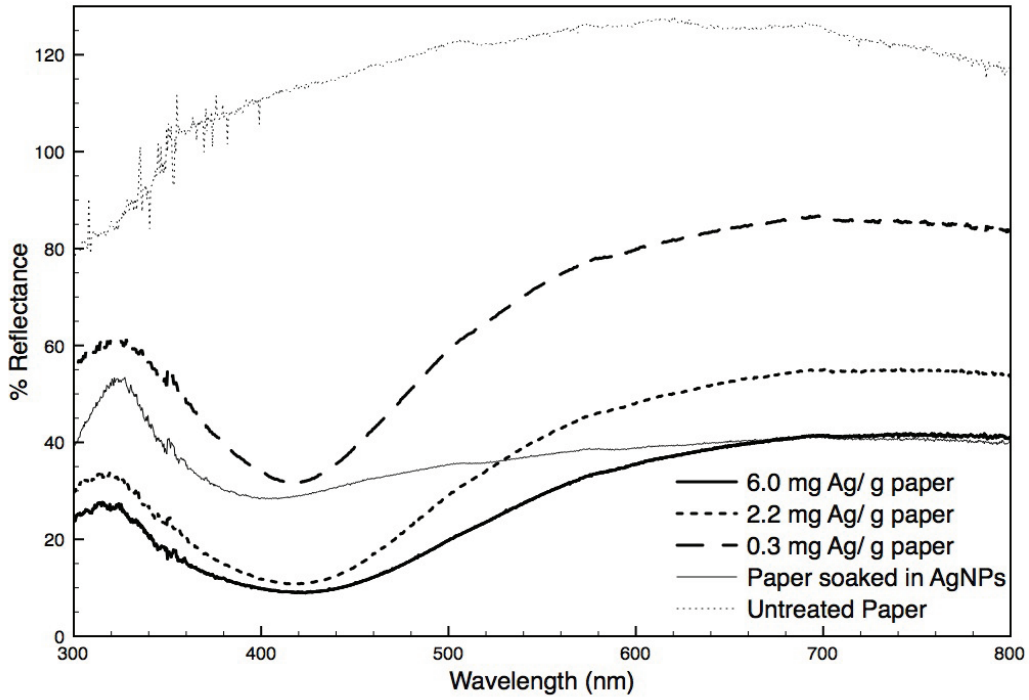

FIGURE 2.3. UV-Visible reflectance spectra of paper sheets with different silver nanoparticle contents.

Following the reduction of silver in the filter paper, the surface of the paper fibers was covered with spherical nanoparticles, as shown in Figure 2.4 and S2.1. In the TEM images, the paper fibers were left unstained, so only silver nanoparticles are visible. The TEM images showed nanoparticles with an average diameter of 7.1 nm and a standard deviation of 3.7 nm, which are typical sizes for silver nanoparticles prepared by borohydride reduction of silver salts [5, 7]. An EDX peak at 3 keV confirms the formation of silver nanoparticles in the filter papers (See supplementary data, Figure S2.1).

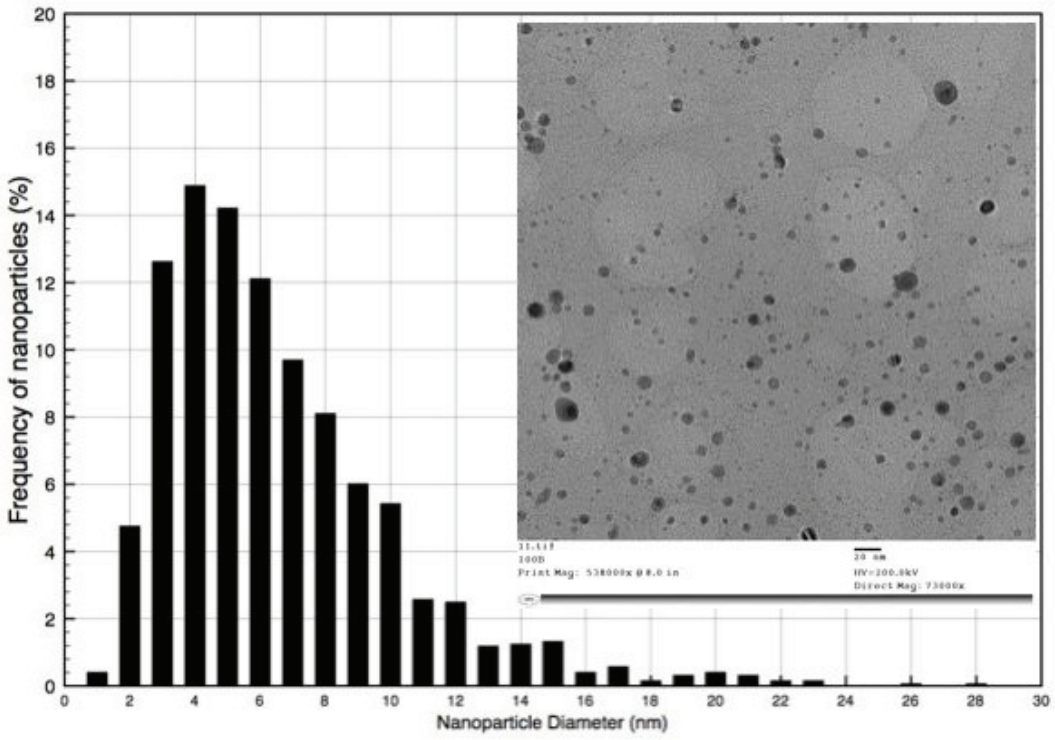

FIGURE 2.4. Histogram of distribution of silver nanoparticle diameters, as measured from TEM image (insert).

The acid digestion of the AgNP papers showed silver content ranging from 0.2 to 20.4 mg Ag per dry gram of paper. The increase in silver content of the paper correlates with the increase in precursor silver ion concentration of the solution in which the papers were soaked, prior to reduction (Table 2.1). The lowest silver content was observed in the papers that were soaked in the pre-formed nanosilver suspension. The size of the nanoparticles did not appear to correlate with the silver content of the paper; the borohydride reduction produced nanoparticles in the range 7.1 ± 3.7 nm for all samples. The AgNPs in the paper soaked in pre-formed nanoparticles did have a significantly larger diameter of 27.5 nm.

TABLE 2.1. Silver content in paper filters, measured by ICP-AES, and average nanoparticle diameters from TEM images, with increasing precursor silver ion concentration.

Precursor Ag^+ ion concentration (mM)	Silver Content (mg Ag/ dry g paper)	Nanoparticle diameter (nm)
1	0.26 ± 0.093	8.8 ± 4.8
5	1.39 ± 0.58	5.0 ± 2.6
10	2.21 ± 0.68	4.9 ± 1.9
25	5.97 ± 1.39	7.1 ± 3.5
50	17.20 ± 0.98	6.1 ± 2.4
100	26.50 ± 6.3	8.4 ± 2.9
Ag NP soaked	0.06 ± 0.045	27.5 ± 9.3
Overall (1-100mM)	- -	7.1 ± 3.7

In what follows, the different paper samples are characterized by their silver content as measured by acid digestion.

2.4.2 Bactericidal effectiveness of AgNP paper

The AgNP paper provided rapid and effective bactericidal activity as model *E. coli* bacteria suspensions were poured through the sheet. The average percolation time for 100 ml of bacteria suspension was 10 minutes. Some *E. coli* bacteria were retained in the filter, but most passed through and were isolated from the effluent by centrifugation and analyzed for viability. The qualitative re-growth experiments in LB broth showed inactivation of bacteria at the highest silver concentration (Figure 2.5). The positive control sample shows the beginning of the exponential growth curve, while the negative control sample shows no growth. The bacteria growth after percolation through the AgNP papers was almost completely deactivated for the paper with the highest silver content (5.9 mg Ag/dry g paper). The papers containing lower silver amounts also showed a reduction in growth compared with the positive control.

To further check the bactericidal effectiveness of AgNP paper, we added the isolated effluent bacteria, after passage through the paper, to nutrient agar plates. The plate count experiments showed log 7.6 (±1.3) and log 3.4 (±0.9) reductions of viable *E.*

coli and *E. faecalis* bacteria, respectively, in the effluent, as compared to the initial concentration of bacteria (10^9 CFU/mL) (Figure 2.6). The positive control also showed a reduction in bacteria by log 0.95 (±0.5), presumably due to some bacteria remaining on the fiber surfaces in the blotting paper. The paper prepared by soaking in preformed nanosilver suspensions did show a modest reduction in bacteria count, with a log reduction of 2.5 (±0.1) and log 2.0 (±0.1) for *E. coli* and *E. faecalis*, respectively, but clearly was less effective than the AgNP papers prepared by the *in situ* reduction method. This is due to the poor adherence of silver to cellulose, which was much lower than for nanoparticles formed *in situ*. The $AgNO_3$ paper showed the best bacterial reduction overall, with a log reduction of 8.7 (±0.1) for *E. coli* and 6.5 (±1.5) for *E. faecalis.*

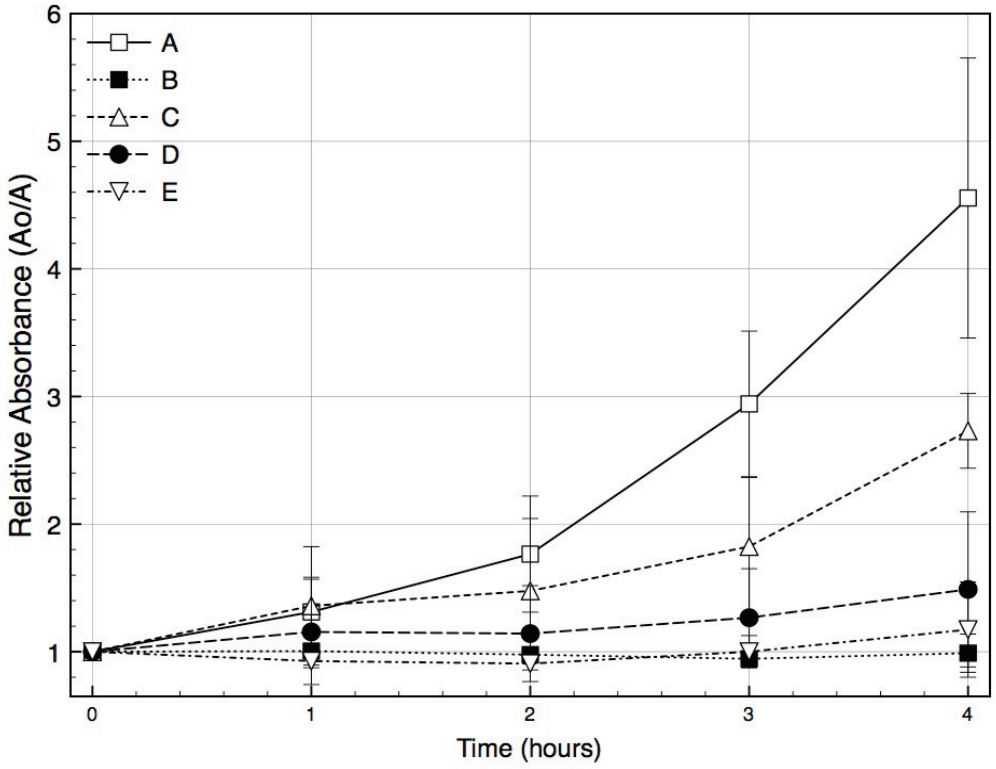

FIGURE 2.5. Relative absorbance of permeate at 600 nm during the first few hours of *E. coli* bacterial growth. (A) Positive Control (no silver in paper). (B) Negative Control (no bacteria added to permeate). (C) 1.6 mg Ag/g paper. (D) 2.3 mg Ag/g paper. (E) 5.7 mg Ag/g paper.

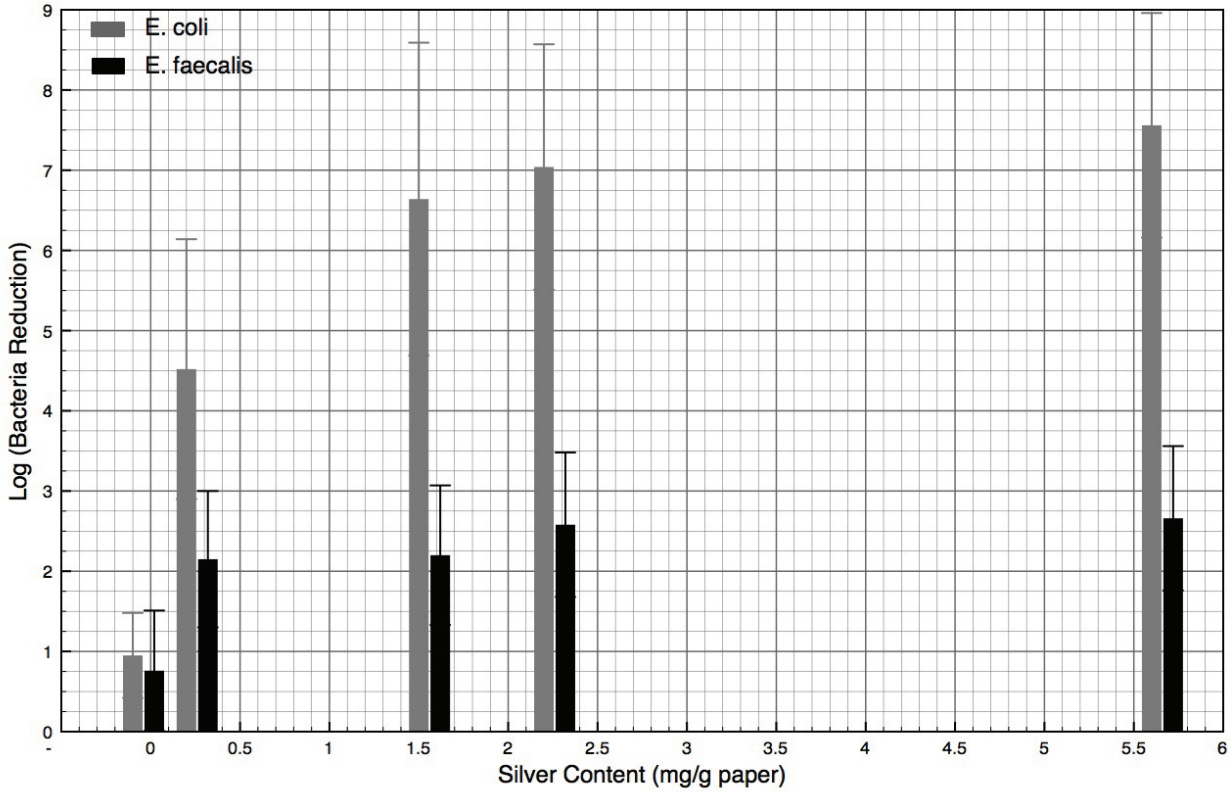

FIGURE 2.6. Log reduction of *E. coli* and *E. faecalis* bacterial count after permeation through the silver nanoparticle paper, at different silver contents in paper. Initial bacterial concentration, 10^9 CFU/mL (log 9). Error bars represent standard deviation.

The mode of bactericidal action in the AgNP sheets is unclear. In bacterial suspensions, the minimal inhibitory concentration (MIC) needed for silver nanoparticles to inactivate bacteria ranges from 5.4-108 ppm [22, 135, 136], where concentrations of bacteria on the order of 10^5 CFU/mL were incubated with various dilutions of silver nanoparticles. The MIC values were dependent upon the AgNP diameters, bacteria concentration, exposure time, and nutrient media. For a given bacterial system, silver nanoparticles with an average diameter of 62 nm gave a MIC of 108 ppm, whereas nanoparticles with an average diameter of 9.2 nm gave a much lower MIC value of 5.4 ppm. In comparison, silver ions have a MIC of 2-5 ppm [22]. In general, silver nanoparticles have been observed to have the largest antibacterial effects with the

smallest particle sizes, with average diameters under 10 nm being most effective. Assuming that the actual bactericidal action is due to silver ions in solution, the higher proportion of surface atoms in smaller particle sizes allows for a more effective release of silver ions from the nanoparticle surface [12, 23]. In the AgNP papers, the silver nanoparticles are not coated with a colloidal stabilizer, such as a polymer or ligand, which can passivate the surface and slow the oxidation and subsequent ion release rate [23].

To provide adequate exposure to silver nanoparticles during percolation, the density of nanoparticles may need to be above the MIC threshold value. The MIC literature is a useful guideline for AgNP paper requirements, but key differences between static and percolation conditions include nanoparticle size and distribution, exposure time to the silver nanoparticles, and the need to achieve an overall log reduction of bacterial activity beyond the MIC threshold. The average particle size in AgNP paper is comparable to that in some of the MIC experiments, but the effect of incorporation on the cellulose fiber surfaces is unclear. However, the MIC value of 15 ppm for 2.7 nm diameter silver nanoparticles embedded in cellulosic fibers was found to be similar to the MIC value for AgNPs in suspension [9]. In the percolation experiment, the exposure time to the embedded AgNPs is much shorter than in the MIC experiments. Typically, 100 mL of bacteria-contaminated water take an average of 10 minutes to percolate through the AgNP sheet, whereas the MIC experiments generally have an exposure time to the silver nanoparticle suspension of up to 24 hours. Clearly, to obtain an effective bactericidal paper, the concentration of AgNPs in the AgNP paper must be much higher than the threshold MIC concentration. In addition, with water purification in mind, we have take into consideration that for a water purification device to meet US EPA standards, it must reduce the bacteria colony count by over five orders of magnitude (log 5) [24].

The bactericidal activity of silver nanoparticles has been attributed to mechanisms such as the release of silver ions from the AgNP surface [20, 25]. Silver ions have been shown to bind preferentially on thiol groups in membrane proteins, and to cause DNA aggregation [25]. Treatment with silver nanoparticles caused pitted membranes, increased membrane permeability, and cytoplasm leakage in *E. coli* [12, 26]. Hwang et al. demonstrated that AgNPs in growing cultures of wild type *E. coli* led to the production of superoxide radicals, which aided silver ion penetration into the cell membrane [27]. In general, the literature is inconclusive on the antibacterial properties of silver in a comparison of Gram negative bacteria with Gram positive bacteria [21, 25, 28].

After percolation through the AgNP sheet, the *E. coli* cells showed significant morphological changes when imaged by TEM (See supplementary data, Fig. S2.2). In some cases, the *E. coli* cell membranes have detached from the cytoplasm and show serious cell wall damage.

2.4.3 Analysis of silver in the effluent

Due to possible human health effects from silver exposure [29], we analyzed the silver content of the effluent water. We used centrifugation to separate the bacteria from the silver (either nanoparticles or ions or both) leached out of the paper. The average silver content in the effluent water was 0.0475 (±0.0177) ppm, as measured by graphite furnace atomic absorption, which measures total silver content (i.e., silver ions and nanoparticles). The amount of silver leaching from the filter papers thus meets the US-EPA guideline for drinking water of less than 0.1 ppm [137] (Figure 2.7). In contrast, the average silver content in the effluent water from the $AgNO_3$ paper was 1.80 (±0.186) ppm. The different samples leached between 0.04% to 2.4% of the initial silver content of the filter papers (See supplementary data, Table S2.1). Higher values for silver leaching were observed with the AgNP soaked paper and the $AgNO_3$ papers, with 6.8%

and 12.9% of total silver content lost, respectively, from the paper sheets (Table S2.1). This demonstrates that the *in situ* preparation of the silver nanoparticles in paper sheets improves silver retention and the longevity of the water purifier.

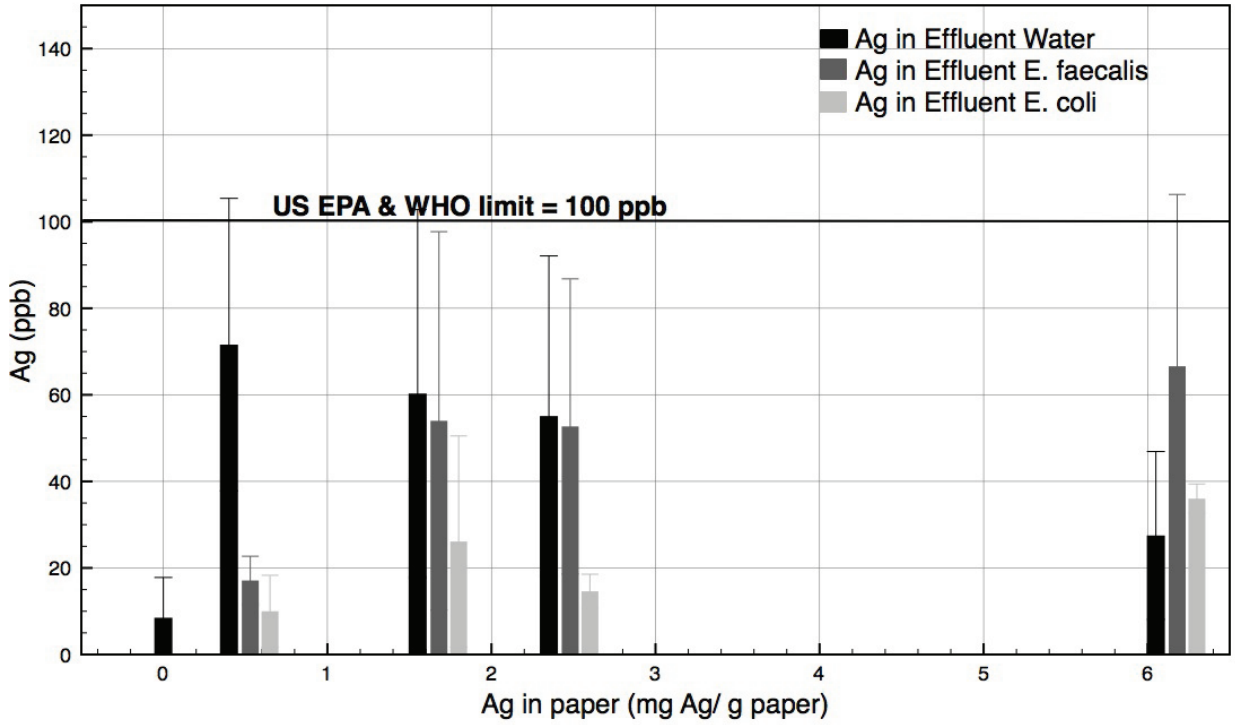

FIGURE 2.7. Silver concentration in effluent water and in effluent *E. faecalis* and *E. coli* bacteria, per 10^8 CFU/mL. The recommended Ag limit for drinking water is 100 ppb.

We also analyzed for the silver taken up by the bacterial cells during percolation through the AgNP sheet. We observed an average silver absorption of 0.0195 (±0.0112) ppm per 108 CFU/mL *E. coli* bacteria cells, and 0.043 (±0.018) ppm per 108 CFU/mL E. faecalis bacteria (Figure 2.7). The *E. coli* bacteria appear to absorb less silver overall, and the *E. faecalis* silver adsorption is comparable to the mean amount of silver present in the effluent water. This is orders of magnitude lower than the minimal inhibitory concentration for both silver ions, 2-5 ppm [22] and silver nanoparticles, 5.4-108 ppm [19-21]. It is possible that *E. faecalis* had higher silver content than *E.*

coli due to the larger surface area, as the size of *E. faecalis* is approximately 0.5 micron and *E. coli* is 1-2 microns.

Although the bactericidal action of the AgNP paper remains to be tested in real-world situations, where disease-causing organisms exist in a medium containing a wide range of other organic, inorganic and colloidal contaminants, the reported results show that it is possible to demonstrate significant biocidal action as bacteria percolate through a paper sheet impregnated with silver nanoparticles. Hopefully, this will provide the basis for a water purification method that is light, cheap and easily deployed in an emergency.

2.5 Acknowledgements

This work was supported by the Sentinel Bioactive Paper Network. We gratefully acknowledge the training and use of facilities at McGill from Glenna Keating (GF-AA), Line Mongeon (SEM), Xue Dong Liu (TEM), Josiane Lafleur and David Duford (ICP-AES), and thank Rosie Gao for help with the microbiology. Rafik Allem and David Wong (FPInnovations, Pointe Claire) helped with SEM and UV-Vis Spectroscopy, respectively.

2.6 References

1. World Health Organization / UNICEF Joint Water Supply: Sanitation Monitoring Programme, ed. *Water for life: making it happen*. 2005.
2. World Health Organization, ed. *Guidelines for drinking-water quality*. 2006: Geneva, Switzerland.
3. Q. Li, S. Mahendra, D.Y. Lyon, L. Brunet, M.V. Liga, D. Li, and P.J.J. Alvarez, *Antimicrobial nanomaterials for water disinfection and microbial control: Potential applications and implications.* Water Research, 2008. **42**(18): p. 4591-4602.
4. A.M. Ferraria, S. Boufi, N. Battaglini, A.M. Botelho Do Rego, and M. Reivilar, *Hybrid systems of silver nanoparticles generated on cellulose surfaces.* Langmuir, 2010. **26**(3): p. 1996-2001.
5. J.H. He, T. Kunitake, and A. Nakao, *Facile in situ synthesis of noble metal nanoparticles in porous cellulose fibers.* Chem Mater, 2003. **15**(23): p. 4401-4406.
6. S. Ifuku, M. Tsuji, M. Morimoto, H. Saimoto, and H. Yano, *Synthesis of silver nanoparticles templated by TEMPO-mediated oxidized bacterial cellulose nanofibers.* Biomacromolecules, 2009. **10**(9): p. 2714-2717.
7. T. Maneerung, S. Tokura, and R. Rujiravanit, *Impregnation of silver nanoparticles into bacterial cellulose for antimicrobial wound dressing.* Carb Polym, 2008. **72**(1): p. 43-51.
8. F. Tang, L. Zhang, Z. Zhang, Z. Cheng, and X. Zhu, *Cellulose filter paper with antibacterial activity from surface-initiated ATRP.* Journal of Macromolecular Science Part A-Pure and Applied Chemistry, 2009. **46**(10): p. 989-996.
9. C. Zhu, J. Xue, and J.H. He, *Controlled in-situ synthesis of silver nanoparticles in natural cellulose fibers toward highly efficient antimicrobial materials.* Journal of Nanoscience and Nanotechnology, 2009. **9**(5): p. 3067-3074.
10. J. Cai, S. Kimura, M. Wada, and S. Kuga, *Nanoporous cellulose as metal nanoparticles support.* Biomacromolecules, 2009. **10**(1): p. 87-94.
11. R. Davies and S. Etris, *The development and functions of silver in water purification and disease control.* Catalysis Today, 1997. **36**(1): p. 107-114.

12. J.R. Morones, J.L. Elechiguerra, A. Camacho-Bragado, K. Holt, J.B. Kouri, J.T. Ramírez, and M.J. Yacaman, *The bactericidal effect of silver nanoparticles.* Nanotechnology, 2005. **16**(10): p. 2346-2353.
13. W. Chou, D. Yu, and M. Yang, *The preparation and characterization of silver-loading cellulose acetate hollow fiber membrane for water treatment.* Polymers for Advanced Technologies, 2005. **16**(8): p. 600-607.
14. K.Y. Yoon, J.H. Byeon, C.W. Park, and J. Hwang, *Antimicrobial effect of silver particles on bacterial contamination of activated carbon fibers.* Environ Sci Technol, 2008. **42**(4): p. 1251-1255.
15. K. Zodrow, L. Brunet, S. Mahendra, D. Li, A. Zhang, Q. Li, and P.J.J. Alvarez, *Polysulfone ultrafiltration membranes impregnated with silver nanoparticles show improved biofouling resistance and virus removal.* Water Research, 2009. **43**(3): p. 715-723.
16. P. Jain and T. Pradeep, *Potential of silver nanoparticle-coated polyurethane foam as an antibacterial water filter.* Biotechnol Bioeng, 2005. **90**(1): p. 59-63.
17. V. Oyanedel-Craver and J. Smith, *Sustainable colloidal-silver-impregnated ceramic filter for point-of-use water treatment.* Environ Sci Technol, 2008. **42**(3): p. 927-933.
18. A. Henglein, *Colloidal silver nanoparticles: photochemical preparation and interaction with O_2, CCl_4, and some metal ions.* Chem. Mater., 1998. **10**: p. 444-450.
19. C. Baker, A. Pradhan, L. Pakstis, D.J. Pochan, and S.I. Shah, *Synthesis and antibacterial properties of silver nanoparticles.* Journal of Nanoscience and Nanotechnology, 2005. **5**(2): p. 244-249.
20. C.-N. Lok, C.-M. Ho, R. Chen, Q.-Y. He, W.-Y. Yu, H. Sun, P.K.-H. Tam, J.-F. Chiu, and C.-M. Che, *Silver nanoparticles: Partial oxidation and antibacterial activities.* J Biol Inorg Chem, 2007. **12**(4): p. 527-534.
21. A. Panacek, L. Kvitek, R. Prucek, M. Kolar, R. Vecerova, N. Pizurova, V. Sharma, T. Nevecna, and R. Zboril, *Silver colloid nanoparticles: Synthesis, characterization, and their antibacterial activity.* J Phys Chem B, 2006. **110**(33): p. 16248-16253.

22. G.J. Zhao and S.E. Stevens, *Multiple parameters for the comprehensive evaluation of the susceptibility of Escherichia coli to the silver ion.* Biometals, 1998. **11**(1): p. 27-32.
23. J. Liu, D.A. Sonshine, S. Shervani, and R.H. Hurt, *Controlled release of biologically active silver from nanosilver surfaces.* ACS Nano, 2010. **4**(11): p. 6903-6913.
24. U.S. Environmental Protection Agency: Office of Pesticide Programs, *Guide standard and protocol for testing microbiological water purifiers*. 1987, Washington, D.C. p. 1-20.
25. Q.L. Feng, J. Wu, G.Q. Chen, F.Z. Cui, T.N. Kim, and J.O. Kim, *A mechanistic study of the antibacterial effect of silver ions on Escherichia coli and Staphylococcus aureus.* J Biomed Mater Res, 2000. **52**(4): p. 662-668.
26. I. Sondi and B. Salopek-Sondi, *Silver nanoparticles as antimicrobial agent: a case study on E. coli as a model for Gram-negative bacteria.* Journal of Colloid and Interface Science, 2004. **275**(1): p. 177-182.
27. E. Hwang, J. Lee, Y. Chae, Y. Kim, B. Kim, B. Sang, and M. Gu, *Analysis of the toxic mode of action of silver nanoparticles using stress-specific bioluminescent bacteria.* Small, 2008. **4**(6): p. 746-750.
28. J. Kim, E. Kuk, K. Yu, J. Kim, S. Park, H. Lee, S. Kim, Y. Park, Y. Park, and C. Hwang, *Antimicrobial effects of silver nanoparticles.* Nanomedicine: Nanotechnology, Biology and Medicine, 2007. **3**(1): p. 95-101.
29. P. Drake and K. Hazelwood, *Exposure-related health effects of silver and silver compounds: A review.* Annals of Occupational Hygiene, 2005. **49**(7): p. 575-585.

2.7 Supplementary Material

Following the strict publication guidelines from the journal "Environmental Science and Technology," the Table S2.1 and Figures S2.1-2 were published as "Supplementary Material" to the article. Because these data are referred to earlier in Chapter 2, it has been included in the thesis.

TABLE S2.1. Silver loss from filter paper during water filtration flow tests. Standard deviations shown.

Silver Content	**Silver Loss in Effluent Water**	
(mg Ag/ g paper)	µg / g paper	% of initial silver
0.26	4.6 ± 3.5	2.40% ± 1.7%
1.39	6.7 ± 4.7	0.57% ± 0.4%
2.21	4.2 ± 3.2	0.25% ± 0.17%
5.97	2.3 ± 1.6	0.05% ± 0.03%
AgNP soaked (0.06)	3.4 ± 1.4	6.80% ± 2.75%
$AgNO_3$ paper (1.4)	150.1 ± 15.5	12.86% ± 1.33%

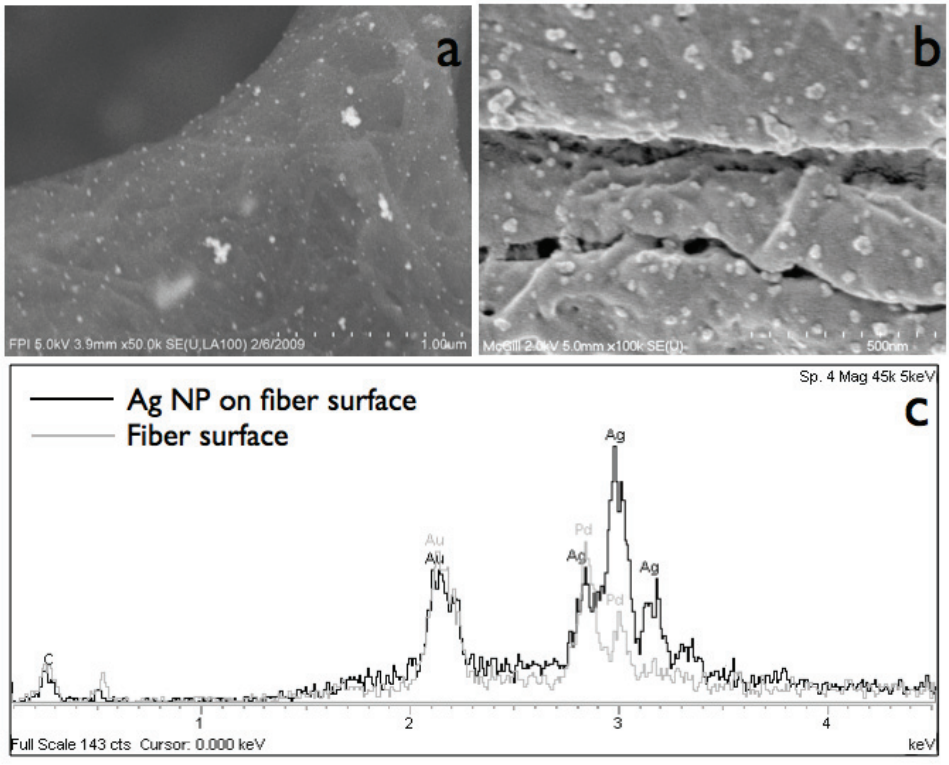

FIGURE S2.1. SEM image of fiber surface coated with silver nanoparticles: (a) 50,000x magnification and (b) 100,000x magnification. (c) EDX spectra of the Ag NP paper. Samples were sputter coated with AuPd.

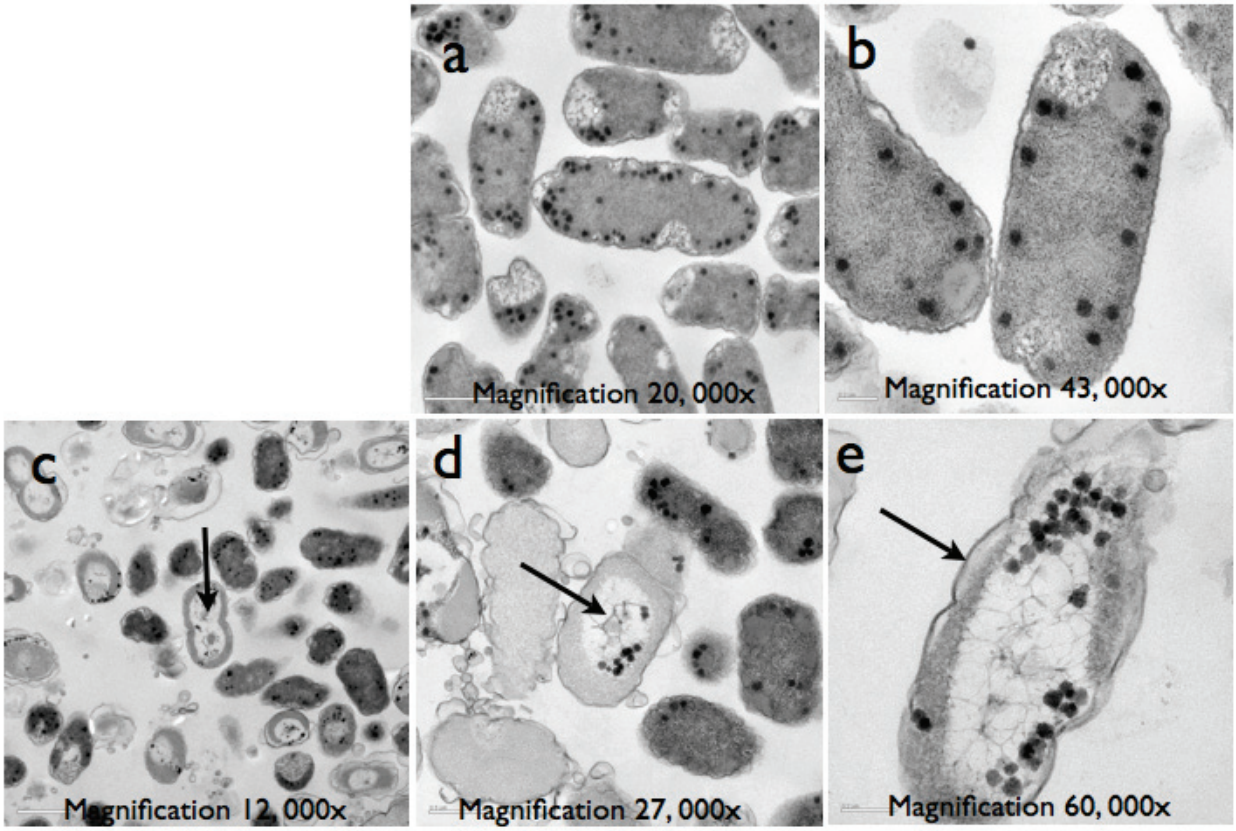

FIGURE S2.2. Internal structure of *E. coli* bacteria imaging by TEM, following percolation experiments. (a) & (b) control paper (no silver). After exposure to AgNP paper (c) low electron density region (arrow) in the centers of the cells. (d) Condensed form of DNA (arrow) in the center of the low electron density region. (e) A gap between the cytoplasm membrane and the cell wall (arrow); the cell wall shows serious damage. Black dots are not AgNP, but electron dense granules typical of *E. coli*.

Chapter 3

Microwave-assisted synthesis of silver nanoparticles in paper

This chapter describes the preparation of blotter papers containing silver nanoparticles using an environmentally benign method. The bactericidal effects are evaluated in a model filter setup, similarly to Chapter 2.

3.1 Abstract

In this work, we report an environmentally benign method for the *in situ* preparation of silver nanoparticles (AgNPs) in paper using microwave irradiation. Microwave heating yields nanoparticles on the surface of cellulose fibers within 3 minutes with an excess of glucose compared to the silver ion precursor. Paper sheets were characterized by electron microscopy, UV-Visible reflectance spectroscopy, and atomic absorption spectroscopy. The nanoparticles appear to be homogeneous and their diameters are <10 nm. The paper sheets containing silver nanoparticles are highly effective antibacterial materials and may be suitable for point-of-use emergency water treatment, wound care, and food packaging.

3.2 Introduction

Metal nanoparticles in solid matrices have potential applications as catalytic, antimicrobial, sensor, and electronic materials. Paper, as a solid matrix, is an attractive material due to its high porosity, mechanical strength, and natural abundance. Additionally, cellulose fibers, the primary component of paper, are highly absorbent materials. Blotter papers in particular, are pure cellulose papers with no additives and are thick (0.5 mm), porous sheets of paper. We recently reported that blotters containing silver nanoparticles show promise in point-of-use water purification [1].

Integration of green and sustainable processes into nanomaterial synthesis has attracted interest over the past decade [2-6]. Some of the key efforts aim to use renewable resources, nontoxic chemicals, and environmentally benign solvents, and to minimize the generation of waste. Previously, deposition of metal nanoparticles on surfaces has generally involved chemical reduction using sodium borohydride,

hydrazine, DMF, etc., and physical reduction using UV irradiation and conventional thermal heat [1, 7-9]. Most of the wet chemistry methods use highly reactive reducing agents such as sodium borohydride and hydrazine, which are not environmentally friendly. As a result, there is considerable interest in the use of nontoxic reducing agents, such as amino acids and reducing sugars, for nanoparticle synthesis [2-6].

Microwave irradiation is emerging as a rapid and green method of heating for nanoparticle synthesis [3, 8]. Microwave heating methods have been shown to increase reaction rates and product yields, compared to conventional thermal heating. This is due to more uniform heating of the sample [8]. In general, microwave irradiation has been used to synthesis nanoparticles in solution, but not extensively in solid matrices. In situ reduction of nanoparticles in the solid paper matrix directly in the microwave oven greatly simplifies the experimental design, reduces energy inputs, and minimizes waste. In cellulose materials, there have been a few reports of physical reduction of metals by thermal treatment [9-12]. However, to achieve uniform nanoparticles by heating, long reaction times are required, and microwave-assisted synthesis could drastically reduce these reaction times. Cellulose-silver nanocomposites have also been prepared in regenerated cellulose via microwave-assisted synthesis [13-15].

In this chapter, we have used microwave irradiation for rapid and uniform synthesis of silver nanoparticles in paper. Although preparation of AgNPs on paper surfaces by reduction of silver nitrate is a straight-forward reaction, achieving uniform nanoparticle size and minimal aggregation requires specific reaction conditions. To accomplish this, we have added the reducing sugar, glucose, to supplement the reducing ends of cellulose chains that may already be present in the paper, thus speeding up the nanoparticle formation.

3.3 Experimental

3.3.1 Materials

We used absorbent blotting papers made from bleached softwood kraft pulp. The blotters (made by Domtar Inc. and kindly supplied by FP Innovations, Pointe-Claire, QC) are used for drying laboratory handsheets during pulp testing, according to PAPTAC Standard C.4. The sheet thickness and grammage for the blotting paper sheets are 0.5 mm and 250 g/m^2, respectively, and the sheets are free from sizing agents, fluorescent agents and chemical additives. Silver nitrate ($AgNO_3$), β-D-glucose, 30% hydrogen peroxide (H_2O_2), concentrated nitric acid (HNO_3), and poly(L-lysine) (0.01% solution) were purchased from Sigma Aldrich and used as received. Water treated with a Barnstead Nanopure system was used throughout.

3.3.2 Preparation of silver nanoparticle paper

We immersed a sheet of the blotting paper (10 cm by 10 cm) in a freshly prepared aqueous solution of glucose (0 to 1.0 M) and silver nitrate (0 to 0.1 M) for 10 minutes. No apparent reaction was observed at room temperature. For nanoparticle formation, the papers were either placed upright in a 400 mL glass beaker in a domestic microwave (Sharp Model No. R-410CWC, 2.45 GHz, 1000W) for 3-7 minutes or in a conventional oven at 105°C for 30-70 minutes. After heating, the AgNP papers were soaked in water for 1-2 hours to remove excess unreacted reagents. For comparison, AgNP papers were also prepared by reduction with sodium borohydride [1]. Following the paper soaking step, the papers were dried in a modified plastic food container with a clamp lock to restrain the paper in order to prevent shrinkage. The top and sides of the container were cut out to maximize air drying (Figure 3.1). The initially wet sheet was placed across the top of the container and clamped in place with the container lid. The dried sheet was trimmed to 6.5 cm by 6.5 cm.

FIGURE 3.1. Image of the plastic food container as a clamp for paper drying. The dimensions of the container are 10 cm by 10 cm by 5 cm.

Due to the possibility of the papers overheating in the microwave oven, several important and simple experimental modifications are necessary. Firstly, the careful placement of papers in the microwave by avoidance of the hot spots[1] while heating in the microwave reduces the occurrence of side reactions of the glucose, i.e. caramelization as evidenced by brown staining. Secondly, if the papers are placed in or partially in a hot spot, the 90° rotation of the papers every 30 seconds reduces the overheating.

[1] The "hot spots" where overheating occurs due to standing waves in the microwave were plotted by a simple experiment. This involved covering a large sheet of parchment paper with a layer of chocolate chips on the microwave carousel plate. The chocolate chips were heated until specific areas started to melt and then these regions, which correspond to the "hot spots," were indicated on the parchment paper. The hot spots map was used for placement of the silver soaked papers in the microwave for the experiments detailed in this chapter. These chocolate experiments were based on a WOW Lab at McGill: http://wowlab-blueprints.mcgill.ca/en/projectpage.php?id=chocolate.

3.3.3 Paper characterization

The presence of AgNPs in the blotting paper was established by measuring the reflectance spectra of the AgNP papers with a diffuse reflectance attachment (Labosphere, DRA-CA-30) on a UV-Vis spectrophotometer (Varian TCA-Cary 300) at wavelengths of 300 to 800 nm. Reflectance was measured relative to a poly(tetrafluoroethylene) powder standard. Spherical silver nanoparticles have a characteristic surface plasmon resonance peak around 400 nm [16]. The shape and size distribution of the silver nanoparticles in the sheet were examined by electron microscopy. Individual paper fibers containing silver nanoparticles from the AgNP sheets were pulled from the papers and deposited on carbon coated copper grids that had been treated with poly(L-lysine), and imaged with a Philips CM200 200 kV transmission electron microscope (TEM). Nanoparticle diameters were measured for greater than 100 particles per sample, with standard deviation values reported. Imaging and analysis of the AgNP paper was performed with a field emission scanning electron microscopy (Hitachi S-4700 FE-SEM) attached to an energy-dispersive X-ray spectroscopy detector (EDX). For SEM, samples were sputter coated with a thin, 24 nm, layer of AuPd prior to imaging.

To quantify the amount of silver in the AgNP papers, we performed an acid digestion of the paper and analyzed the amount of dissolved silver with a flame atomic absorption (FAA) spectrometer (Perkin Elmer AAnalyst 100) as described previously [1]. The silver content reported is five replicates per sample concentration with standard deviation error bars. To analyze for the deposition of glucose oxidation products on the AgNP sheets, we used the following methods. First, we evaluated the weight difference before and after nanoparticle formation. Second, we soaked the paper sheets in water for 120 minutes to remove the sugars and analyzed the aqueous extracts for reaction byproducts with a UV-Vis spectrophotometer at wavelengths of 200 to 700 nm. Absorbance at 280 nm corresponds to conjugated carbonyl intermediate byproducts,

while absorbance at 420 nm is used to determine the extent of brown polymer formation [17]. Lastly, we assessed for changes in silver content through FAA analysis of discolored spots on the paper from excessive glucose oxidation.

3.3.4 Bactericidal testing

AgNP papers were evaluated for bactericidal effectiveness by a simple water filter test, as detailed in Chapter 2 [1]. Suspensions of model *Escherichia coli* bacteria were passed through the paper, and the effluent water was analyzed for viable bacteria by plating on nutrient agar plates and incubating at 37°C for 24 hours. Five replicates were performed per paper, and the standard deviations were reported.

3.3.5 Analysis for silver in effluent

After passing through the AgNP paper, the effluent was analyzed for silver content by graphite furnace atomic absorption spectrometry (GF-AA, Perkin Elmer AAnalyst 100), as described previously [1]. Five replicates were performed per paper, and the standard deviations were reported.

3.4 Results and discussion

3.4.1 Paper characterization

The silver nanoparticles were readily formed by both microwave irradiation (MW) and conventional oven heating of a silver nitrate solution absorbed in the blotting paper. Higher concentrations of the reducing sugar, glucose (1 M), gave more uniform and smaller nanoparticles, and shortened the reaction times in both the microwave and conventional oven (Table 3.1). In both of these cases, the reduction of silver nitrate to metal nanoparticles occurred during the drying of the solution-soaked paper sheets.

TABLE 3.1. Comparison of various methods to incorporate silver nanoparticles into blotting paper sheets.

Heating method	Reducer	Concentration (M)	Synthesis time* (min)	Nanoparticle Diameter (nm)
Microwave	none	n/a	20	13.4 ± 10.2
Microwave	Glucose	0.01	9	7.1 ± 3.2
Microwave	Glucose	0.1	5	7.2 ± 2.6
Microwave	Glucose	1	3	3.2 ± 1.6
Oven	none	n/a	8 days	5.5 ± 2
Oven	Glucose	0.01	90	7.1 ± 3
Oven	Glucose	0.1	75	6.9 ± 4.8
Oven	Glucose	1	40	7.5 ± 2.2
n/a	$NaBH_4$**	0.26	15	7.1 ± 3.7

* Time required to generate overall yellow/orange color on the paper

** Results from Chapter 2, (Dankovich and Gray, 2011 [138])

The sheets changed color from white to yellow/orange/brown with increasing precursor silver ion and glucose concentrations (Figure 3.2). The color changes in the paper sheets are due to the surface plasmon resonance (SPR) of silver nanoparticles. UV-Vis reflectance spectroscopy (Figure 3.3) showed a peak at 420 nm, which falls in the characteristic SPR range (390-420 nm) for a suspension of spherical silver nanoparticles [16]. The broader peak at 420 nm for the higher concentrations of AgNPs from blotting paper also is indicative of a wider size distribution than for AgNPs formed in solution and of surface effects of the paper substrate. For papers with the same precursor silver concentration, the AgNP papers formed by glucose reduction showed a slightly broader peak at 420 nm and a greater reflectance at long wavelengths (greater than 600nm) than the AgNP paper formed by sodium borohydride reduction from Chapter 2 (Figure 3.4), which resulted in a more orange colored sheet.

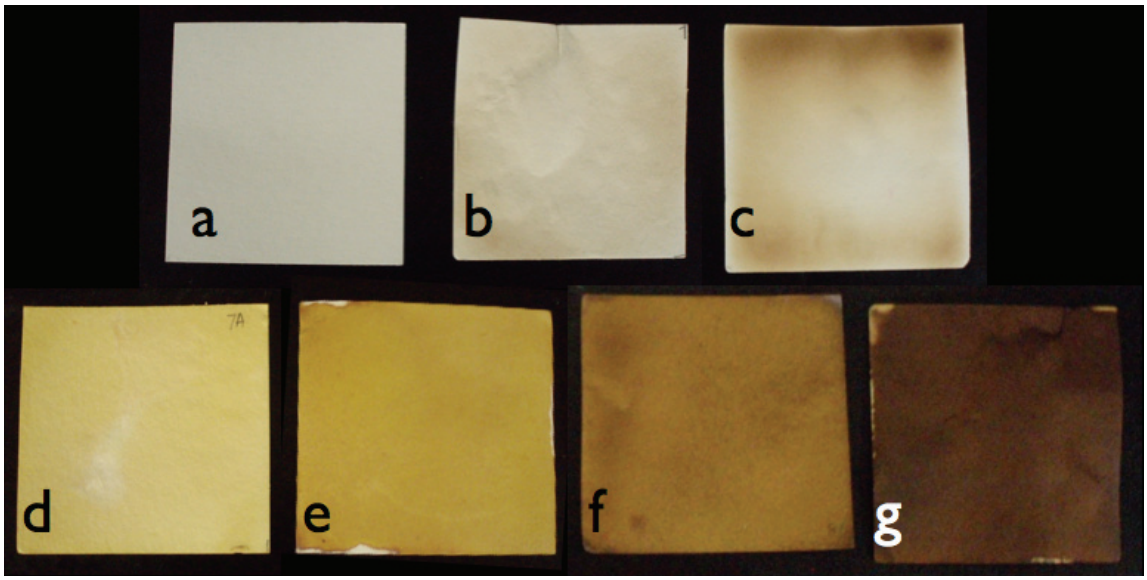

FIGURE 3.2. Blotter papers without any silver (a) untreated, (b) heated in the microwave for 30 minutes, and (c) heated in the microwave for 6 minutes with glucose. Blotter papers were heated in the microwave for 4-6 minutes with 1M glucose and the following $AgNO_3$ concentrations: (d) 1 mM (e) 10 mM (f) 25 mM, and (g) 100 mM (each sheet is 6.5 x 6.5 cm) to form silver nanoparticles in the sheets.

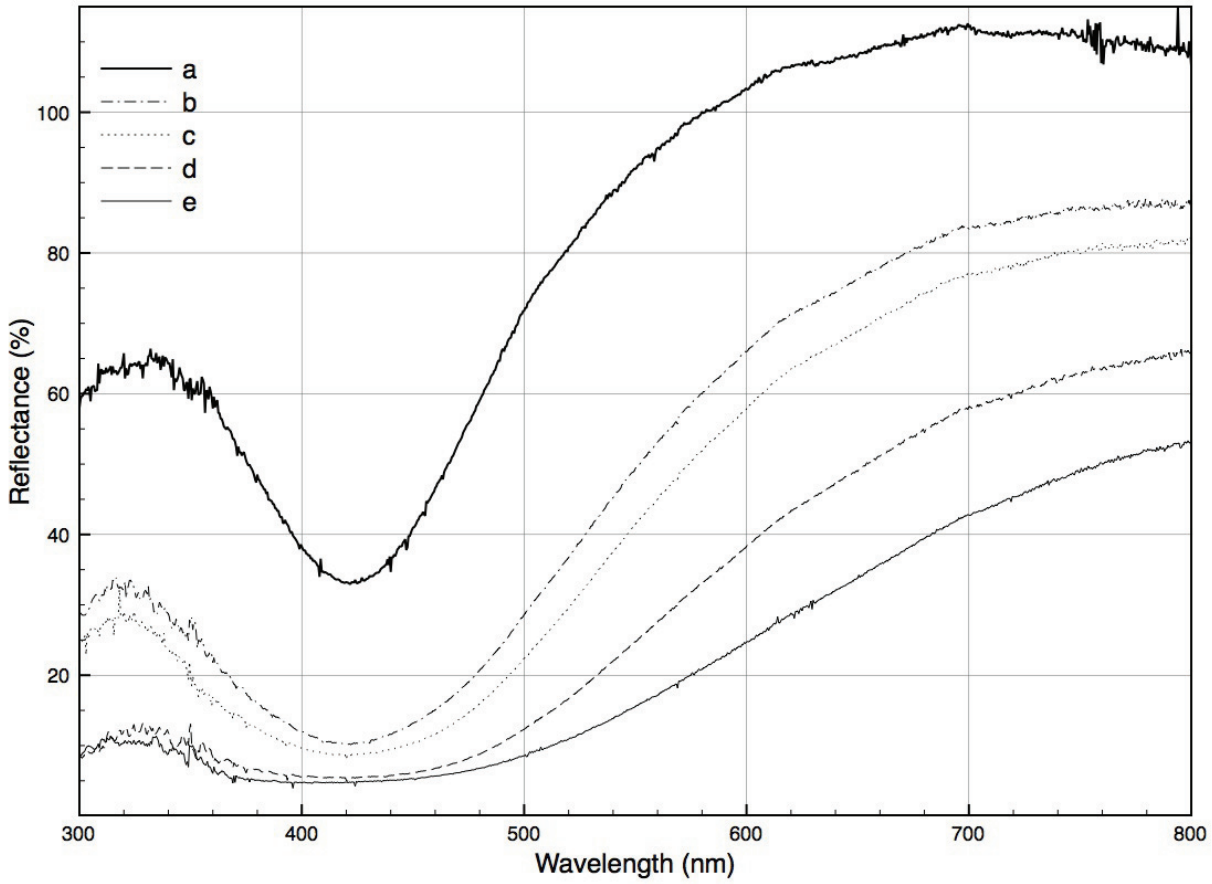

FIGURE 3.3. UV-Visible reflectance spectra of paper sheets after being soaked with 1M glucose and increasing silver nitrate concentrations: a) 1 mM, b) 5 mM, c) 10 mM, d) 25 mM, and e) 50 mM, and then heated by microwave irradiation.

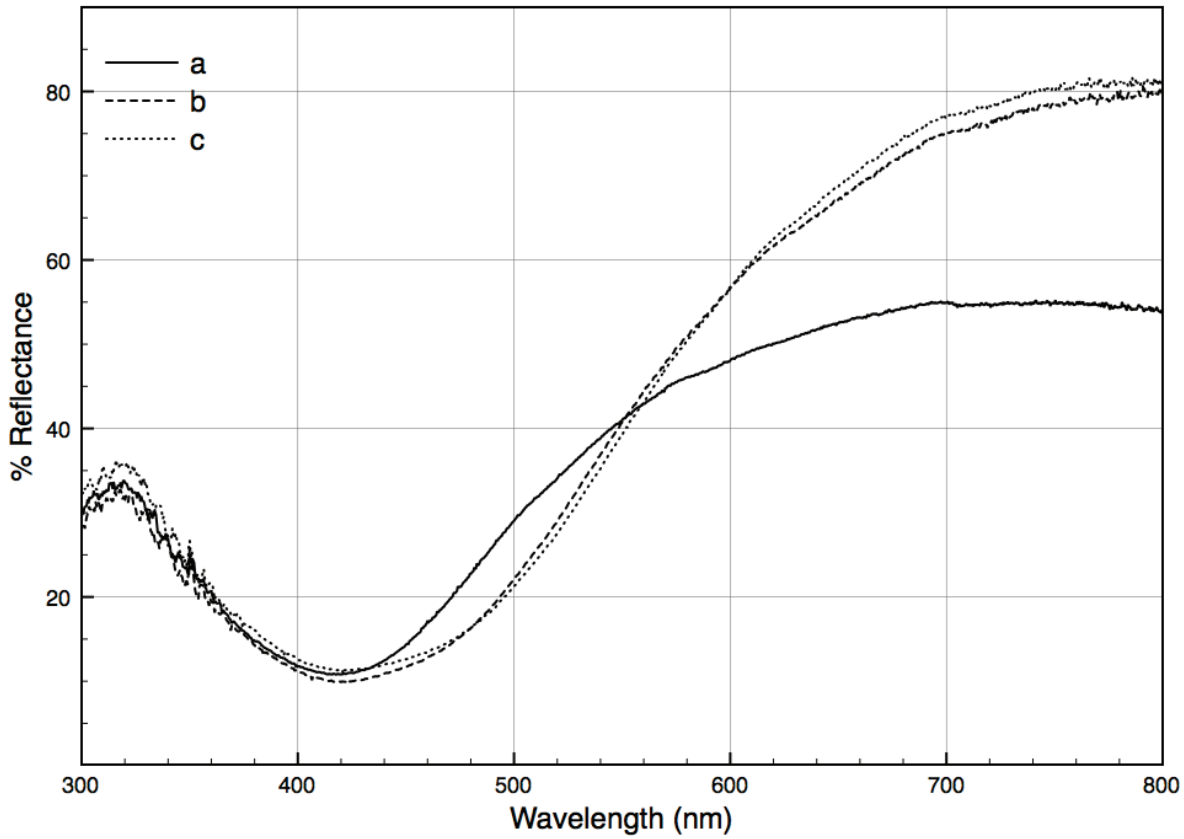

FIGURE 3.4. UV-Visible reflectance spectra of AgNP paper sheets prepared with sodium borohydride (a), and glucose, with the heat source either a microwave (b) or an oven at 105°C (c). All paper sheets had the same precursor Ag^+ concentration of 10 mM.

Following the microwave-assisted reduction of silver in the filter paper, the surface of the paper fibers was covered with mostly small spherical nanoparticles and a few larger cubic nanoparticles, as shown in the SEM images in Figure 3.5. From the TEM images, the average diameter of the AgNPs was 5.5 nm with a standard deviation of 3.6 nm. (Table 3.1 and Figure 3.6). Generally, the electron microscopy images showed similarities in sizes and shapes of the nanoparticles for both the oven and microwave heating methods. These are typical sizes for silver nanoparticles prepared *in situ* on cellulosic fibers [47, 53, 138, 139], although only spherical nanoparticles were observed after sodium borohydride reduction [1]. Other studies have shown a greater

proportion of silver nano-cubes than spherical silver nanoparticles with higher synthesis temperatures [18,19]. Samples heated in the microwave without any glucose had the largest nanoparticles with an average diameter of 13.4 nm and the most variety in particle sizes with a standard deviation of 10.2 nm. Samples heated in the microwave with only glucose and no silver nitrate showed similar SEM images as untreated paper. An EDX peak at 3 keV confirms the formation of silver nanoparticles in the papers (Figure 3.7). The untreated paper had silicon and magnesium EDX peaks, which were not present in the AgNP samples.

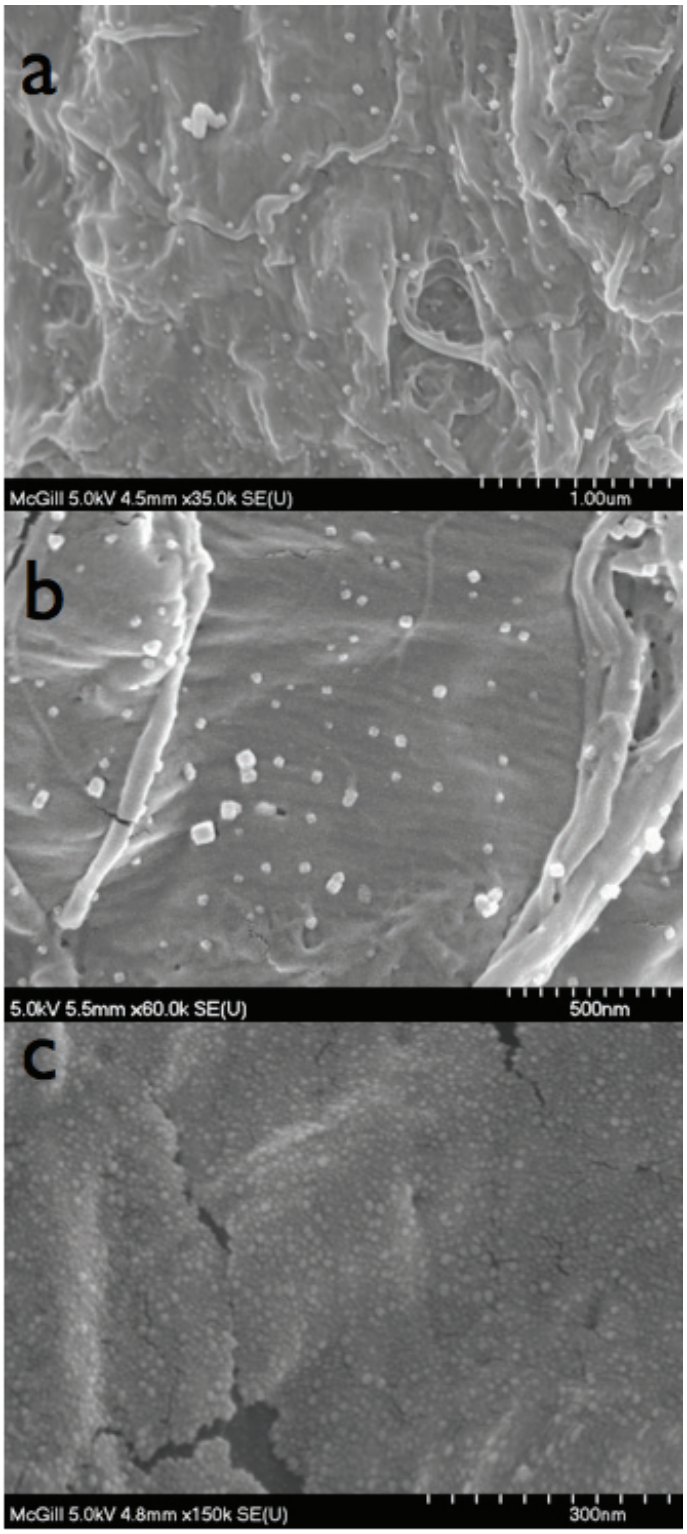

FIGURE 3.5. Scanning electron microscope image of AgNP paper, prepared by soaking the paper in 10 mM silver nitrate and 1 M glucose and heated in microwave oven: (a) 35,000 x, (b) 60,000 x, and (c) 150,000 x magnification.

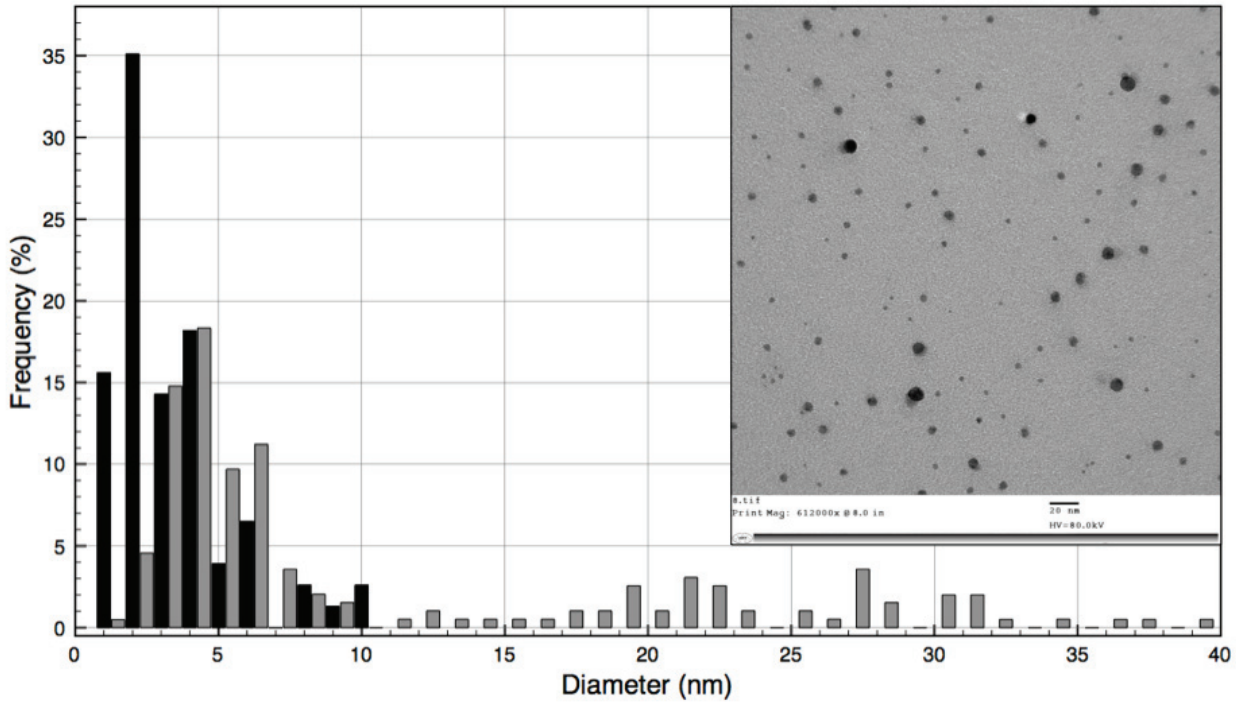

FIGURE 3.6. Nanoparticle diameter size histogram of silver nanoparticles in blotting paper with 1M glucose concentration (black bars) and no glucose (gray bars), and heated in the microwave. Inset of TEM image of silver nanoparticles formed with glucose reduction and microwave irradiation.

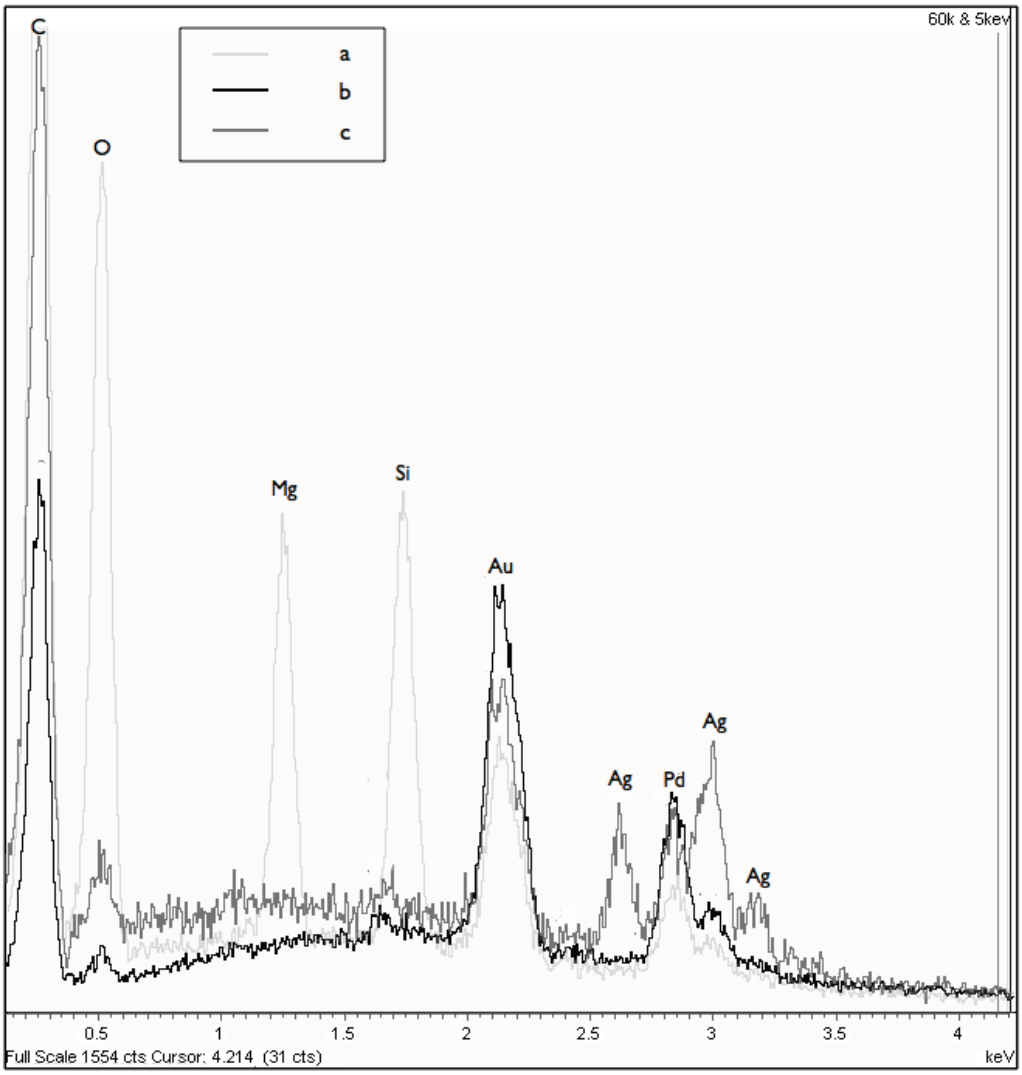

FIGURE 3.7. EDX spectra of (a) untreated, (b) glucose (1M), and (c) AgNP/glucose papers. Samples were sputter coated with Au Pd.

The acid digestion of the AgNP papers showed silver content ranging from 0.53 to 10.1 mg Ag per gram of paper (Table 3.2). The increase in silver content of the paper correlates with the increase in precursor silver ion concentration of the solution in which the papers were soaked, prior to the reduction. Immediately following the heat treatment, we observed that the amount of silver present in the AgNP papers was significantly lower than the retained sugars. For a typical experiment, the initial glucose

concentration in the reagent bath was 1M, and following NP synthesis, the dried paper had a weight gain of 260 (±10.9) mg of glucose per gram of paper, as compared to paper samples prepared without glucose (Figure 3.8). However, following soaking in water for two hours, much of the sugar was removed from the paper, as the total weight gain was 42.2 (±28.3) mg of glucose per gram of paper. The water only acted to remove excess sugar, as the silver content in the AgNP papers remained the same (data not shown). Overall, the optimal molar ratio of glucose:Ag^+ was greater than 75, based on the speed of NP formation and overall uniformity of NP sizes (Table 3.1).

TABLE 3.2. Silver content in paper filters, measured by Flame Atomic Absorption Spectrometry, with increasing precursor silver ion concentration.

Precursor Ag^+ ion concentration (mM)	Silver Content (mg Ag/g paper)	
	Microwave	Oven (105°C)
1	0.5 ± 0.4	0.7 ± 0.2
5	1.4 ± 0.5	1.5 ± 0.4
10	2.4 ± 0.8	2.4 ± 0.7
25	5.2 ± 1.3	5.3 ± 1.4

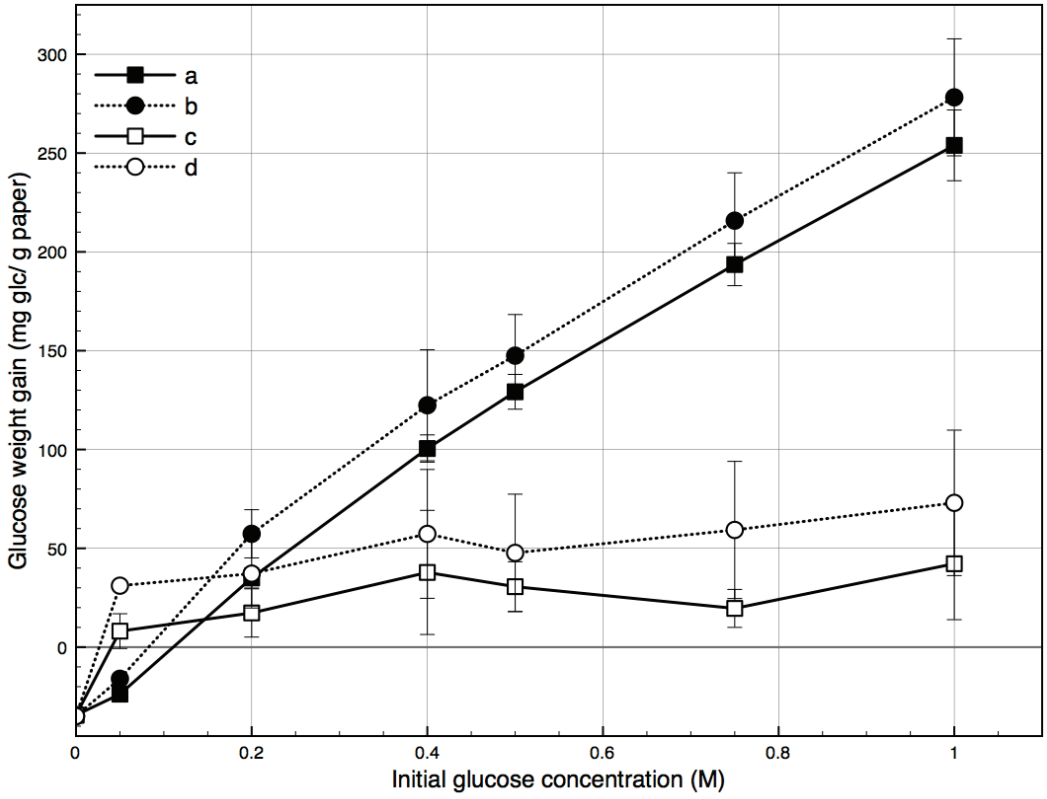

FIGURE 3.8. Glucose content in AgNP papers, as heated by the microwave oven (a) and conventional oven at 105°C (b), and after soaking in deionized water for 120 minutes and drying for samples a (c), and samples b (d).

3.4.2 Effect of glucose

The preparation of silver nanoparticles in paper was first conducted without any glucose as chemical reductant. This method was slow to produce nanoparticles, with reaction times of over 15 minutes for microwave irradiation and over several days for conventional oven heating (Table 3.1). The sheets with the lowest silver concentration barely showed any nanoparticle formation, as indicated by the sheet color. The sheets with the highest silver concentration appeared non-homogeneous with larger, agglomerated particles in some areas and only a few nanoparticles in other spots. Similarly to the combination reduction of heat treatment and glucose, the heat treatment alone also resulted in the formation of a mixture of spherical and cubic shaped

nanoparticles. Generally, without any glucose, as the silver ion concentration increased, the nanoparticles formed more quickly and were more likely to aggregate. It seems that the number of reducing end groups present on the cellulose surface was insufficient to generate significant amounts of silver nanoparticles.

The addition of glucose as reductant greatly sped up the reaction. The microwave-assisted formation of silver nanoparticles occurred in 3-7 minutes with a glucose concentration of 1.0 M. As the glucose concentration was increased from 0.01 to 1.0 M, the nanoparticle formation time decreased and less particle aggregation was observed. The reflectance spectra from UV-Vis measurements showed a deeper orange color with higher glucose concentrations (Figure 3.9). The average nanoparticle diameter decreased from 7.2 nm for 0.01 M glucose to 3.2 nm for 1 M glucose (Table 3.1). Glucose appeared to facilitate the nucleation of silver nanoparticles. Similar trends were observed with oven heating. Higher concentrations of glucose lead to a greater deposition in the paper sheets, resulting in increased paper stiffness and brittleness (Figure 3.8), presumably due to deposition of solid crystalline glucose in the intra- and inter-fiber interstices of the paper. Following nanoparticle synthesis, soaking in water extracted the excess sugar, the paper brittleness greatly decreased, as the glucose was extracted. Overall, the paper stiffness was not changed in the final AgNP paper compared to the untreated paper.

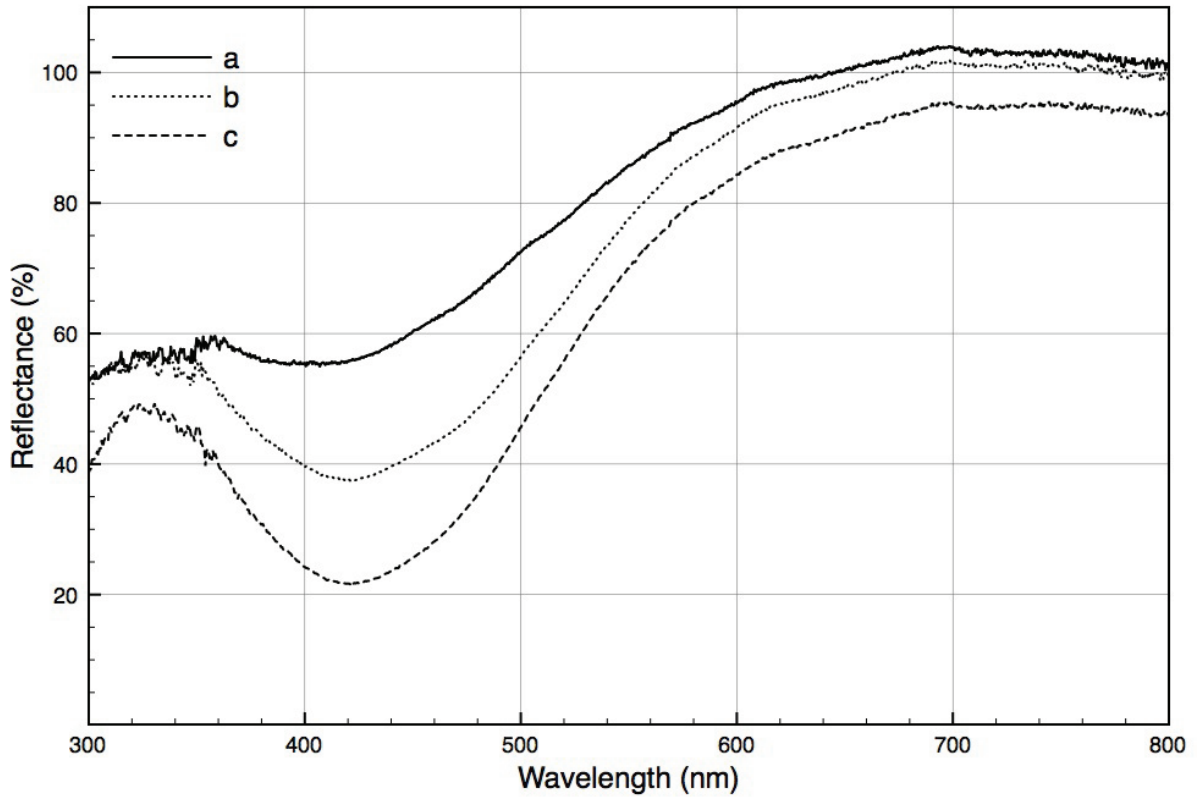

FIGURE 3.9. UV-Visible reflectance spectra of paper sheets with different initial glucose concentrations: a) 0.01 M b) 0.1M and c) 1.0 M, and 1 mM $AgNO_3$ as the initial silver ion concentration, prepared by oven heating at 105°C for 70 minutes.

3.4.3 Effect of heat source

As discussed above, the domestic microwave heating was inhomogeneous due to the formation of standing waves, which result in some spots overheating, so called "hot spots". A paper sheet saturated with an aqueous glucose solution (1M) showed considerably more browning from microwave heating than an untreated sheet (Figure 3.2); no discoloration was observed when a similar glucose-saturated sheet was dried in a conventional oven. The microwave-dried sheet emitted a pleasant caramel odor. Glucose undergoes complex caramelization reactions at temperatures greater than 160°C, resulting in hundreds of chemical products, including furans, furanones, pyrones, and carbocyclics [17]. The initial caramelization stages include the oxidation of

glucose to gluconic acid and the isomerization of glucose to fructose; subsequent reactions include fragmentation and polymerization reactions [20]. To detect caramel byproducts, we used UV-Vis spectroscopy to measure the spectra of aqueous extracts from AgNP paper sheets. The low molecular weight caramel byproducts, such as 5-(hydroxymethyl)furfural (HMF), are detected in the range 270-300 nm, and the kinetics of caramelization can be monitored by the measurement of HMF concentration [17,21]. Overall, the microwave-dried samples showed minor spectral variations due to spots overheating in the microwave. However, the brown caramel spots showed the greatest absorbance in the 270-300 nm range (Figure 3.10). The samples heated in the conventional oven did not show any spectrophotometric evidence of caramelization. There was no clear trend for variations in glucose or silver content and the subsequent caramel byproduct formation.

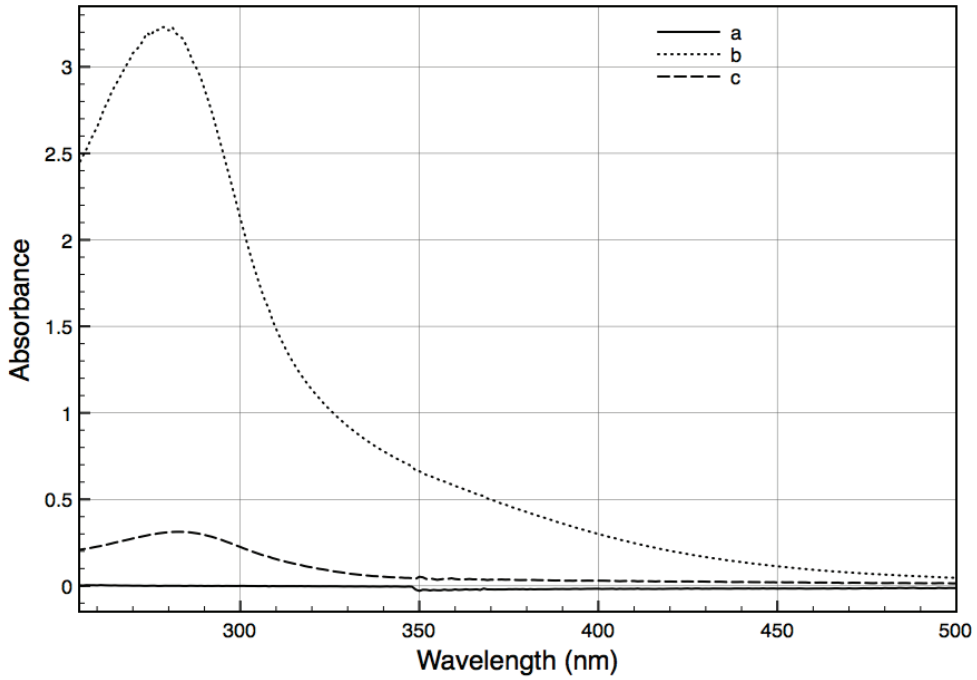

FIGURE 3.10. UV-Vis spectra of effluent water from rinsing AgNP paper with the same glucose concentration, 1 M, the same $AgNO_3$ concentration, 10 mM, and varying heating conditions: (a) heated in the oven at 105°C, (b) paper placed in a "hot spot" in the microwave, and (c) paper placed in a "cold spot" in the microwave.

Compared with the silver content in non-caramelized AgNP papers, the silver content of the brown caramel spots was 30% reduced (data not shown). This suggests that caramelization is acting as a competing reaction. Care should be taken experimentally to avoid overheating of the papers during AgNP formation. The formation of caramel in the microwaved paper seemed to be directly related to the energy absorbed by glucose during heating. If the paper was not placed in a hot spot in the microwave, then no caramelization was observed, and only silver nanoparticle synthesis occurred.

The impact of byproduct formation due to overheating was monitored by measuring the absorbance at 280 nm and 420 nm (Figure 3.11). A simple and effective strategy to reduce the degree of caramelization was periodic rotation of the papers while heating in the microwave oven. With this rotation, even if the paper was placed in a hot spot in the microwave oven, very minor formation of caramel byproducts was observed (Figure 3.11).

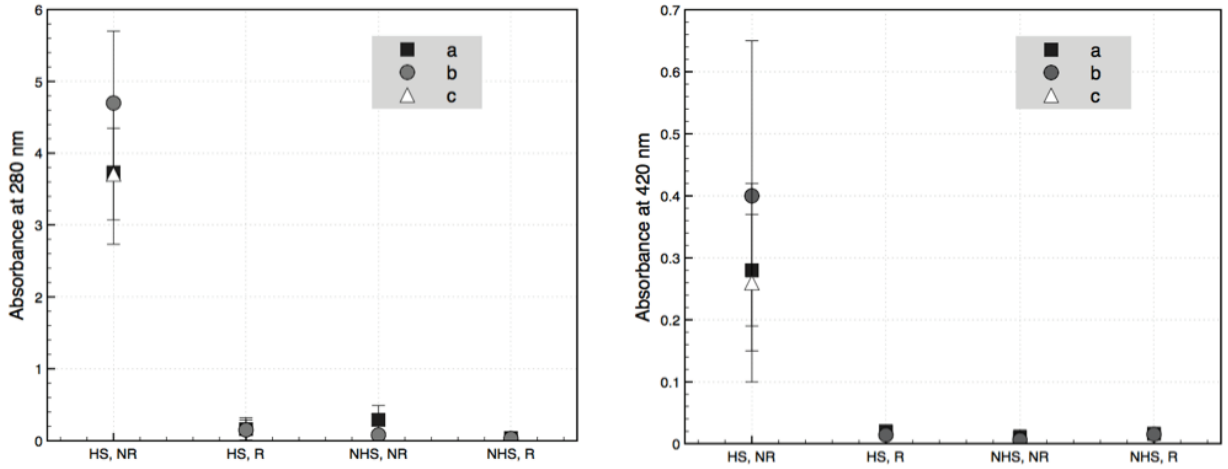

FIGURE 3.11. UV-Visible absorbance measurements of extracted caramel byproducts generated by different microwave treatments: HS, hot spot, NHS, non hot spot, R, rotation, NR, not rotated, with differing silver concentrations: (a) 1 mM $AgNO_3$, (b) 10 mM $AgNO_3$, and (c) 0 mM $AgNO_3$.

3.4.4 Antibacterial activity

The antibacterial activity of sheets prepared by both microwave and conventional heating was measured, as described previously [1]. To assess the bactericidal effectiveness of AgNP paper, we added the isolated effluent bacteria, after passage through the paper, to nutrient agar plates. The plate count experiments showed log 8.1 and log 2.3 reductions of viable *E. coli* and *E. faecalis* bacteria, respectively, in the effluent, as compared to the initial concentration of bacteria (10^9 CFU/mL) (Figure 3.12). The paper prepared by soaking in only glucose solutions did not show any difference from the control sample for the reduction in bacteria count, with a log reduction of 0.5 and a log increase of 0.2, for *E. coli* and *E. faecalis*, respectively. Caramelization byproducts do not show any synergistic effects with AgNPs, and some intermediates, such as furfural and HMF, have been suggested to be used as an alternative growth media source for enteric bacteria [22]. Additionally, the AgNP papers lost very little silver during filtration experiments, with an average value of 40.7 ± 38.9 ppb in the effluent water. These results are comparable to the results from Chapter 2 [2].

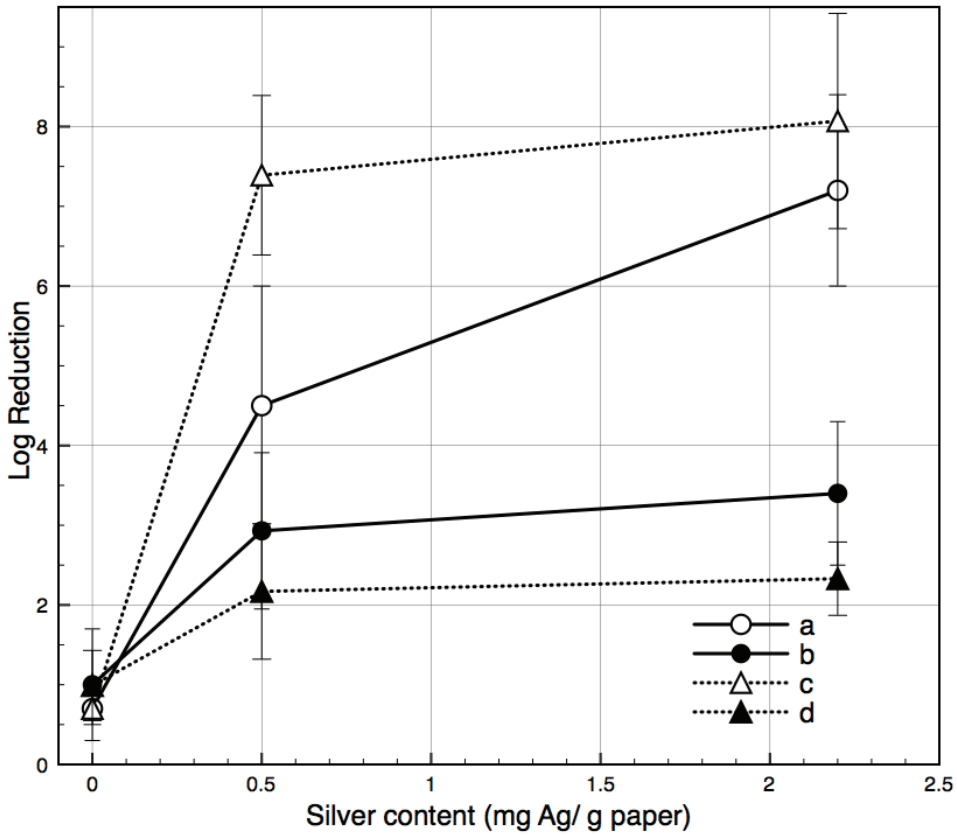

FIGURE 3.12. Log reduction of *E. coli* (a), (c), and *E. faecalis* (b), (d), bacterial count after permeation through the silver nanoparticle paper, at different silver contents in paper. (a) and (b) represent AgNP papers formed via sodium borohydride reduction. (c) and (d) represent AgNP papers formed via glucose and heat reduction. Initial bacterial concentration, 10^9 CFU/mL (log 9). Error bars represent standard deviation.

3.5 Conclusion

Silver nanoparticles can be deposited on paper by either microwave irradiation or conventional oven heating in combination with glucose reduction. The nanoparticles were well dispersed and stabilized on the paper fiber surfaces. The size of the silver nanoparticles can be controlled by initial silver ion concentration, glucose concentration, temperature, and duration of reaction. Local overheating, i.e. “hot spots,” during microwave heating of the sheets can be avoided by periodic rotation. The combination

of microwave irradiation and glucose reduction is more benign than the reduction with sodium borohydride used previously. Most importantly, the resultant AgNP paper is just as effective in deactivating bacteria during percolation through the sheet, as in Chapter 2 [1].

3.6 Acknowledgements

This work was supported by the Sentinel Bioactive Paper Network. We gratefully acknowledge the training and use of facilities at McGill from Glenna Keating and Isabelle Richer (Flame - AA), Line Mongeon (SEM), Xue Dong Liu (TEM), and thank Ruoxi Gao and Sangjin Bae for lab assistance. David Wong (FPInnovations, Pointe Claire) helped with UV-Vis Spectroscopy.

3.7 References

1. T.A. Dankovich and D.G. Gray, *Bactericidal paper impregnated with silver nanoparticles for point-of-use water treatment.* Environ Sci Technol, 2011. **45**(5): p. 1992-1998.
2. B. Baruwati, V. Polshettiwar, and R.S. Varma, *Glutathione promoted expeditious green synthesis of silver nanoparticles in water using microwaves.* Green Chem., 2009. **11**(7): p. 926-930.
3. P. Raveendran, J. Fu, and S. Wallen, *A simple and "green" method for the synthesis of Au, Ag, and Au-Ag alloy nanoparticles.* Green Chemistry, 2006. **8**(1): p. 34-38.
4. A. Panacek, L. Kvitek, R. Prucek, M. Kolar, R. Vecerova, N. Pizurova, V. Sharma, T. Nevecna, and R. Zboril, *Silver colloid nanoparticles: Synthesis, characterization, and their antibacterial activity.* J Phys Chem B, 2006. **110**(33): p. 16248-16253.
5. S. Horikoshi, H. Abe, K. Torigoe, M. Abe, and N. Serpone, *Access to small size distributions of nanoparticles by microwave-assisted synthesis. Formation of Ag nanoparticles in aqueous carboxymethylcellulose solutions in batch and continuous-flow reactors.* Nanoscale, 2010. **2**(8): p. 1441-1447.
6. B. Hu, S.-B. Wang, K. Wang, M. Zhang, and S.-H. Yu, *Microwave-assisted rapid facile "green" synthesis of uniform silver nanoparticles: Self-assembly into multilayered films and their optical properties.* J Phys Chem C, 2008. **112**(30): p. 11169-11174.
7. J.H. He, T. Kunitake, and A. Nakao, *Facile in situ synthesis of noble metal nanoparticles in porous cellulose fibers.* Chem Mater, 2003. **15**(23): p. 4401-4406.
8. J.A. Gerbec, D. Magana, A. Washington, and G.F. Strouse, *Microwave-enhanced reaction rates for nanoparticle synthesis.* J Am Chem Soc, 2005. **127**(45): p. 15791-15800.

9. S. Ifuku, M. Tsuji, M. Morimoto, H. Saimoto, and H. Yano, *Synthesis of silver nanoparticles templated by TEMPO-mediated oxidized bacterial cellulose nanofibers.* Biomacromolecules, 2009. **10**(9): p. 2714-2717.
10. N. Kotelnikova, V. Demidov, G. Wegener, and E. Windeisen, *Mechanisms of diffusion-reduction interaction of microcrystalline cellulose and silver ions.* Russian Journal of General Chemistry, 2003. **73**(3): p. 427-433.
11. R. Gottesman, S. Shukla, N. Perkas, L.A. Solovyov, Y. Nitzan, and A. Gedanken, *Sonochemical coating of paper by microbiocidal silver nanoparticles.* Langmuir, 2011. **27**(2): p. 720-726.
12. J. Cai, S. Kimura, M. Wada, and S. Kuga, *Nanoporous cellulose as metal nanoparticles support.* Biomacromolecules, 2009. **10**(1): p. 87-94.
13. A.R. Silva and G. Unali, *Controlled silver delivery by silver-cellulose nanocomposites prepared by a one-pot green synthesis assisted by microwaves.* Nanotechnology, 2011. **22**(31): p. 315605.
14. S.-M. Li, N. Jia, M.-G. Ma, Z. Zhang, Q.-H. Liu, and R.-C. Sun, *Cellulose silver nanocomposites: Microwave-assisted synthesis, characterization, their thermal stability, and antimicrobial property.* Carbohydrate Polymers, 2011. **86**(2): p. 441-447.
15. S.-M. Li, N. Jia, J.-F. Zhu, M.-G. Ma, F. Xu, B. Wang, and R.-C. Sun, *Rapid microwave-assisted preparation and characterization of cellulose silver nanocomposites.* Carbohydrate Polymers, 2011. **83**(2): p. 422-429.
16. A. Henglein, *Colloidal silver nanoparticles: photochemical preparation and interaction with O_2, CCl_4, and some metal ions.* Chem. Mater., 1998. **10**: p. 444-450.
17. L.W. Kroh, *Caramelisation in food and beverages.* Food chemistry, 1994. **51**(4): p. 373-379.
18. Y.G. Sun and Y.N. Xia, *Gold and silver nanoparticles: A class of chromophores with colors tunable in the range from 400 to 750 nm.* Analyst, 2003. **128**(6): p. 686-691.

19. T. Zhao, J.-B. Fan, J. Cui, J.-H. Liu, X.-B. Xu, and M.-Q. Zhu, *Microwave-controlled ultrafast synthesis of uniform silver nanocubes and nanowires.* Chemical Physics Letters, 2011. **501**(4-6): p. 414-418.
20. R.S. Shallenberger and G.G. Birch, *Sugar Chemistry*. 1975, Westport, Connecticut: AVI Publishing Company, Inc.
21. K. Licht, C. Smith, and J. Mendoza, *Characterization of caramel colour IV.* Food and Chemical Toxicology, 1992. **30**(5): p. 365-373.
22. R. Boopathy, H. Bokang, and L. Daniels, *Biotransformation of furfural and 5-hydroxymethyl furfural by enteric bacteria.* Journal of Industrial Microbiology and Biotechnology, 1993. **11**(3): p. 147-150.

Supplementary Material

Chapters 2 and 3

Effects of bacteria percolation on time exposure to silver nanoparticles

A.1 Introduction

In the previous two chapters, the two types of bacteria tested, *E. coli* and *E. faecalis*, showed a considerable difference in susceptibility to silver toxicity, with *E. faecalis* being more resistant [1]. This may be due to several reasons such as different cell wall structure (gram positive vs. gram negative), the size of the bacteria, and the exposure time to AgNPs. In this section, we have explored the differences in the two types of bacteria in relation to the percolation time through the AgNP paper and by extension, the exposure time to the biocide.

A.2 Experimental

A.2.1 Bactericidal testing

Following the method previously described, the bactericidal activity of the AgNP paper was tested using *Enterococci faecalis* (ATCC #47077) [1]. To determine the approximate cell density of the bacteria suspensions, we measured the optical density at 600 nm using a UV-Vis spectrophotometer. The bacteria suspension corresponded to approximately 10^8 colony-forming units (CFU)/mL. This suspension (100 mL), a model for contaminated water, was passed through a sheet of AgNP paper, which was laid flat on a large, plastic grid with vertical walls to support the uniform 1-D flow. The effluent water was tested for viable bacteria, as follows. The effluent bacteria were removed

from the effluent water by centrifugation, which separated the excess silver leachate in the effluent water from the bacteria. The effluent bacteria were plated on mE nutrient agar plates. The nutrient agar plates were incubated overnight at 37°C for 24 hours and the colonies were counted. Three replicates were performed per paper. Standard deviation was reported.

A.2.2 Observations of Bacteria Morphology

Before and after percolation through the AgNP paper, bacteria samples were imaged through transmission electron microscopy (FEI Tecnai 12 120 kV TEM) and scanning electron microscopy (Hitachi model S-4700). For both types of microscopy, the samples were fixed in 2.5% glutaraldehyde overnight, and were dehydrated with increasing ethanol/water mixtures to 100% ethanol. For TEM preparation, following dehydration, the samples were cured with epoxy and sectioned with an ultramicrotome into 100 nm thick slices. The epoxied bacteria slices were deposited on carbon coated copper grids. In the preparation for SEM imaging, the samples were placed on a glass slide coated with poly-L-lysine, allowed to air dry, and sputter coated with Au Pd with a thickness of ~24 nm.

A.3 Results and Discussion

A.3.1 Comparison of percolation time of *E. coli and E. faecalis* as limiting biocide exposure

During the bactericidal tests, the percolation time was recorded to determine the flow rate through the AgNP papers. The flow rates were considerably faster for *E. faecalis* compared to *E. coli* (Figure A.1). The untreated blotter papers show the slowest flow rate out of all the different paper treatments for *E. coli* bacteria and pure Millipore

water. To assess the proportion of bacteria that passes through the blotter papers during bactericidal tests, the optical density before and after the percolation was measured (Figure A.2). The difference between the influent and effluent cell densities of bacteria was larger with *E. coli* than with *E. faecalis,* which suggests that a greater proportion of *E. coli* bacteria are retained in the blotter paper. Likewise, the log reduction following percolation through the untreated control blotter papers was larger for *E. coli* than for *E. faecalis*, log 1.81 (± 0.81) and log 0.99 (± 0.44), respectively, as reported in Chapter 3. Additionally, the size differences between *E. coli* and *E. faecalis* are shown by comparing Figures S2.2 from Chapter 2 and A.3, which show *E. coli* nearly twice the size of *E. faecalis.* The *E. faecalis* bacteria average size is 0.5 μm and *E. coli* is 1 by 2 μm.

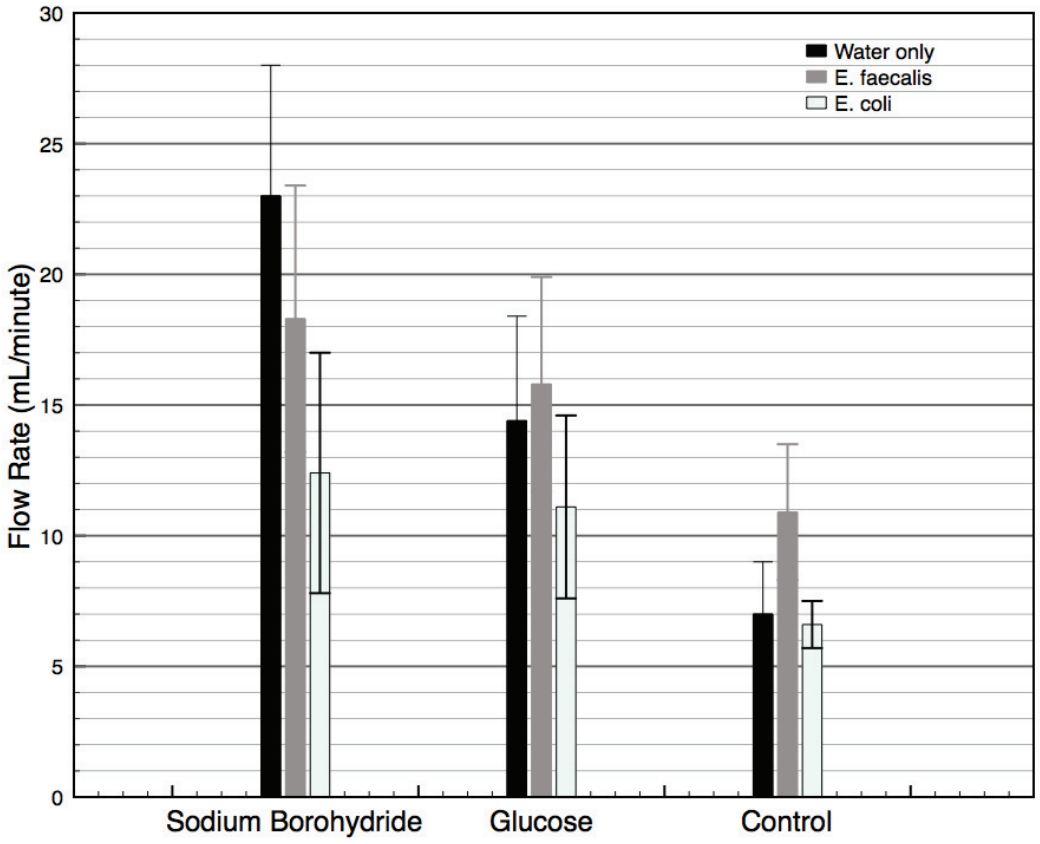

FIGURE A.1. Flow rate of bacterial suspensions and deionized water through AgNP papers and untreated control papers.

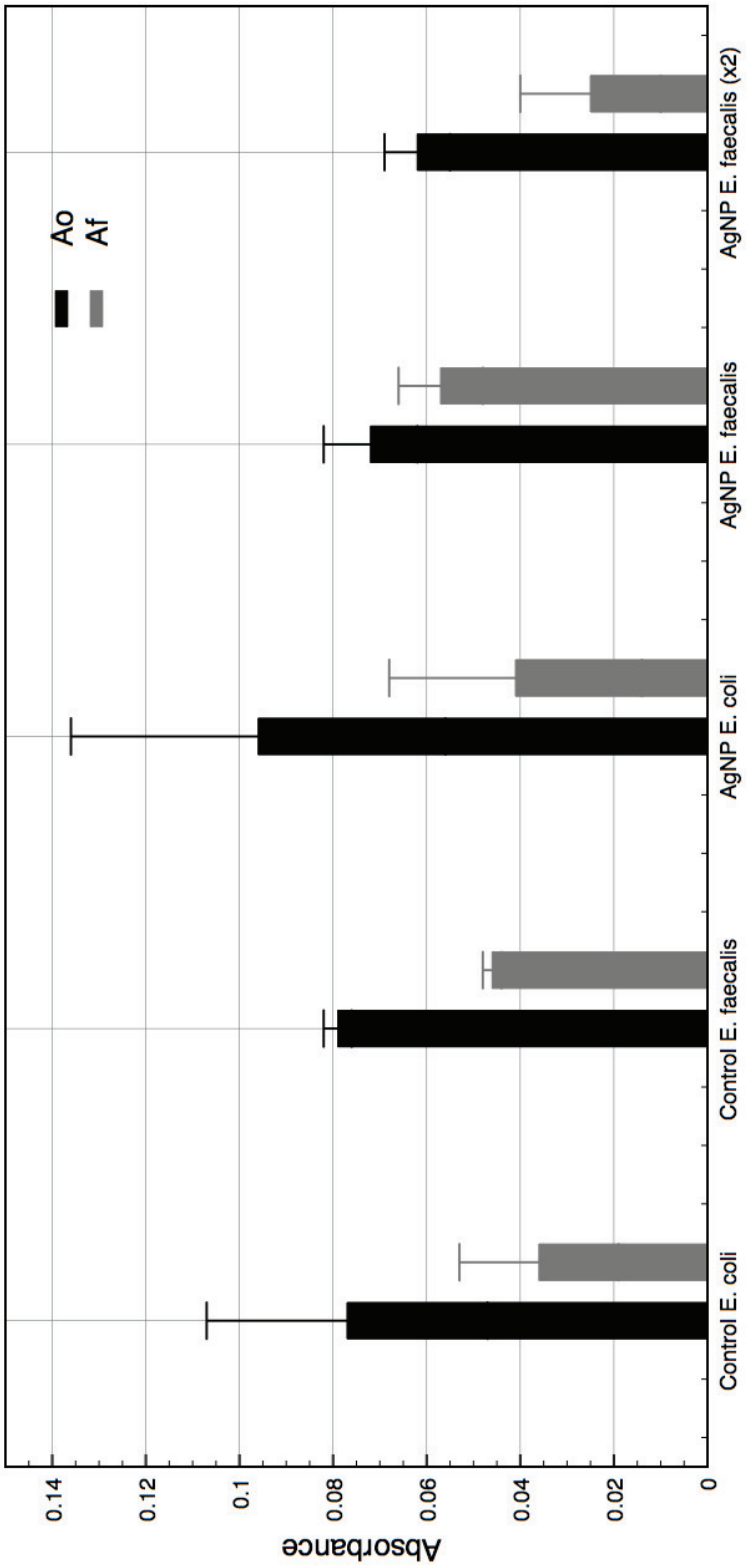

FIGURE A.2. Absorbance measurements before (A_o) and after (A_f) percolation through the blotter papers. The control is untreated blotter paper, and the AgNP paper was formed by glucose reduction. The AgNP paper x2 refers to two sheets of AgNP papers in the flow tests.

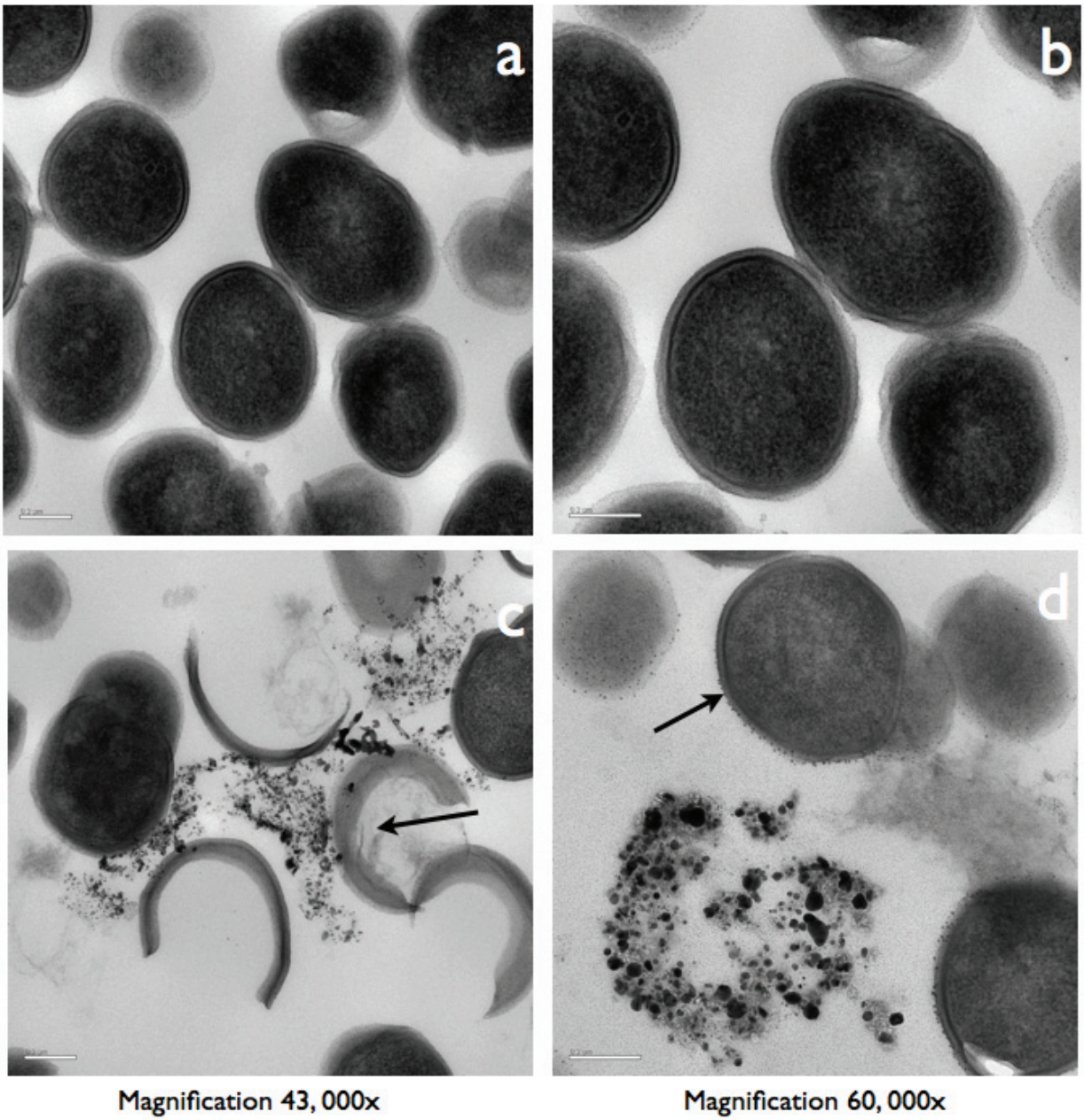

FIGURE A.3. Images of *E. faecalis* bacteria by TEM, following percolation experiments: (a) and (b) control paper (no silver), and after exposure to AgNP paper: (c) cell wall crescents remaining after AgNP exposure (arrow), and (d) attachment of AgNPs onto the bacterial cell wall. Magnification of (a) and (c) was 43,000x, and of (b) and (d) was 60,000x.

As previously shown in Chapters 2 and 3, *E. faecalis* was not as effectively inactivated as *E. coli* [1]. The smaller size of *E. faecalis* was shown to contribute to a faster flow rate through the AgNP paper, and therefore to reduce the overall time of exposure to AgNPs. To test the parameter of exposure time to the biocide, a new experiment was designed, where two sheets of AgNP papers were stacked in parallel in the filter unit and the rest of the bactericidal experiment was carried out. In general, a much higher log reduction of *E. faecalis* bacteria was observed by the double AgNP sheets tests, with an average log reduction of 4.8 (±2.5), than by single AgNP sheets, log 2.5 (±0.9) (Figure A.4). The flow rate of *E. faecalis* through the double sheets was nearly half as fast as the single sheets , which increased the exposure time to the biocide (Table A.1).

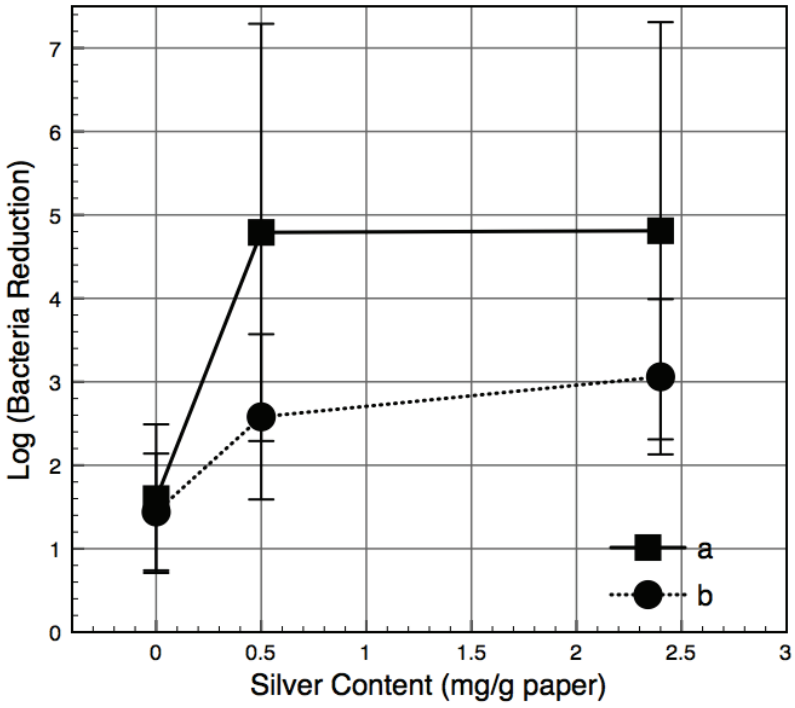

FIGURE A.4. Log reduction of *E. faecalis* bacterial count after permeation through the silver nanoparticle paper, at different silver contents in paper: (a) represents 2 stacked sheets of AgNP papers and (b) represents a singular AgNP paper. Initial bacterial concentration, 10^9 CFU/mL (log 9). Error bars represent standard deviation.

TABLE A.1. Change in flow rate of *E. faecalis* bacteria through the paper sheets with varying sheet counts.

Sample	Flow Rate (mL/minute)	
Control Paper	10.94	± 2.6
1 sheet AgNP	15.77	± 4.1
2 sheets AgNP	7.39	± 2.0

A.3.2 Morphological changes in bacteria

After percolation through the AgNP sheet, *E. faecalis* cells showed significant morphological changes when imaged by TEM (Figure A.3). In some cases, the *E. faecalis* cell membranes have detached from cytoplasm and left crescent shaped shells. Additionally, the deposition of AgNPs on the cell surface was observed in Figure A.3(d) In the SEM images, the *E. coli* cells exposed to silver nanoparticles appear to be shrunken due to structural collapse and have a scaly, porous, and rough surface (Figure A.5).

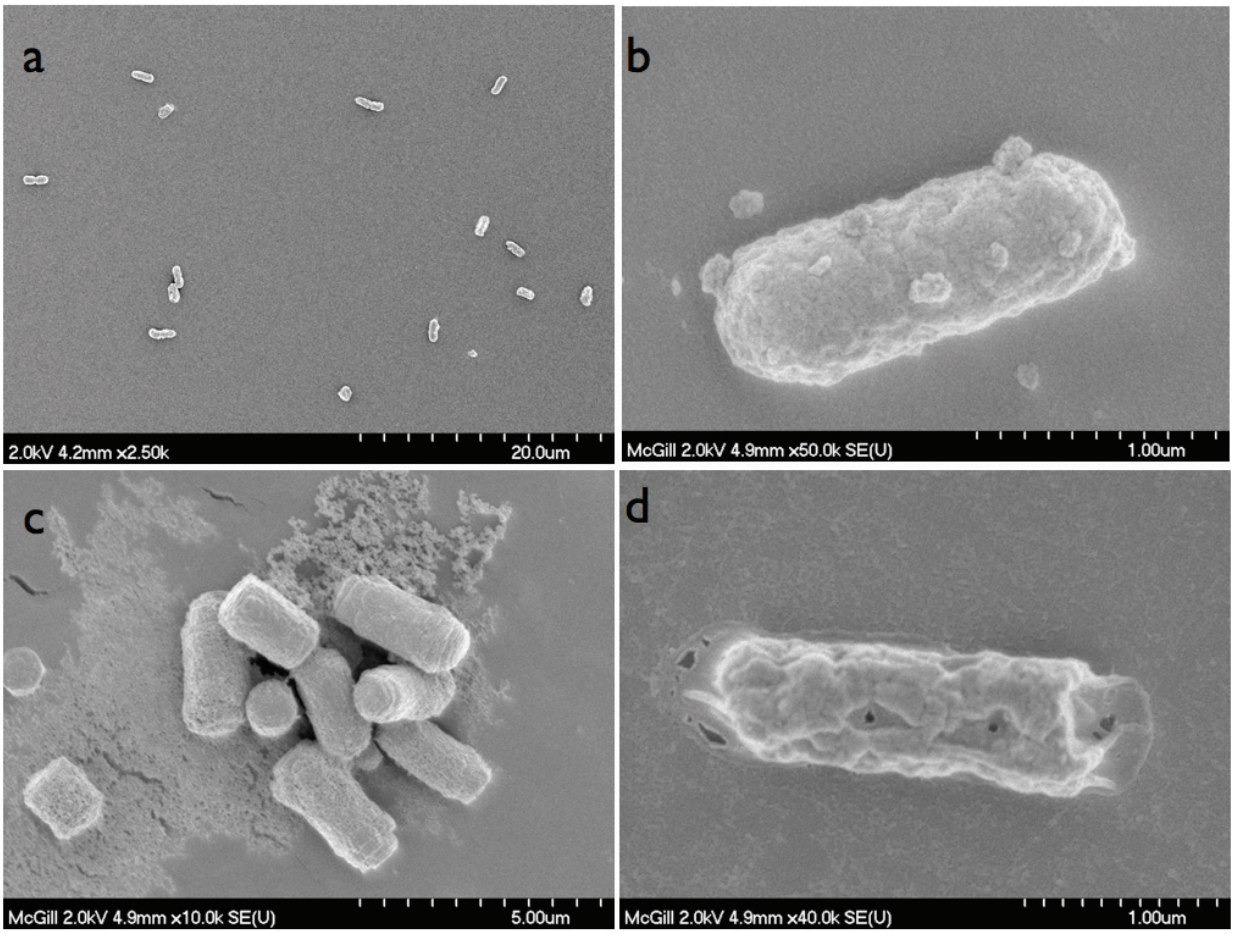

FIGURE A.5. SEM images of *E. coli* bacteria, following percolation experiments. (a) & (b) control paper (no silver). After exposure to AgNP paper: (c) scaly membranes and cytoplasm leakage and (d) shrinkage of cell wall structure.

A.3.3 Discussion

In the literature, specific understanding of how AgNPs inactivate bacterial cells is still being debated. The discussion centers around whether the release of silver ions, the release of reactive oxygen species, or the actual endocytosis of the whole nanoparticle are the causes for bacteria toxicity [2-6]. While we do not attempt to answer this question with this work, the understanding of disinfection kinetics for AgNPs is still unclear. Generally, the simplest model for disinfection kinetics relates the effectiveness to the biocide concentration multiplied by the exposure time to the biocide

[7]. This work supports the idea that different types of bacteria may need longer exposure time to AgNPs for effective disinfection. In practice, this implies that engineering design of a filter unit containing AgNP paper will have to take into account that the rate of disinfection for different microorganisms is variable.

A.4 References

1. T.A. Dankovich and D.G. Gray, *Bactericidal paper impregnated with silver nanoparticles for point-of-use water treatment.* Environ Sci Technol, 2011. **45**(5): p. 1992-1998.
2. C.-N. Lok, C.-M. Ho, R. Chen, Q.-Y. He, W.-Y. Yu, H. Sun, P.K.-H. Tam, J.-F. Chiu, and C.-M. Che, *Silver nanoparticles: partial oxidation and antibacterial activities.* J Biol Inorg Chem, 2007. **12**(4): p. 527-534.
3. A. Panacek, L. Kvitek, R. Prucek, M. Kolar, R. Vecerova, N. Pizurova, V. Sharma, T. Nevecna, and R. Zboril, *Silver colloid nanoparticles: Synthesis, characterization, and their antibacterial activity.* J Phys Chem B, 2006. **110**(33): p. 16248-16253.
4. I. Sondi and B. Salopek-Sondi, *Silver nanoparticles as antimicrobial agent: a case study on E-coli as a model for Gram-negative bacteria.* Journal of Colloid and Interface Science, 2004. **275**(1): p. 177-182.
5. J.R. Morones, J.L. Elechiguerra, A. Camacho-Bragado, K. Holt, J.B. Kouri, J.T. Ramírez, and M.J. Yacaman, *The bactericidal effect of silver nanoparticles.* Nanotechnology, 2005. **16**(10): p. 2346-2353.
6. E. Hwang, J. Lee, Y. Chae, Y. Kim, B. Kim, B. Sang, and M. Gu, *Analysis of the toxic mode of action of silver nanoparticles using stress-specific bioluminescent bacteria.* Small, 2008. **4**(6): p. 746-750.
7. K.H. Cho, J.E. Park, T. Osaka, and S.G. Park, *The study of antimicrobial activity and preservative effects of nanosilver ingredient.* Electrochimica Acta, 2005. **51**(5): p. 956-960.

Chapter 4

Silver nanoparticle stability on model nanocrystalline cellulose surfaces

This expands upon research in the previous chapters by investigating a model film of cellulose embedded with silver nanoparticles. The particular concerns include the long term stability and behavior of silver nanoparticles in nano-composite materials. The films of nanocrystalline cellulose are very much smoother that the paper substrates described in previous chapters, and this facilitates imaging, spectroscopic examination, and contact angle measurements on the silver nanoparticle-cellulose system. This work has not yet been published.

4.1 Abstract

The broad spectrum bactericidal properties of silver nanoparticles (AgNPs) have led to their widespread use in consumer products. These applications require consideration of their possible chemical and physical changes during the product's lifespan and the potential end-of-life impact on the environment. Many nanotechnology consumer products do not contain free nanoparticles, but rather embedded nanoparticles in polymer matrices or on surfaces. This study investigates the stability and aggregation of AgNP cellulose materials, as a model nanocomposite material. In this study, we formed AgNP on nanocrystalline cellulose (NCC) thin films, which can be used as a model to study the behavior of AgNPs formed on other cellulose materials, such as cotton fabric, paper, and bacterial cellulose. Thin cast films of NCC provide a model for flat cellulose surfaces, without the complex morphology of natural cellulose fibers [1]. Such flat surfaces facilitate interpretation of contact angle, electron microscopy, and spectroscopic measurements. Additionally, changes in the films were studied for the stability of AgNPs after a two year time period. Nanoparticle aggregation was more pronounced after exposure to high salt concentrations than over a two year time period. This research represents a novel way to investigate the aggregation behavior of nano-Ag on solid surfaces.

4.2 Introduction

Because silver nanoparticles inactivate a broad spectrum of bacteria [2], they have been used in various consumer products, such as cosmetics, textiles, medical devices, water filters, etc. [3]. Often in these applications, the AgNPs are embedded in a polymer matrix or coated on the surface of a solid material, referred to as a

nanocomposite material. The interactions of Ag nanocomposites with aqueous solutions is an important aspect for many antibacterial applications. Depending upon the specific dissolved compounds present in solutions in contact with the Ag nanocomposites, the AgNPs may become unstable and may release silver in the form of ions, particles or aggregates [4]. Consequently, the AgNP-containing product may become less effective as a biocide. Knowledge of the aggregation behavior and ion release of silver nanoparticles in nanomaterial hybrids can lead to better product design. Previously, researchers have evaluated the degradation and fate of AgNPs embedded in solids via indirect methods, such Ag ion and particle release measurements [4-6], and more recently, through particle immobilization and weathering on TEM grids [7].

The motivation for studying thin nanocrystalline cellulose (I) films embedded with silver nanoparticles is to analyze the stability of AgNPs in a model solid system. Previously, suspensions of cellulose nanocrystals have been used to stabilize or form silver nanoparticles [8-10]. We have formed the silver nanoparticles directly on the surface of the pure NCC film, instead of in suspension, as previously done [4-6]. Researchers have previously made composite films of NCC, AgNPs, and polylactic acid polymer films [11]. The complexities of a paper or cotton fiber system, such as rough, non-flat surfaces have been avoided by use of a NCC model film. The silver nanoparticles formed on NCC films are more easily characterized than AgNPs on cellulose fibers. The NCC films are translucent, which facilitates UV-Vis spectrophotometry for the characterization of surface plasmon resonance peaks from AgNPs. The non-porous surfaces of NCC films limit the formation of nanoparticles within the material, which results in the formation of AgNPs only on the surface of the films. Whereas in contrast, for other metal nanoparticles formed in cellulosic fibers, other researchers have observed a fraction of platinum nanoparticles in the interior of the fibers [12].

In this study, NCC AgNP films were examined as a model material to study aggregation phenomena of AgNPs in a nano-composite, rather than in a suspension. Previously, aggregation phenomena of AgNPs have been studied primarily in suspension [13-17]. Key differences with studying nanoparticles embedded in a surface compared to in suspension include to the methods employed for analysis. In suspensions, previously used methods include dynamic light scattering, transmission electron microscopy, spectrophotometry, atomic absorption for Ag ion and particle release, and zeta potential [13, 15, 16]. Of these methods, the TEM analysis, for primary particle size and morphology, and spectrophotometry, for changes in SPR peaks, can overlap between characterization of the nanoparticles in solids compared to in suspensions. In addition, we also used SEM to study changes in particle morphology.

Substances dissolved in the aqueous media are expected to affect the stability of AgNPs. Some of the dissolved compounds that have also been studied by other authors with respect to aggregation phenomena include: dissolved organic matter, dissolved solids (i.e. magnesium, calcium, sulfate, phosphate, etc), and proteinaceous matter. Other parameters that can also contribute include the pH, ionic strength, and ionic composition of the media [13, 14, 16, 18]. We have examined the AgNP aggregation behavior with respect to time stability and salt solutions, although we have not tested for some of the commonly encountered solutes, such as proteins, natural organic matter, pH, etc. For real world applications, e.g. water treatment, silver nanocomposites may be exposed to brackish waters, so the understanding of AgNP aggregation behavior in saline solutions is highly relevant.

In this study, silver nanoparticles were formed by an *in situ* reduction on the surface of NCC cellulose films. We examined the impact of salts solutions and lengthy time periods on the aggregation behavior of AgNPs embedded in NCC films, via UV-Vis spectrophotometry absorbance, TEM, and SEM. We also characterized the wetting

properties of AgNP NCC films, to better understand the aqueous interactions with these nanocomposites. From our previous work, ease of wetting was established as an important criterion for the use of the AgNP paper in water purification [19], and the use of the smooth model films simplifies the interpretation of contact angle measurements.

4.3 Experimental

4.3.1 Materials

Colloidal suspensions of cellulose nanocrystals were made from cotton fibers (Whatman No.1 filter paper) following a previously published method [1]. Silver nitrate ($AgNO_3$), sodium borohydride (NaBH4), 30% hydrogen peroxide (H_2O_2), concentrated nitric acid (HNO_3), poly(L-lysine) (0.01% solution), and sodium chloride were purchased from Sigma Aldrich and used as received. Water treated with a Barnstead Nanopure system was used throughout.

4.3.2 Preparation of silver nanoparticle (AgNP) cellulose thin films and suspensions

We prepared cellulose films from nanocrystalline suspensions on polystyrene (PS) Petri dishes. To form a thick and free-standing film, we evaporated 5 mL aliquots of 2.65% (w/w) cellulose nanocrystal suspension on the PS petri dish at 60°C overnight. The film thickness was approximately 130 μm for the NCC films. To stabilize the films and prevent the re-dispersion of the nanocrystals, we heated them at 105°C for 20-30 minutes. The heat treatment removes sulfate groups from the surface of the cellulose nanocrystals [20].

Silver nanoparticles were formed on the surface of the NCC films through similar methods to those described in Chapter 2 [19]. The films were soaked in 1-10 mM silver

nitrate solutions, then blotted dry, and placed into a sodium borohydride bath with a concentration of 0.25 M. Following reduction, the films were soaked in a water bath for an hour. The films were subsequently air dried and stored in glass petri dishes wrapped in aluminum foil until further use.

Similarly, AgNPs were synthesized in NCC suspensions. To a 20 mL volume of 0.2% NCC suspension, silver nitrate concentrations from 1 mM to 100 mM were added and stirred well. The silver ions were reduced by a 0.02M solution of sodium borohydride.

4.3.3 Characterization of AgNP cellulose films and suspensions

The color changes of the AgNP NCC films were established by measuring the absorbance spectra on a UV-Vis spectrophotometer (Varian TCA-Cary 300) at wavelengths of 300 to 800 nm. The translucent films were placed in cuvettes and immersed in Millipore water to measure the absorbance spectra. Silver nanoparticles show surface resonance peaks (SPR) in the visible spectra between 400-600 nm, with different maximum intensities related to the shape of the nanoparticle [21, 22]. The shape and size distribution of the silver nanoparticles in the film were examined by electron microscopy. Small pieces of the AgNP NCC films were deposited on carbon coated copper grids that had been treated with poly(L-lysine), and imaged with a Philips CM200 200 kV transmission electron microscope (TEM). Nanoparticle diameters were measured for greater than 100 particles per sample, with standard deviation values reported. Imaging and elemental analysis of the AgNP NCC films was performed with a field emission scanning electron microscopy (Hitachi S-4700 FE-SEM) attached to an energy-dispersive X-ray spectroscopy detector (EDX). For SEM, samples were sputter coated with a thin 24 nm layer of AuPd prior to imaging and analysis. To quantify the amount of silver in the AgNP NCC films, we performed an acid digestion of the films and analyzed the amount of dissolved silver with a flame atomic absorption spectrometer

(Perkin Elmer AAnalyst 100), as described previously in Chapter 2 [19]. The silver content reported is five replicates per sample concentration with standard deviation error bars.

4.3.4 Stability of AgNPs in cellulosic materials

To investigate the potential for silver nanoparticle aggregation in cellulosic materials, we used the AgNP NCC films as a model material. Following AgNP formation, the AgNP NCC films were either set aside to age or exposed to salt solutions. The former were kept in the glass petri dishes for 2.5 years. The latter were soaked in a 10 mL solution of 1M NaCl for 60 minutes, removed from the salt solution, and allowed to air dry. Subsequently, the films were characterized via methods in section 4.3.3.

4.3.5 Contact angle measurement

Contact angles were measured on sessile drops with a goniometer (contact angle system OCA20, Dataphysics, Germany) and a CCD camera at room temperature (23°C) in air with a relative humidity of 10–25%. A 3 µL drop volume of the probe liquid was placed on the cellulose surface from a micro-syringe (Hamilton-Bonaduz). To determine the advancing contact angles, θ_a, we added ~2 µL more liquid to the drop on the surface in order to gently advance the contact line. For receding contact angles, θ_r, liquid was withdrawn with the syringe needle until the contact line retracted (Figure 4.1). Measurements were made on ten or more drops and averaged. Unless stated otherwise, each measurement was made on a new spot.

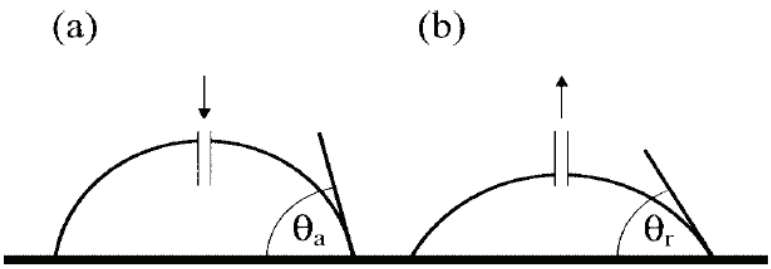

FIGURE 4.1. Side view of a sessile liquid drop on a solid surface showing advancing and receding contact angles, θ_a and θ_r. (a) Liquid is added to the drop and the contact angle advances. (b) As liquid is withdrawn, the contact line remains pinned until the contact angle decreases to θ_r, then the contact angle recedes [23].

4.4 Results and discussion

4.4.1 AgNP characterization on cellulose substrates

The silver nanoparticles were readily formed on the surface of the NCC substrate by reduction of silver ions with an excess of sodium borohydride. Similarly, the AgNPs were formed in suspension with a dilute concentration of NCC and a 2:1 molar ratio of sodium borohydride to silver nitrate. The films changed color from translucent white to yellow/orange with increasing precursor silver ion concentrations (Figure 4.2). Similar color changes were observed in AgNP NCC suspensions (Figure 4.2). The color changes in the NCC films are due to the surface plasmon resonance (SPR) of silver nanoparticles. UV-Vis absorbance spectroscopy (Figure 4.3, dashed lines) showed a peak at 420 nm, which falls in the characteristic SPR range (390-420 nm) for spherical silver nanoparticles [21]. The AgNP NCC suspensions showed a narrower SPR peak at 385 nm as compared to the AgNP NCC films (Figure 4.3, solid lines). The broader SPR peak in the NCC film spectra may be due to an increase in polydispersity of the

nanoparticles. The untreated NCC films do not show any absorbance in the UV-Vis spectra, and thus are not included in Figure 4.3.

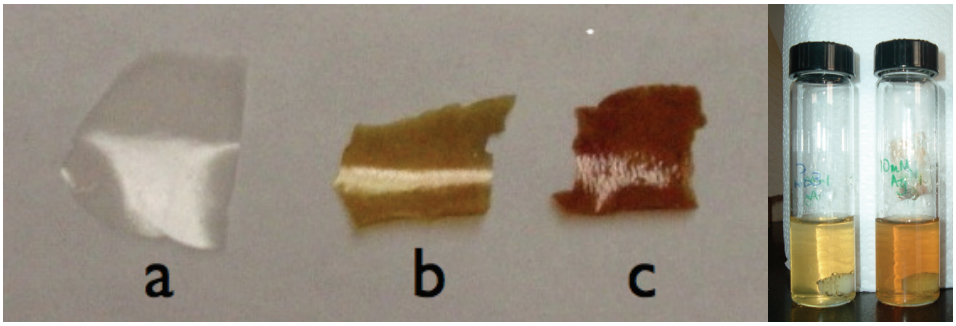

FIGURE 4.2. Nanocrystalline cellulose films , (a) unmodified (no silver), and with silver nanoparticles: (b) 1.6 mg Ag/ g film and (c) 4.3 mg Ag/ g film. Each film is approximately 1-2 cm, with irregular shapes due to the brittle nature of NCC films. The two vials contain NCC suspensions with AgNPs, with precursor silver concentrations of 2 mM (left) and 10 mM (right).

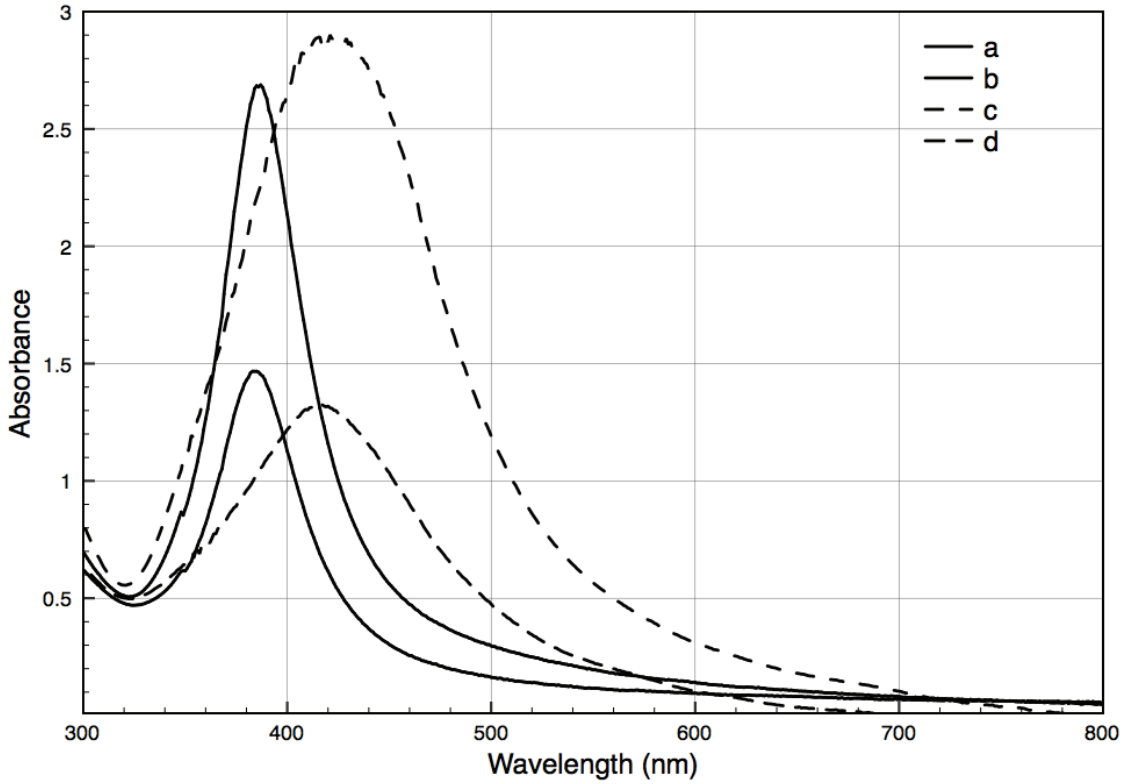

FIGURE 4.3. UV-Visible absorbance spectra of NCC films and suspensions with different silver nanoparticle contents, (a) 2 mM Ag suspension, (b) 10 mM Ag suspension, (c) 1.6 mg Ag/ g film, and (d) 4.3 mg Ag/ g film. The lower absorbance peaks correspond to the lower silver concentrations. The solid line represents the suspension and the broken line pattern represents the films. Film thickness is ~ 130 micrometers.

The AgNPs formed on the model NCC films appeared quite similar to the ones formed in blotter papers, in terms of particle size, size distribution, and morphology [19]. Spherical nanoparticles were observed by SEM (Figure 4.4 (a)) and TEM (Figure 4.5 (a)). The average diameter of the AgNPs in the model NCC films was 5.2 ± 2.4 nm, as determined through TEM imaging and analysis (Figures 4.5 (a) and 4.6 (black bars)).

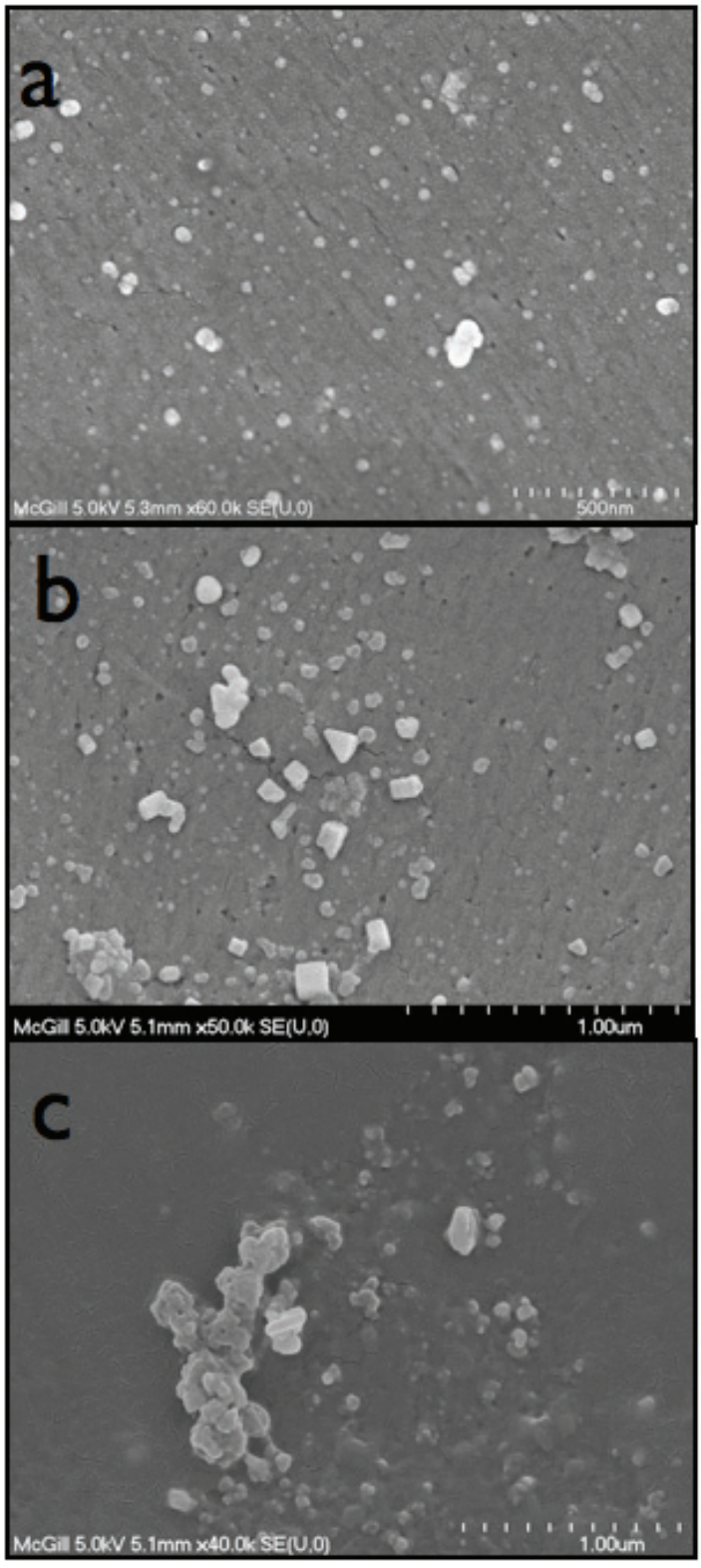

FIGURE 4.4. SEM images of NCC AgNP films (a) freshly prepared, (b) following 1M NaCl soaking and drying, and (c) as in (a) following aging 2.5 years.

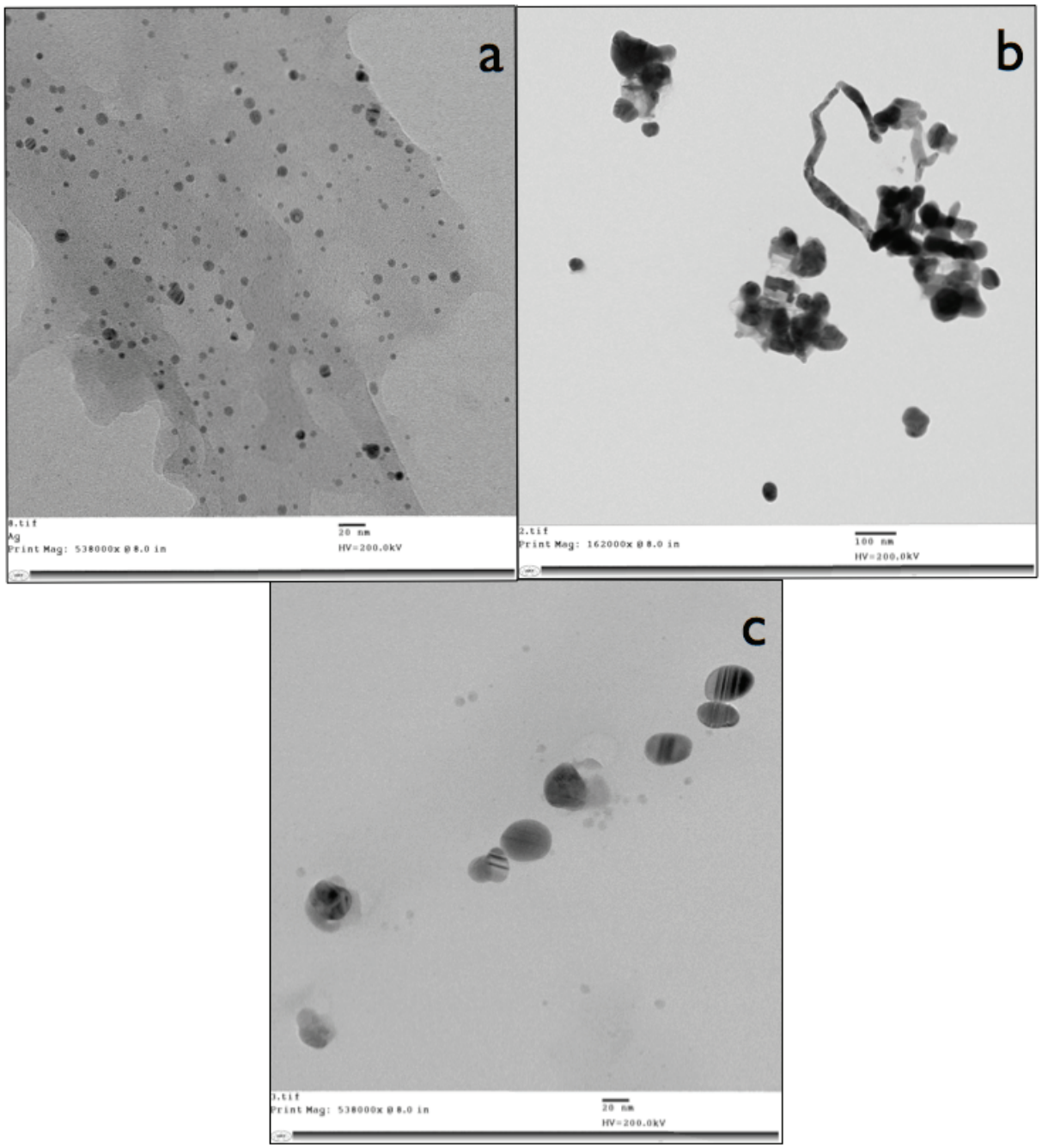

FIGURE 4.5. TEM images of NCC AgNP films (a) freshly prepared, (b) following 1M NaCl soaking and drying, and (c) as in (a) following aging 2.5 years. Note that the scale bar on (b) is 100 nm, while it is 20 nm on (a) and (c).

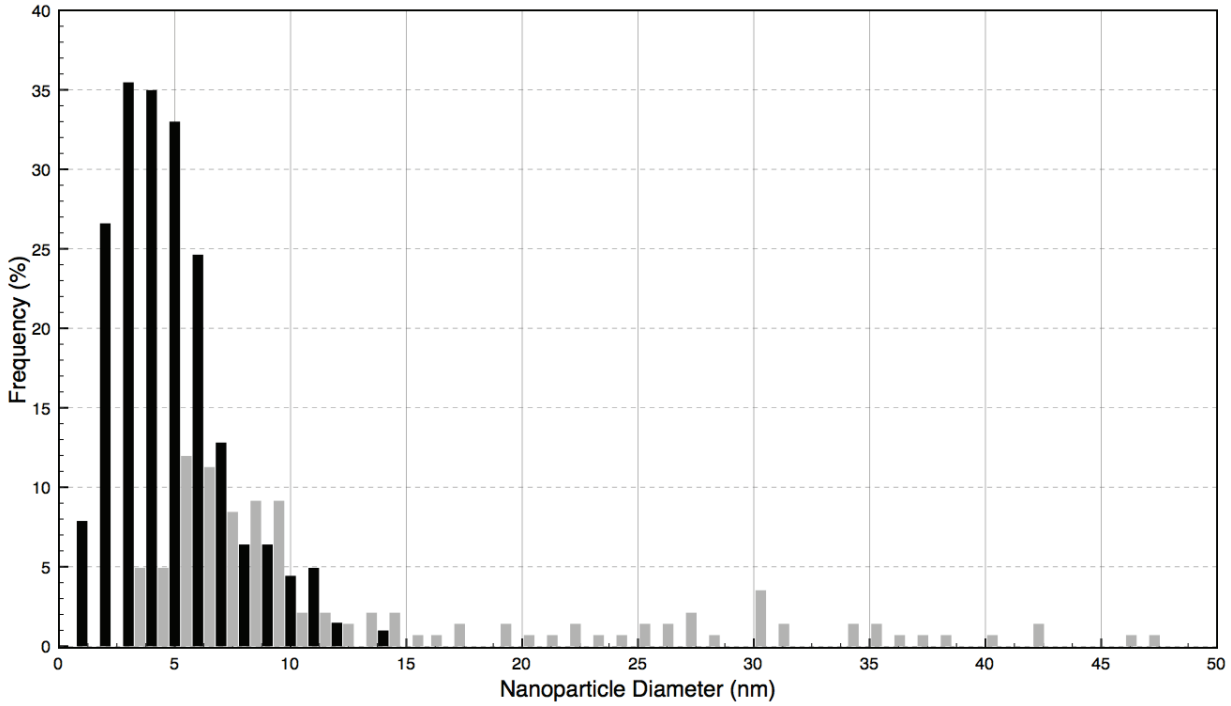

FIGURE 4.6. Nanoparticle diameter size histogram of silver nanoparticles on NCC films: freshly prepared (black bars) and aged 2.5 years (gray bars).

4.4.2 Stability of AgNP cellulosic materials

The stability of AgNPs in cellulosic materials is dependent upon a number of factors. Firstly, silver is sensitive to UV light, and so silver compounds, nanoparticle suspensions and nano-composite materials should always be stored in the dark. Even films carefully wrapped in aluminum foil show some color change after a couple of years (Figure 4.7 (b)), indicating some particle aggregation. Over several months, these films do not show any notable color changes when stored in the dark and are generally considered stable. Secondly, the solution chemistry can cause more extreme silver particle aggregation, as we observed from exposure to concentrated NaCl solutions (Figure 4.7 (c)).

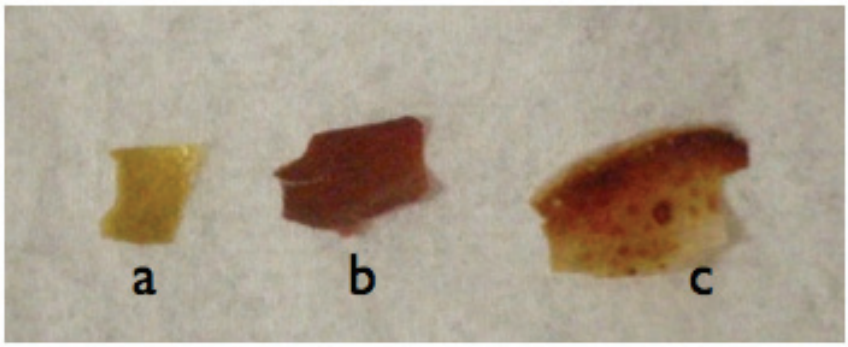

FIGURE 4.7. Color changes in the AgNP NCC films: (a) freshly prepared AgNP NCC film, (b) AgNP NCC film aged 2.5 years, and (c) AgNP NCC film soaked in 0.1 M NaCl.

In general, when silver nanoparticles begin to aggregate on cellulosic surfaces, the color changes to a purple and/or red colored material, instead of the typical yellow/ orange color for non-aggregated silver nanoparticles. This results in a red shift in the SPR peak in the absorbance spectra (Figure 4.8). Some of the changes observed include the formation of cubic and/or prism shaped nanoparticles and the grape-like agglomeration of spherical nanoparticles (Figure 4.4). The former seems more typical for AgNP exposure to 1M NaCl solutions, as depicted in Figure 4.4 (b), and the SPR peak of 465 nm in Figure 4.8. The latter agglomeration seems more typical of the formation of agglomerates over a long time period (Figure 4.4 (c)), which shows two SPR peaks, one of the spherical particles at 406 nm and one red shifted at 480 nm. Through TEM analysis, the average particle diameter sizes were observed with a much higher increase for the NaCl exposure (45.1 ± 23.9 nm) than for aged NCC AgNP films (16.6 ± 12.8 nm) (Figures 4.5 (b,c) and 4.6 (gray bars). Another observation of nanoparticle degradation is shown by the diffraction patterns seen in Figure 4.5 (c), which result from defects in the crystalline structure of the nanoparticles.

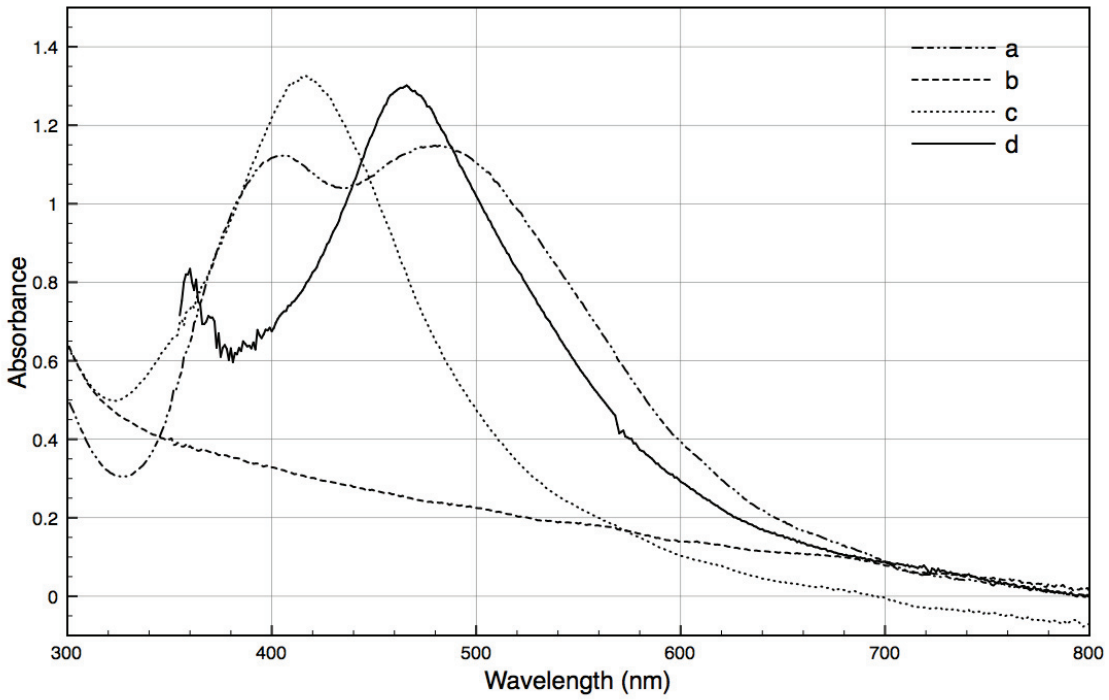

FIGURE 4.8. UV-Vis spectrophotometry changes in the AgNP NCC films: a) AgNP NCC film aged 2.5 years, (b) control (unmodified NCC), (c) freshly prepared AgNP NCC film, and (d) AgNP NCC film soaked in 0.1 M NaCl and subsequently dried.

UV/visible spectrophotometry can be used to help characterize nanoparticle agglomeration since the localized SPR bands change upon agglomeration [13, 24]. The spectral red shift observed following exposure of AgNP NCC films to 1M NaCl may be representative of the SPR peak for cubic AgNPs [22] or larger spherical AgNPs with a diameter greater than 60 nm [14, 25], as supported by large particle size increases and morphological changes observed via electron microscopy (Figures 4.4, 4.5).

In the aged AgNP NCC films, there was a slight increase in the average particle size from the freshly prepared AgNP NCC films, and the emergence of a bimodal particle size distribution (Figure 4.6). The mixture in particle sizes is also shown directly by TEM imaging in Figure 4.5(c) and indirectly through the two SPR peaks in Figure 4.8. With the adsorption of a thin aqueous layer from the humidity, some of the surface may dissolve as silver nitrate and subsequently can recrystallize on larger particles. This can

create a disordered crystalline structure in the nanoparticles, which can account for the diffraction pattern seen in the TEM image (Figure 4.5(c)).

The greater impact on the stability of AgNPs in NCC films came from the 1M NaCl solutions. The EDX spectra of NCC AgNP films exposed to NaCl shows the peaks of sodium and chloride in addition to silver (Figure 4.9). EDX can only qualitatively describe the metal speciation, and a more thorough assessment would require X-ray absorption spectroscopy [26]. Due to the distinctive peaks for sodium, chloride, and silver in the EDX spectra, this suggests the formation of AgCl. Over a period of several months, the NCC AgNP films exposed to NaCl turn a cloudy white color with a UV-Vis absorbance spectrum similar to that of the control NCC films (data not shown). This also supports the idea that AgNPs have disappeared and AgCl and NaCl salt particles have formed on the NCC films. The possibility of conversion of AgNPs into “AgCl nanoparticles” is unlikely, and we did observe an absorbance peak at 250 nm, as is typical for AgCl NPs [27]. In AgNP suspensions, the literature suggests that the addition of a high concentration of chloride ions can lead to initial particle aggregation, the formation of AgCl precipitates, and eventually facilitate Ag dissolution [17, 18].

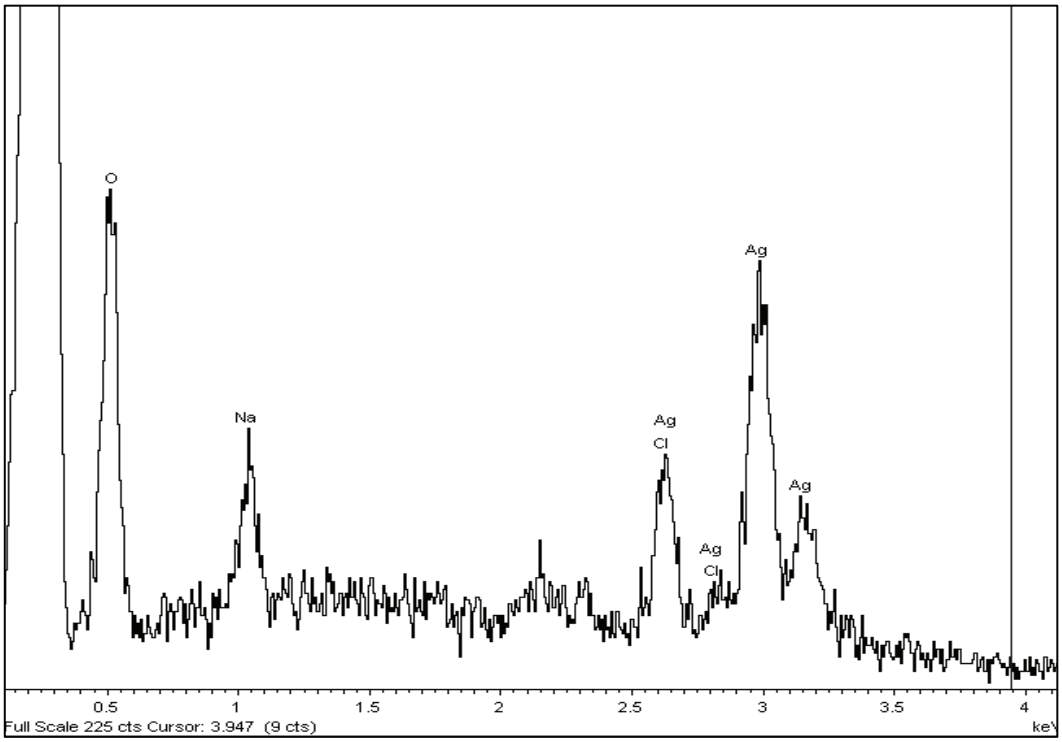

FIGURE 4.9. EDX spectrum of the NCC AgNP film exposed to NaCl. Samples were sputter coated with Au Pd.

4.4.3 Contact Angle Measurement of AgNP NCC films

The advancing and receding contact angles on the surfaces of unmodified free-standing nanocrystalline cellulose [28] and on the cellulose surfaces modified with silver nanoparticles are summarized in Table 4.1. The overall difference in water contact angles between the AgNP NCC films and unmodified NCC films is relatively minor. The free-standing nanocrystalline cellulose films had the lowest advancing water contact angle (29.2°), the lowest receding contact angle (15.5°) and hence the lowest hysteresis value of 13.7° [70]. The AgNP NCC films showed slightly higher advancing and receding contact angles (θ_A = 40.3-41.8°, θ_R = 18.1-21.8°) and higher hysteresis (20.0-22.2°), and did not differ in relation to silver content, at these levels. These differences are not expected to greatly impact the properties related to interactions with aqueous solutions.

TABLE 4.1. Advancing (θ_A) and receding (θ_R) contact angles and hysteresis (θ_A - θ_R) (in degrees) with standard deviations for water on cellulose film surfaces with silver nanoparticles.

Surface	θ_A	θ_R	(θ_A - θ_R)
Nanocrystalline Cellulose (I)			
Free-standing Film	29.2 ± 2.7	15.5 ± 2.4	13.7 ± 1.7
Nanocrystalline Cellulose (I) with AgNPs			
1.6 mg Ag/ g cellulose	40.3 ± 7.0	18.1 ± 7.1	22.2 ± 6.4
4.3 mg Ag/ g cellulose	41.8 ± 5.1	21.8 ± 4.9	20.0 ± 4.3

Silver metal is a high energy solid with a measured surface free energy of 1200 mJ/m^2 [29], and would be expected increase the hydrophilicity of the AgNP NCC film surface [30]. This is contrary to the results in Table 4.1. However, silver metal has been observed to adsorb hydrophobic compounds from the air, and the advancing water contact angle on silver metal has shown increases from 40 to 95 degrees over a short time period of a few minutes [30]. This suggests that the NCC film contributes more significantly to the water contact angle measurements. To estimate the surface coverage of NCC and silver nanoparticles from contact angle measurements, the Cassie-Baxter equation can be used. The Cassie-Baxter equation describes the effective contact angle, θ_c, of a liquid on a heterogenous surface [31]:

$$\cos\theta_c = f_1 \cos\theta_1 + f_2 \cos\theta_2$$

where θ_1 is the contact angle for component 1 with fraction f_1 and θ_2 is the contact angle for component 2 with fraction f_2 present in the composite material. Using the value of 95° for silver (θ_2) with absorbed hydrophobic compound [30], the advancing contact angles for the unmodified NCC film, and the two AgNP NCC films in Table 4.1, the surface area fractions were determined. The apparent AgNP surface area fractions (f_2) ranged from 11.5% to 13.3%.

4.5 Conclusion

NCC films prepared with AgNPs were flat, smooth and translucent samples. These properties made them easy to characterize and to follow their aggregation processes from UV-Vis spectrophotometry, electron microscopy, and contact angle measurements. The AgNP NCC films are generally stable for several months in the dark. Under very high ionic strength conditions, the stability of AgNPs is reduced and strong signs of aggregation were observed. This study represents a novel way to examine the changes in metal nanoparticles on solid surfaces under various environmental conditions, such as salinity, moisture, pH, etc.

4.6 Acknowledgements

This work was supported by the Sentinel Bioactive Paper Network. We gratefully acknowledge the training and use of facilities at McGill from Line Mongeon (SEM) and Xue Dong Liu (TEM).

4.7 References

1. C.D. Edgar and D.G. Gray, *Smooth model cellulose I surfaces from nanocrystal suspensions.* Cellulose, 2003. **10**(4): p. 299-306.
2. R. Davies and S. Etris, *The development and functions of silver in water purification and disease control.* Catalysis Today, 1997. **36**(1): p. 107-114.
3. E. Fauss, *The Silver nanotechnology commercial inventory.* Project on Emerging Nanotechtnologies, 2008: p. 21.
4. T.M. Benn and P. Westerhoff, *Nanoparticle silver released into water from commercially available sock fabrics.* Environ Sci Technol, 2008. **42**(11): p. 4133-4139.
5. C.A. Impellitteri, T.M. Tolaymat, and K.G. Scheckel, *The speciation of silver nanoparticles in antimicrobial fabric before and after exposure to a hypochlorite/ detergent solution.* Journal of Environment Quality, 2009. **38**(4): p. 1528.
6. L. Geranio, M. Heuberger, and B. Nowack, *The behavior of silver nanotextiles during washing.* Environ Sci Technol, 2009. **43**(17): p. 6458-6462.
7. R.D. Glover, J.M. Miller, and J.E. Hutchison, *Generation of metal nanoparticles from silver and copper objects: Nanoparticle Dynamics on Surfaces and Potential Sources of Nanoparticles in the Environment.* ACS Nano, 2011. **5**(11): p. 8950-8957.
8. Y. Shin, I.-T. Bae, B.W. Arey, and G.J. Exarhos, *Facile stabilization of gold-silver alloy nanoparticles on cellulose nanocrystal.* J Phys Chem C, 2008. **112**(13): p. 4844-4848.
9. H. Liu, D. Wang, Z. Song, and S. Shang, *Preparation of silver nanoparticles on cellulose nanocrystals and the application in electrochemical detection of DNA hybridization.* Cellulose, 2011. **18**(1): p. 67-74.
10. N. Drogat, R. Granet, V. Sol, A. Memmi, N. Saad, C. Klein Koerkamp, P. Bressollier, and P. Krausz, *Antimicrobial silver nanoparticles generated on cellulose nanocrystals.* Journal of Nanoparticle Research, 2011. **13**(4): p. 1557-1562.

11. E. Fortunati, I. Armentano, Q. Zhou, A. Iannoni, E. Saino, L. Visai, L.A. Berglund, and J.M. Kenny, *Multifunctional bionanocomposite films of poly(lactic acid), cellulose nanocrystals and silver nanoparticles.* Carbohydrate Polymers, 2011: p. 1-37.
12. H. Dong and J.P. Hinestroza, *Metal nanoparticles on natural cellulose fibers: Electrostatic assembly and in situ synthesis.* ACS Appl. Mater. Interfaces, 2009. **1**(4): p. 797-803.
13. J.M. Zook, R.I. Maccuspie, L.E. Locascio, M.D. Halter, and J.T. Elliott, *Stable nanoparticle aggregates/agglomerates of different sizes and the effect of their size on hemolytic cytotoxicity.* Nanotoxicology, 2010. **5**(4): p. 517-530.
14. A.M. El Badawy, T.P. Luxton, R.G. Silva, K.G. Scheckel, M.T. Suidan, and T.M. Tolaymat, *Impact of environmental conditions (pH, ionic strength, and electrolyte type) on the surface charge and aggregation of silver nanoparticles suspensions.* Environ Sci Technol, 2010. **44**(4): p. 1260-6.
15. R.C. Murdock, L. Braydich-Stolle, A.M. Schrand, J.J. Schlager, and S.M. Hussain, *Characterization of nanomaterial dispersion in solution prior to in vitro exposure using dynamic light scattering technique.* Toxicological Sciences, 2008. **101**(2): p. 239-253.
16. X. Jin, M. Li, J. Wang, C. Marambio-Jones, F. Oeng, X. Huang, R. Damoiseaux, and E.M.V. Hoek, *High-throughput screening of silver nanoparticle stability and bacterial inactivation in aquatic media: Influence of specific ions.* Environ Sci Technol, 2010: p. 1-8.
17. J. Liu, D.A. Sonshine, S. Shervani, and R.H. Hurt, *Controlled release of biologically active silver from nanosilver surfaces.* ACS Nano, 2010. **4**(11): p. 6903-6913.
18. J. Liu and R.H. Hurt, *Ion Release kinetics and particle persistence in aqueous nano-silver colloids.* Environ Sci Technol, 2010. **44**(6): p. 2169-2175.
19. T.A. Dankovich and D.G. Gray, *Bactericidal paper impregnated with silver nanoparticles for point-of-use water treatment.* Environ Sci Technol, 2011. **45**(5): p. 1992-1998.

20. J Revol, L Godbout, and Derek G Gray, *Solid self-assembled films of cellulose with chiral nematic order and optically variable properties.* Journal of Pulp and Paper Science, 1998. **24**(5): p. 146-149.
21. A. Henglein, *Colloidal silver nanoparticles: photochemical preparation and interaction with O_2, CCl_4, and some metal ions.* Chem. Mater., 1998. **10**: p. 444-450.
22. T. Zhao, J.-B. Fan, J. Cui, J.-H. Liu, X.-B. Xu, and M.-Q. Zhu, *Microwave-controlled ultrafast synthesis of uniform silver nanocubes and nanowires.* Chemical Physics Letters, 2011. **501**(4-6): p. 414-418.
23. C.W. Extrand, *Water contact angles and hysteresis of polyamide surfaces.* J Coll Interf Sci, 2002. **248**: p. 136-142.
24. S.L. Chinnapongse, R.I. Maccuspie, and V.A. Hackley, *Persistence of singly dispersed silver nanoparticles in natural freshwaters, synthetic seawater, and simulated estuarine waters.* Science of the Total Environment, 2011. **409**(12): p. 2443-2450.
25. R.I. MacCuspie, K. Rogers, M. Patra, Z. Suo, A.J. Allen, M.N. Martin, and V.A. Hackley, *Challenges for physical characterization of silver nanoparticles under pristine and environmentally relevant conditions.* J. Environ. Monit., 2011. **13**(5): p. 1212.
26. R. Kaegi, B. Sinnet, S. Zuleeg, H. Hagendorfer, E. Mueller, R. Vonbank, M. Boller, and M. Burkhardt, *Release of silver nanoparticles from outdoor facades.* Environmental Pollution, 2010. **158**(9): p. 2900-2905.
27. M. Husein, E. Rodil, and J. Vera, *Formation of silver chloride nanoparticles in microemulsions by direct precipitation with the surfactant counterion.* Langmuir, 2003. **19**(20): p. 8467-8474.
28. T.A. Dankovich and D.G. Gray, *Contact angle measurements on smooth nanocrystalline cellulose (I) Thin Films.* J Adhes Sci Technol, 2010. **25**(6): p. 699-708.
29. V.K. Kumikov and K.B. Khokonov, *On the measurement of surface free-energy and surface-tension of solid metals.* J Appl Phys, 1983. **54**(3): p. 1346-1350.

30. F.E. Bartell and P.H. Cardwell, *Reproducible contact angles on reproducible metal surfaces I Contact angles of water against silver and gold.* J Am Chem Soc, 1942. **64**: p. 494-497.
31. A.B.D. Cassie and S. Baxter, *Wettability of porous surfaces.* Trans. Faraday Soc., 1944. **40**: p. 546.

Chapter 5

Impact of the influent water composition on bacterial inactivation by a silver nanoparticle paper

This expands upon research in the previous chapters by adapting the model filtration system to include more real-world variables. In addition to bacteria, the raw water feed for any real-world purification systems may contain a wide range of other materials. These contaminants may inhibit the effectiveness of the bactericidal action described in the previous chapters. Here, an attempt is made to model the most likely contaminants, namely natural organic matter, proteins, and salts, and to investigate how the model contaminants influence the bactericidal effectiveness of the AgNP paper. This work has not yet been published.

5.1 Abstract

Previously, we demonstrated a method to deactivate bacteria by percolation through a paper sheet containing silver nanoparticles (AgNP) [1]. We have investigated the effects of influent water composition on the effectiveness of the AgNP paper during water purification. In this work, typical environmental and biological contaminants, such as salt, nutrient media, and natural organic matter (NOM), were added to the influent water. Following water treatment, the silver loss was characterized by atomic absorption and UV-Visible spectroscopy. We assessed whether the test waters affected *Escherichia coli* bacterial inactivation. The viability of *E. coli* decreased from 8 log for deionized water to 4 log when nutrient broth was added to the influent. However, the addition of phosphate buffered saline and NOM did not impact the bacterial inactivation ability of the AgNP paper. The protein in the nutrient media may be complexing the silver. We conclude that bactericidal effectiveness of AgNPs is dependent upon the influent solution chemistry.

5.2 Introduction

Due to inadequate water and sanitation services in many parts of the world, over one billion people do not have access to clean, potable water sources [2]. This causes the spread of preventable water-borne diseases by microbial contaminants, such as giardiasis, cholera, cryptosporidiosis, gastroenteritis, etc. [3]. One of the possible solutions to reducing the microbial contamination of drinking water is small-scale or point-of-use (POU) systems for water treatment. POU systems are not connected to a central network, have low energy inputs, and can be used in emergency response following disasters. Functional nanomaterials, such as AgNPs, carbon nanotubes, and

titania nanoparticles, have been suggested for POU treatment [1, 4-7]. Recently, for POU applications, we have designed a paper sheet embedded with silver nanoparticles to purify drinking water contaminated with bacteria [1].

Silver nanoparticles are well-known to be broad spectrum, potent antimicrobial agents [8, 9], and are easily incorporated into cellulosic materials [10]. Previously, we demonstrated the bactericidal effectiveness of the AgNP papers by passing model bacterial suspensions through an AgNP paper sheet, and analyzing the effluent water for viable bacteria. Our work has provided the proof-of-concept under ideal laboratory conditions, yet the overall bactericidal performance under various solution chemistries has not been presented. The objective of this paper is to examine bacterial inactivation by the AgNP paper for bacteria in solutions containing a selection of environmental and biological media, such as natural organic matter, salt, and nutrient media.

In surface waters, natural organic matter is often present in various forms, such as humic and fulvic acids, and in concentrations varying from 0 to 30 mg/L [11]. Both are diverse compounds with many functional groups, including phenolics, carboxylic acids, quinones, hydroxyls, methoxyls, aldehydes, ketones, and thiols. Fulvic acids are generally lower molecular weight compounds with higher oxygen and lower carbon contents than humic acids [12]. A proposed model structure for fulvic acid is represented in Figure 5.1 [13]. Due to the potential release of AgNPs into the environment, researchers have examined the interactions of natural organic matter and AgNPs to predict their fate and transport [14-17]. In this study, we evaluated the effects of fulvic acid, as a representative compound for natural organic matter, on the AgNP paper.

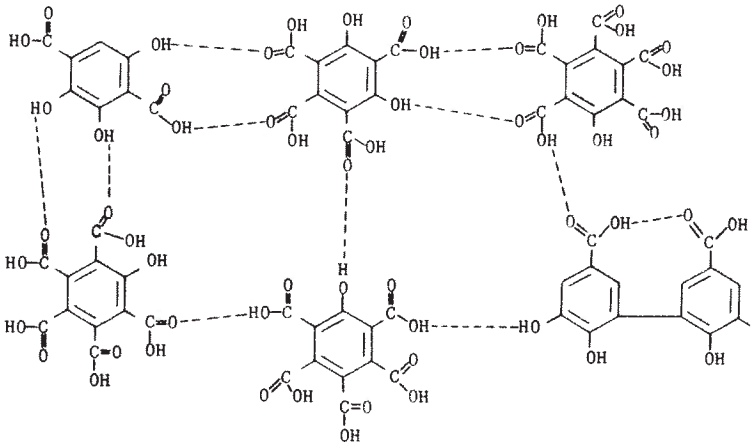

Figure 5.1. Hypothetical chemical structure of fulvic acid, as propsed by Schnitzer and Khan [13].

In biological nutrient media, a complex mixture of salts, protein digests, and yeast or beef extracts provides the appropriate composition of nutrients for bacterial or yeast growth in laboratory conditions, either in suspension or on agar plates. In many studies, researchers have observed changes in the aggregation behavior of AgNPs in complex media and as a result, there are inconsistent findings on the necessary threshold concentration for optimal AgNP bactericidal activity [18-21]. Interactions between AgNPs and various forms of biological media are highly relevant for many product applications, such as biomedical devices, bandages, food packaging, cosmetics, etc. In our case, we used a nutrient broth as proxy for the proteinaceous components of contaminated water.

In this study, we tested AgNP paper sheets made following a previously described method from our research group [1]. We examined the impact of fulvic acid, salt, and biological nutrient media on the inactivation of *E. coli* bacteria. The various test solutions were combined with bacterial suspensions and passed through the AgNP paper sheet in a simple flow percolation experiment, as previously described [1]. In this work, the presence of fulvic acid, phosphate buffered saline (PBS), and nutrient broth media on the bactericidal performance of AgNP sheets has been evaluated.

5.3 Experimental

5.3.1 Materials

We used absorbent blotting papers made from bleached softwood kraft pulp. The blotters (made by Domtar Inc. and kindly supplied by FP Innovations, Pointe-Claire, QC) are used for drying laboratory handsheets during pulp testing. The sheet thickness and grammage for the blotting paper sheets are 0.5 mm and 250 g/m^2, respectively, and the sheets are free from sizing agents, fluorescent agents and chemical additives. Silver nitrate ($AgNO_3$), 30% hydrogen peroxide (H_2O_2), concentrated nitric acid (HNO_3), poly(L-lysine) (0.01% solution), and sodium chloride were purchased from Sigma Aldrich and used as received. Nutrient broth media (Luria Bertani and Lauryl Sulfate broths), tryptone, yeast extract, β-D glucose, phosphate buffered saline (PBS), and Endo agar were purchased from VWR and used as received. Suwannee River fulvic acid was purchased from the International Humic Substances Society (IHSS), St. Paul, MN. The fulvic acid powder was dissolved into deionized water and stirred until dissolved, for approximately one hour. The concentrated fulvic acid stock solution was stored at 4°C in the dark until use. All solutions with the exception of fulvic acid were autoclaved prior to use. During the experiments, the diluted fulvic acid solution was not protected from light exposure. Phosphate buffered saline (PBS), sodium chloride, tryptone, and Luria Bertani (LB) broth are frequently used in bacteria nutrient media, and representative of concentrations encountered in biomedical applications. The concentration of test solutions is given in Table 5.1. Water treated with a Barnstead Nanopure system was used throughout.

TABLE 5.1. Range of components used in influent solutions.

Influent Test Solutions	Concentration(s)
Deionized water	-
NaCl	0.1-1.0 M
PBS	0.14 M
LB broth	0.25-2.5%
Tryptone	1.0%
Tryptone and NaCl	2.0%
Fulvic Acid	0.1-0.5%

5.3.2 Preparation of silver nanoparticle (AgNP) paper

As described in Chapter 3, the AgNP papers were prepared by an *in situ* reduction using glucose in a domestic microwave oven (Sharp Model No. R-410CWC, 2.45 GHz, 1000W). The silver contents of the AgNP papers were 0.5 to 2.4 mg Ag per gram of paper, as previously determined in Chapter 3.

5.3.3 Bactericidal testing

The bactericidal activity of the AgNP paper was tested against a nonpathogenic strain of *Escherichia coli* (ATCC #11229), a Gram-negative bacterium, commonly used as an indicator organism for water contamination. To test for the bactericidal activity, we used a modification of the method previously described in Chapter 2 [1] and schematically in Figure 5.2, Scheme A. Specific test liquids, including fulvic acid, LB broth, tryptone, and PBS, were added separately to the bacterial suspension which was then passed through a sheet of AgNP paper. The effluent bacteria were isolated from the aqueous effluent through centrifugation, 1228 x g for 10 minutes, and plated on endo nutrient agar plates. The nutrient agar plates were incubated overnight at 37°C for 24 hours and the colonies were counted and reported as colony forming units (CFU). Three replicates were performed per paper. Standard deviation values were reported.

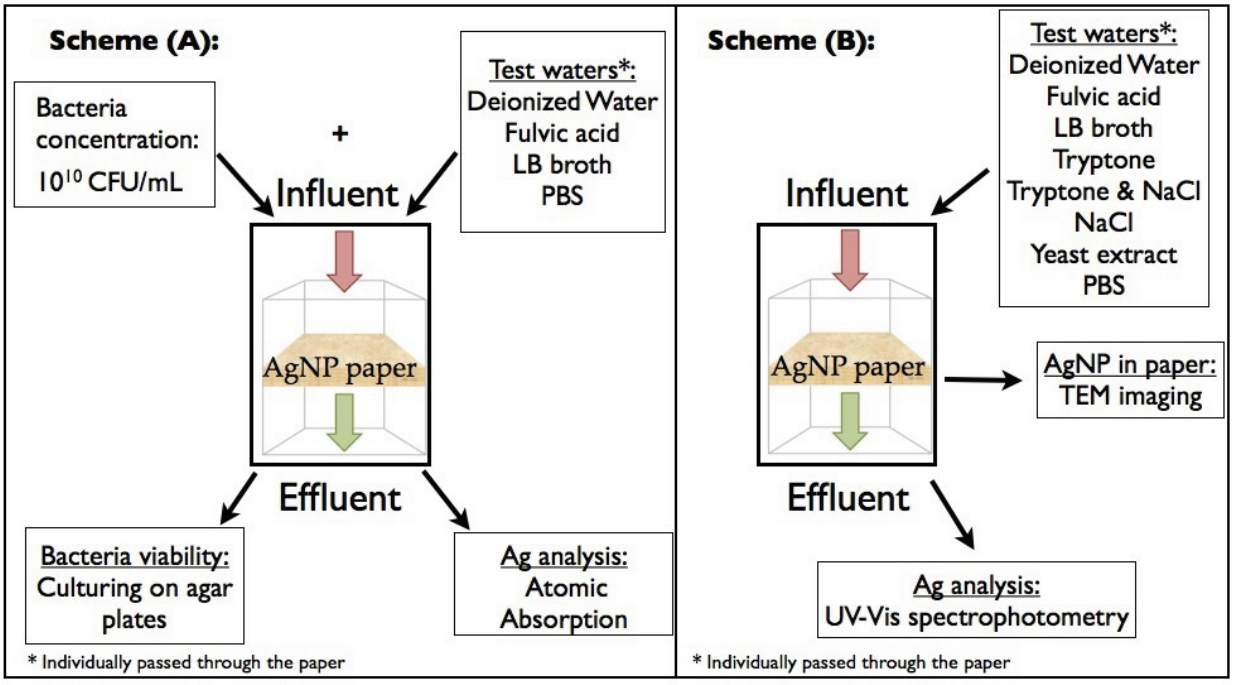

FIGURE 5.2. Schematic of experimental designs, (A) bactericidal testing, and (B) silver leaching.

5.3.4 Analysis for silver in effluent

The effluent after passing through the AgNP paper was analyzed for silver content by two methods: UV/Visible spectrophotometry (TCA - Cary 300, Varian) and Graphic Furnace Atomic Absorption spectrometry (GF-AA, Perkin Elmer AAnalyst 100). The spectrophotometric method qualitatively detects silver nanoparticles by the presence of a surface plasmon resonance peak around 390-420nm [22]. The GF-AA technique detects all forms of silver present.

Following the bactericidal testing (Figure 5.2 (A)), the effluent water was centrifuged to separate the bacteria from the supernatant. Both the supernatant and bacterial pellet were analyzed for silver by GF-AA. The bacterial pellet was digested prior to analysis as described in Chapter 2, following a previously published method [1]. The silver content reported is five replicates per sample concentration with standard deviation error bars.

To investigate the impact of specific influent solutions on the leaching of silver nanoparticles in the effluent, we passed the influent solutions described in Table 5.1 through the AgNP papers without bacteria, Figure 5.2 (B). To determine which broth components contribute to AgNP leaching, we first separated the Luria Bertani broth into its major components: tryptone, a protein digest, sodium chloride (0.14M), and yeast extract. Following this, the effluent water was analyzed for the presence of silver nanoparticles by UV-Vis spectrophotometry.

5.3.5 Characterization of AgNP papers

The shape and size distribution of the silver nanoparticles in the sheet were examined by electron microscopy. Individual paper fibers containing silver nanoparticles from the AgNP sheets were deposited on carbon coated copper grids that had been treated with poly(L-lysine), and were imaged with a Philips CM200 200 kV transmission electron microscope (TEM). Nanoparticle diameters were measured for greater than 100 particles per sample, with standard deviation values reported. The silver loss from the AgNP papers in 100 mL effluent was estimated from the GF-AA values for silver concentration in the effluent water. This value was expressed as a percentage of the total silver mass contained in the papers.

5.4 Results and discussion

Our aim of this study was to assess the impact of dissolved environmental and biological media on the bactericidal performance of the AgNP paper. Firstly, we have previously demonstrated the rapid and effective bactericidal activity of the AgNP sheets with a pristine suspension of *E. coli* bacteria percolated through the paper (Chapters 2 and 3). Briefly, to determine the bactericidal effects of the AgNP paper, we first passed a model suspension of 10^9 - 10^{10} *E. coli* bacteria in deionized water through the paper, following Scheme A in Figure 5.2. The effluent water contained nearly zero viable

bacteria, with a log reduction of 8.1 ± 1.4 (Chapter 3). Unless otherwise noted, these log reduction values are for the sheets containing 2.4 mg Ag per g of paper.

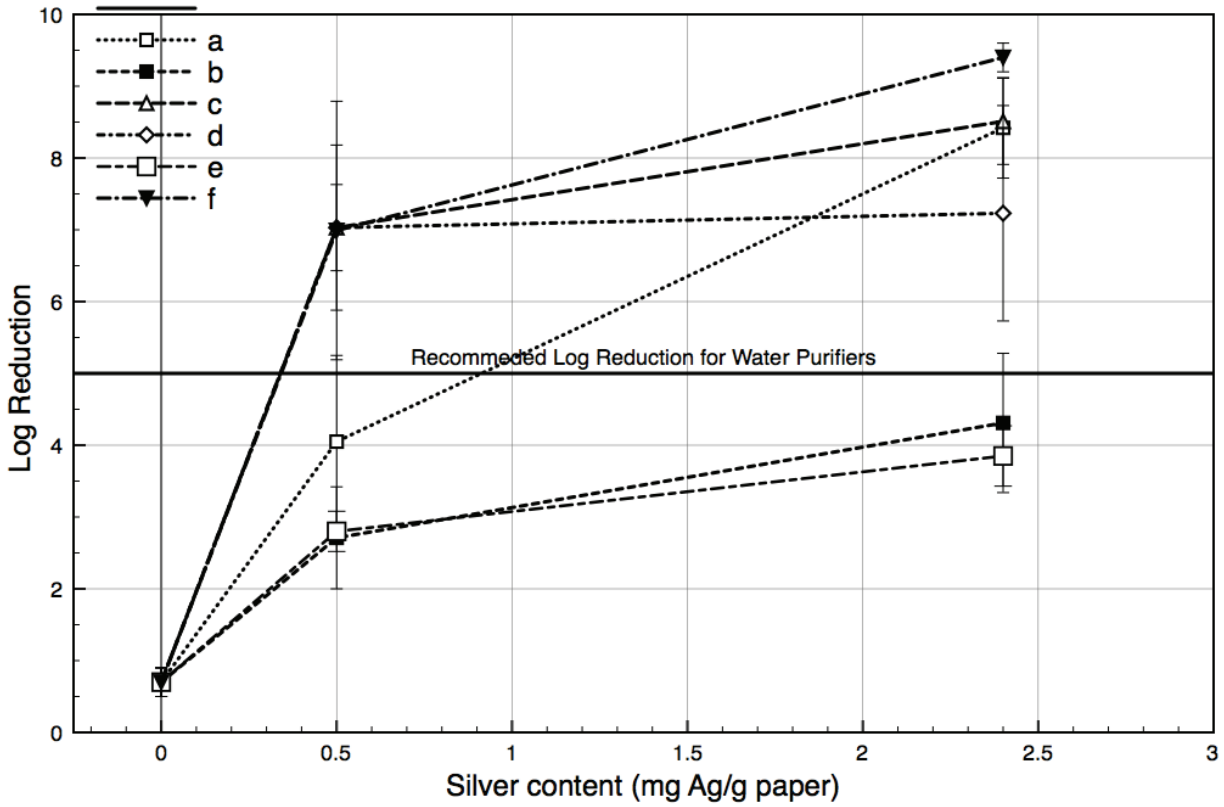

FIGURE 5.3. Log reduction of *E. coli* bacterial count after permeation through the silver nanoparticle paper, at with different dissolved solids in the filter influent water: (a) 10% LB broth, (b) 100% LB broth, (c) deionized water, (d) PBS, (e) tryptone (10 g/L), and (f) fulvic acid (50 mg/L) . Initial bacterial concentration, 10^{10} CFU/mL (log 10). Error bars represent standard deviation.

Following percolation through the AgNP paper, we used centrifugation to separate the bacteria from the silver (either nanoparticles or ions or both) leached out of the paper. The average silver content in the effluent water for deionized water influent was 0.055 ±0.037 ppm, as measured by graphite furnace atomic absorption, which measures total silver content (i.e., silver ions and nanoparticles). Somewhat less bound silver to the effluent bacteria was observed, with average values of 0.015 ±0.004 ppm.

In either case, the amount of silver leaching from the filter papers thus meets the US-EPA guideline for drinking water of less than 0.1 ppm (Table 5.2) [3].

TABLE 5.2. Silver in effluent water and in effluent bacteria, in ppm, as determined by Graphite Furnace Atomic Absorption measurements. Standard deviation is reported.

	Effluent Water				Effluent Bacteria			
	0.5		2.4		0.5		2.4	
Solution	mg Ag/ g paper				mg Ag/ g paper			
Deionized Water	0.072	± 0.034	0.055	± 0.037	0.010	± 0.008	0.015	± 0.004
PBS	0.390	± 0.004	0.346	± 0.043	-	-	-	-
Fulvic Acid	0.074	± 0.022	0.096	± 0.022	0.047	± 0.034	0.181	± 0.093
Tryptone	0.542	± 0.265	1.640	± 0.324	0.001	± 0.0002	0.007	± 0.001
LB Broth	0.197	± 0.280	1.369	± 0.532	0.008	± 0.003	0.007	-

5.4.1 Impact of natural organic matter on bactericidal activity

In this study, the concentrations of fulvic acid used were 10 and 50 mg/L, which is in the high range of the amount of NOM found in surface waters. At both concentrations analyzed, the fulvic acid had no detrimental effect on the log reduction of *E. coli (*9.4 ± 0.3), and in some cases actually out-performed deionized water (Figure 5.3). With the fulvic acid solutions, we observed the highest concentration of silver associated with the bacterial pellet (0.05 - 0.18 ppm) out of all the test solutions, and a similar level of silver in the effluent water (Table 5.2). It is likely that the fulvic acid is being adsorbed to the bacteria surface and complexing the silver, which would explain the high amount of silver found in the effluent bacteria following percolation. TEM images have shown the association of humic acids with AgNPs on the surface of bacteria [14, 15], but there are conflicting results for the bactericidal effects of this association in the literature. Fabrega et al. demonstrated less bactericidal activity of *Pseudomonas fluorescens* with higher humic acid concentrations due to a physical barrier limiting silver ion release [15]. Diagne et al. showed that humic acid had no detrimental effect on biocidal properties of AgNPs embedded in a membrane, which

may be due to nanoAg being fixed to a surface instead of in suspension [98]. Dasari et al. [14] showed a greater log reduction in mixed aquatic bacterial assemblages with humic acids in the light compared to the dark. These authors attribute the difference between light and dark conditions to the reactive oxygen species formation from the humic acid [14], which possibly occurred with our experimental conditions as no precautions were taken to prevent light exposure.

Another factor that influences the behavior of NOM on Ag transport into bacterial cells is the NOM quality. For example, if the NOM is “recent”, then it is more likely to contain more lipid and protein-derived organic matter (derived from phytoplankton), therefore more sulfhydryl bonding sites than “older” NOM (derived from plants) [24]. Fulvic acid is a subdivision of NOM, and its chemical functional groups are not entirely representative of the organic material found in natural waters. The IHSS reports that the standard fulvic acid used in this study has no detectable amino acids containing sulfur groups (cysteine or methionine) [25]. Other work suggests that NOM generally contains sufficient S(II-) to have ambient Ag(I) bound as either an Ag-thiolate or as an Ag-metal sulifde complex associated with the NOM [26]. Higher concentrations of NOM slowed the silver ion release rate from AgNPs in suspensions [27]. Generally, the entry of silver into cells from the Ag-NOM complexes can be completed either by endocytosis or by ligand exchange to a protein cysteine group, then followed by transport into the cell [26].

5.4.2 Impact of biological growth media on bactericidal activity

The biological growth media evaluated for its impact on bactericidal activity of AgNPs included PBS, LB broth, and tryptone. These test solutions had concentrations within the range of proteinaceous material and salts in physiological solutions. In contaminated natural water sources, these components are encountered at lower concentrations in domestic waste waters and brackish waters (Table 1.2) [28].

Phosphate buffered saline had no detrimental effect on the log reduction of *E. coli* (7.9 ± 1.3) (Figure 5.3), although PBS caused a much higher silver loss into the effluent water with values of 0.35 ± 0.04 ppm compared to 0.06 ± 0.04 ppm for deionized water (Table 5.2). This increased silver leaching is most likely due to the high NaCl concentration (0.14M) in PBS.

The concentration range for LB broth was typical of recommendations for optimal bacteria growth (100%) and 10% of this value, which corresponds to 2.5 g/L and 0.25 g/ L of dissolved proteins, salts, and yeast extract. The tryptone and LB nutrient broth showed a negative effect on the log reduction of *E. coli* bacteria, with values of 3.9 ± 0.4 and 4.3 ± 1.0, respectively (Figure 5.3). A lower LB broth concentration (10% of that recommended for growth media) resulted in a higher log reduction of 7.8 ± 1.6 (Figure 5.3). From the LB broth and tryptone samples, an unexpected observation followed from the silver content analysis of effluent water and bacteria. LB broth and tryptone showed the highest silver loss in the effluent water with values of 1.4 and 1.6 ppm, respectively, and the lowest silver content in the effluent bacteria with the same value of 0.007 ppm (Table 5.2). The very low silver absorption by the bacteria pellet and the reduced bactericidal effectiveness with the LB broth and tryptone solutions suggest that these protein-containing solutions are limiting silver ion release to the bacteria.

Following the flow tests with LB broth, the effluent water became a bright yellow color. To determine the source of the yellow color, we first separated the LB broth into its major components: tryptone, a protein digest, sodium chloride (0.14M), and yeast extract. Next, we passed the various broth components (without bacteria) through the AgNP paper in 100 mL aliquots at the same concentrations as in the LB broth, following Scheme B in Figure 5.2. Following this, the effluent water was analyzed for the presence of silver nanoparticles by UV-Vis spectrophotometry.

With LB broth and tryptone media, the presence of silver nanoparticles in the effluent water was shown by its characteristic peak at 420 nm in the UV-Vis spectrum

(Figure 5.4). The SPR peak from the tryptone was rather poorly formed and only the combination of tryptone and NaCl showed the same characteristic SPR peak for AgNPs as the LB broth did. In contrast, the NaCl rinse alone did not show any peaks in the UV-Vis spectrum, nor did the rinses with PBS, yeast extract, or fulvic acid. It is likely that tryptone coats the surface of AgNPs and acts as stabilizer for the AgNPs in suspension. Proteins have been shown to form a coating on the surface of silver nanoparticles [21]. The deposition of protein on the surface of the AgNPs either in the paper or in the effluent water could be what limits the silver ion release to the bacteria. Due to the high silver content in the effluent water, LB broth proteins also appear to stabilize NPs in solution. Other researchers also have reported that AgNPs will aggregate in nutrient media with a high electrolyte content, and that the presence of proteins within the suspension can stabilize the silver nanoparticles against aggregation [20].

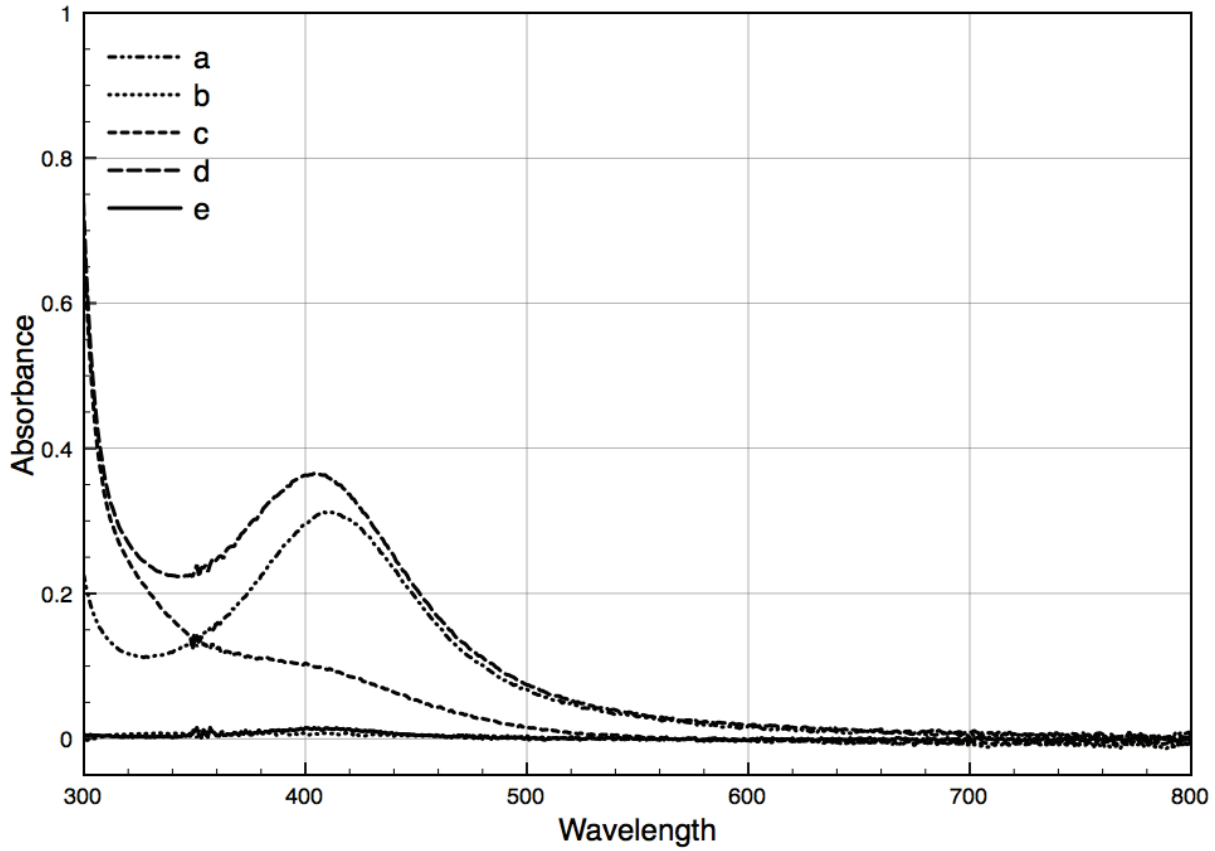

FIGURE 5.4. UV-Vis spectrophotometry of effluent waters: (a) 2.5 g/L LB broth, (b) deionized water, (c) 1 g/L tryptone, (d) 1 g/L tryptone and 0.14M NaCl, and (e) 0.1M NaCl. Note that the peaks at 420 nm indicate the presence of AgNPs in the effluent.

5.4.3 Effect of test liquids on AgNP paper

In general, following passage of the test liquids through the AgNP papers, there was little visible change in the papers themselves (Figure 5.5 (a)). The main exception was for NaCl solutions, where the AgNP paper turned a purple color when dried, and back to orange again when wetted (Figure 5.5 (b)). Similarly, we observed aggregation behavior on AgNP NCC films from NaCl exposure (Chapter 4). Additionally, care must be taken in storage of these materials. To protect the papers from UV light, which can also initiate particle aggregation, the AgNP papers were wrapped in aluminum foil. If

these papers were not completely dry when wrapped, some reactions with the aluminum foil was observed, which resulted in paper discoloration (Figure 5.5 (c)).

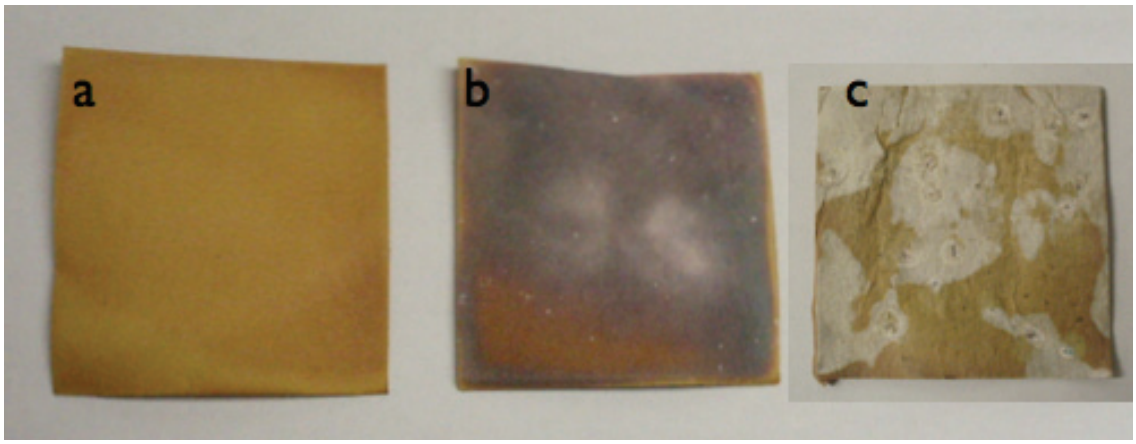

FIGURE 5.5. Color changes in the AgNP papers. a) Untreated AgNP paper b) AgNP paper rinsed with 0.1M NaCl, and c) AgNP paper reaction with Al foil wrapping. With the other rinses, no color changes were observed.

A small change in particle sizes was observed through TEM analysis following test liquid rinses (Scheme B in Figure 5.2 and Table 5.3). The average particle diameter sizes were observed with the most pronounced shift for the 1M NaCl rinse (14.0 ± 10.0 nm) compared to the deionized water rinse (4.5 ± 2.1 nm) (Table 5.3 and Figure 5.6). The changes in particle diameter sizes were rather small overall, and the particle shapes are mostly spherical before and after the test liquid rinses. Longer time exposure to the solutions than the 10-15 minutes for the flow test experiments may result in increased nanoparticle aggregation. For example, previous work with AgNP NCC films showed much greater changes in particle sizes following exposure to 1M NaCl solutions for 1 hour, with an increase to 45.1 nm (Chapter 4).

TABLE 5.3. Average nanoparticle diameters of AgNPs on paper fibers, determined through TEM analysis, following bacterial tests. Nanoparticle diameters were measured for greater than 100 particles per sample, with standard deviation values reported.

	Nanoparticle Diameter (nm)		
Rinse Solution	**Average**	**Std Dev.**	**Median**
Deionized water	4.5	± 2.1	4.3
0.1 M NaCl	5.4	± 1.5	5.3
1M NaCl	14.0	± 10.0	11.2
PBS	10.0	± 5.2	9.7
LB broth	8.7	± 4.9	7.5

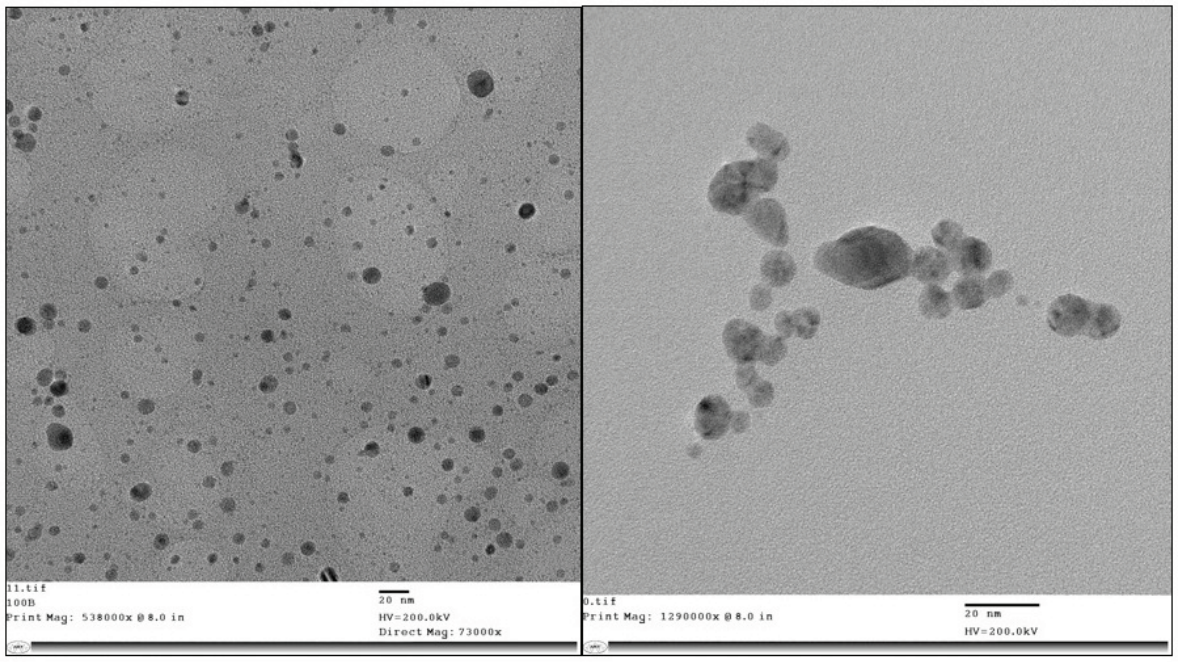

FIgure 5.6. TEM images of AgNPs in paper fibers following rinses with deionized water (left) and 1M NaCl solution (right). Scale bar is 20 nm.

The different samples leached between 0.12% to 10.85% of the initial silver content of the filter papers (Table 5.4). The lowest values for silver loss were observed for the natural organic matter solution and for deionized water. Highest values for silver leaching were observed with the tryptone rinse, with 10.85% and 6.83% of total silver content lost for the 0.5 and 2.4 mg Ag/ g paper sheets, respectively (Table 5.4). This

demonstrates that exposure to proteinaceous material will decrease the bactericidal capacity of AgNP.

In general, the silver loss from AgNP papers is similar to that which has been reported in the literature for fibrous substrates. Silver release from consumer products, notably socks [29, 30] and other water filters containing silver nanoparticles [7, 31] has been investigated. Overall, the release of silver in the wash water of textiles varied considerably, from 3 to 1300 ppb (1-68 μg/g) for distilled water washes [29]. The silver release during washes with surfactants and oxidizers was slightly higher, with a range of 0.3 - 377 μg/g [30]. This was ascribed to specific interactions of chloride anions from detergents with AgNPs to form insoluble AgCl, and hydrogen peroxide oxidation of AgNPs to silver ions. Other filters containing silver nanoparticles showed variable silver release, depending upon the composition of the filter material. For example, polysulfone ultrafiltration membranes impregnated with silver nanoparticles released a high value of 34 ppb silver in the filter effluent, following by a decrease in silver concentration, and resulting in a 10% mass loss of silver from the filter membrane [31]. The ceramic filters with a colloidal silver coating showed an initially high silver concentration in the effluent water of 500 ppb, and over time, this dropped to under 100 ppb [7]. Polyether sulfone membranes with multilayers containing silver nanoparticles showed an average silver release of 5 ppb, which stabilized after an initial depletion period [23].

TABLE 5.4. Silver loss from AgNP paper following the antibacterial flow tests with the test liquids. Standard deviations shown.

	0.5 mg Ag/ g paper		2.4 mg Ag/ g paper	
Solution	Ag µg/ g paper	Percent Ag loss	Ag in µg/ g paper	Percent Ag loss
Deionized Water	3.01 ± 2.73	0.36% ± 0.33%	0.99 ± 0.92	0.12% ± 0.11%
PBS	65.00 ± 0.06	7.80% ± 0.01%	12.02 ± 1.48	1.44% ± 0.18%
Fulvic Acid	12.27 ± 3.69	1.47% ± 0.44%	3.34 ± 0.75	0.40% ± 0.09%
Tryptone	90.39 ± 44.1	10.85% ± 5.3%	56.94 ± 11.3	6.83% ± 1.35%
Broth (100%)	32.83 ± 46.7	3.94% ± 5.6%	47.52 ± 18.5	5.70% ± 2.2%

5.4.4 AgNP stabilization and toxicity

The presence of complex media, stabilizers, and surface ligands all contribute to the interactions of AgNPs with living cells [18, 21, 27, 32]. The impact of these components on the toxicity of AgNPs is highly variable, and the mechanisms are not well established. Nevertheless, there is ample evidence in the literature that the stabilization of AgNP often leads to a decrease in toxicity, either due to particle aggregation or to complexation of dissociated silver ions. Thus, for example, nutrient media bind to free silver ions, which reduces the toxicity of AgNPs to human mesenchymal stem cells [21]. AgNPs stabilized with sodium dodecyl sulfate showed no antibacterial activity due to the lack of interaction between the negatively charged surface groups and the negatively charged bacteria surface [32]. Nanoparticle agglomeration into fractal shapes due to media-AgNP interactions resulted in less hemolysis with larger agglomerates [18].

In the case of our AgNP paper, the nanoparticles are not coated with surface ligands or stabilizing polymers, which results in more silver ion release than with coated nanoparticles. However, some of the dissolved model contaminants discussed above do lower the effectiveness of the AgNP paper. The mechanism is unclear, but the amount of silver in the bacterial portion of the effluent remains constant, while that in the

effluent solution is elevated in the case of the proteinaceous materials (Tables 5.2 and 5.4). This suggests that the decrease in antibacterial activity of the AgNP paper is not simply due to adsorption of proteins on the silver nanoparticles, but that silver is being removed from the paper surface, possibly as stabilized nanoparticles or complexed ionic species.

5.5 Conclusion

The AgNP papers effectively purify water contaminated with bacteria, but water contaminated with bacteria alone is unlikely to be encountered under field conditions. The effect of some model contaminants on the effectiveness of the AgNP paper has been examined. As a model humic material, fulvic acid had essentially no negative effect on the bactericidal action. However, nutrient growth media, as models for proteinaceous contaminants, did lower the effectiveness of the AgNP paper. To mitigate these effects, it may be necessary to protect the AgNPs in the paper sheet by a ligand or polymer coating.

5.6 Acknowledgements

This work was supported by the Sentinel Bioactive Paper Network. We gratefully acknowledge the training and use of facilities at McGill by Glenna Keating and Isabelle Richer (Flame - AA), Line Mongeon (SEM) and Xue Dong Liu (TEM). We thank Ruoxi Gao and Sangjin Bae for lab assistance. David Wong (FPInnovations, Pointe Claire) helped with UV-Vis Spectroscopy.

5.7 References

1. T.A. Dankovich and D.G. Gray, *Bactericidal paper impregnated with silver nanoparticles for point-of-use water treatment.* Environ Sci Technol, 2011. **45**(5): p. 1992-1998.
2. World Health Organization / UNICEF Joint Water Supply: Sanitation Monitoring Programme, ed. *Water for life: making it happen*. 2005.
3. World Health Organization, ed. *Guidelines for drinking-water quality*. 2006: Geneva, Switzerland.
4. P. Jain and T. Pradeep, *Potential of silver nanoparticle-coated polyurethane foam as an antibacterial water filter.* Biotechnol Bioeng, 2005. **90**(1): p. 59-63.
5. A.S. Brady-Estévez, T.H. Nguyen, L. Gutierrez, and M. Elimelech, *Impact of solution chemistry on viral removal by a single-walled carbon nanotube filter.* Water Research, 2010. **44**(13): p. 3773-3780.
6. L. Ye, C.D.M. Filipe, M. Kavoosi, C.A. Haynes, R. Pelton, and M.A. Brook, *Immobilization of TiO_2 nanoparticles onto paper modification through bioconjugation.* J Mater Chem, 2009. **19**(15): p. 2189-2198.
7. V.A. Oyanedel-Craver and J.A. Smith, *Sustainable colloidal-silver-impregnated ceramic filter for point-of-use water treatment.* Environ Sci Technol, 2008. **42**(3): p. 927-933.
8. R. Davies and S. Etris, *The development and functions of silver in water purification and disease control.* Catalysis Today, 1997. **36**(1): p. 107-114.
9. J.R. Morones, J.L. Elechiguerra, A. Camacho-Bragado, K. Holt, J.B. Kouri, J.T. Ramírez, and M.J. Yacaman, *The bactericidal effect of silver nanoparticles.* Nanotechnology, 2005. **16**(10): p. 2346-2353.
10. J.H. He, T. Kunitake, and A. Nakao, *Facile in situ synthesis of noble metal nanoparticles in porous cellulose fibers.* Chem Mater, 2003. **15**(23): p. 4401-4406.
11. M.N. Jones and N.D. Bryan, *Colloidal properties of humic substances.* Advances in colloid and interface science, 1998. **78**(1): p. 1-48.

12. F.J. Stevenson, *Humus chemistry: genesis, composition, reactions*. 1982, New York: Wiley.
13. M. Schnitzer and S.U. Khan, *Humic substances in the environment*. 1972, New York: Marcel Dekker.
14. T.P. Dasari and H.-M. Hwang, *The effect of humic acids on the cytotoxicity of silver nanoparticles to a natural aquatic bacterial assemblage.* Science of the Total Environment, 2010. **408**(23): p. 5817-5823.
15. J. Fabrega, S.R. Fawcett, J.C. Renshaw, and J.R. Lead, *Silver nanoparticle impact on bacterial growth: Effect of pH, concentration, and organic matter.* Environ Sci Technol, 2009. **43**(19): p. 7285-7290.
16. N. Akaighe, R.I. MacCuspie, D.A. Navarro, D.S. Aga, S. Banerjee, M. Sohn, and V.K. Sharma, *Humic acid-Induced silver nanoparticle formation under environmentally relevant conditions.* Environ Sci Technol 2011. **45**(9): p. 3895-3901.
17. R.I. MacCuspie, K. Rogers, M. Patra, Z. Suo, A.J. Allen, M.N. Martin, and V.A. Hackley, *Challenges for physical characterization of silver nanoparticles under pristine and environmentally relevant conditions.* J. Environ. Monit., 2011. **13**(5): p. 1212.
18. J.M. Zook, R.I. Maccuspie, L.E. Locascio, M.D. Halter, and J.T. Elliott, *Stable nanoparticle aggregates/agglomerates of different sizes and the effect of their size on hemolytic cytotoxicity.* Nanotoxicology, 2010. **5**(4): p. 517-530.
19. R.I. MacCuspie, *Colloidal stability of silver nanoparticles in biologically relevant conditions.* Journal of Nanoparticle Research, 2011. **13**(7): p. 2893-2908.
20. R.C. Murdock, L. Braydich-Stolle, A.M. Schrand, J.J. Schlager, and S.M. Hussain, *Characterization of nanomaterial dispersion in solution prior to in vitro exposure using dynamic light scattering technique.* Toxicological Sciences, 2008. **101**(2): p. 239-253.
21. S. Kittler, C. Greulich, J.S. Gebauer, J. Diendorf, L. Treuel, L. Ruiz, J.M. Gonzalez-Calbet, M. Vallet-Regi, R. Zellner, M. Köller, and M. Epple, *The influence of proteins on the dispersability and cell-biological activity of silver nanoparticles.* J. Mater. Chem., 2010. **20**(3): p. 512.

22. A. Henglein, *Colloidal silver nanoparticles: photochemical preparation and interaction with O_2, CCl_4, and some metal ions.* Chem. Mater., 1998. **10**: p. 444-450.
23. F. Diagne, R. Malaisamy, V. Boddie, R.D. Holbrook, B. Eribo, and K.L. Jones, *Polyelectrolyte and silver nanoparticle modification of microfiltration membranes to mitigate organic and bacterial fouling.* Environ Sci Technol, 2012, **46**(7): p. 4025–4033.
24. A.W. Andren and T.W. Bober, eds. *Silver in the environment: Transport, fate, and effects*. 2002, SETAC Press: Pensacola, Florida.
25. International Humic Substance Society. Cited on November 2, 2011. Available from: http://www.humicsubstances.org/aminoacid.html.
26. H. Manolopoulos, N.H.W. Adams, M. Peplow, J.R. Kramer, and R.A. Bell. *S(II-) and its presence in oxic waters*. in *7th Nordic symposium on humic substances in soil and water*. 1999. Kristiansand, Norway: Adgar College.
27. J. Liu and R.H. Hurt, *Ion release kinetics and particle persistence in aqueous nano-silver colloids.* Environ Sci Technol, 2010. **44**(6): p. 2169-2175.
28. U.S. Environmental Protection Agency: Office Of Water, *National interim primary drinking water regulations*. 1977, Washington, D.C. p. 59566-59589.
29. T. Benn and P. Westerhoff, *Nanoparticle silver released into water from commercially available sock fabrics.* Environ Sci Technol, 2008. **42**(11): p. 4133-4139.
30. L. Geranio, M. Heuberger, and B. Nowack, *The behavior of silver nanotextiles during washing.* Environ Sci Technol, 2009. **43**(17): p. 6458-6462.
31. K. Zodrow, L. Brunet, S. Mahendra, D. Li, A. Zhang, Q. Li, and P.J.J. Alvarez, *Polysulfone ultrafiltration membranes impregnated with silver nanoparticles show improved biofouling resistance and virus removal.* Water Research, 2009. **43**(3): p. 715-723.
32. K.H. Cho, J.E. Park, T. Osaka, and S.G. Park, *The study of antimicrobial activity and preservative effects of nanosilver ingredient.* Electrochimica Acta, 2005. **51**(5): p. 956-960.

Chapter 6

Conclusions, original contributions to knowledge, and future work

6.1 Conclusions and original contributions to knowledge

Our most important contribution has been showing that a sheet of paper coated with silver nanoparticles can eliminate bacteria in contaminated water passing through the sheet. This has not been previously demonstrated. Our proof-of-concept model experiment offered a potential use of the AgNP paper for point-of-use water purification. Silver has a low toxicity for humans, and the silver content in the effluent meets the US EPA guidelines for drinking water regulations.

The simplicity and low cost of AgNP formation and incorporation into paper makes this project more likely to become a realized application. The pathway to find an easy, straightforward method for AgNP formation and incorporation into paper was a rather winding path in the laboratory. Initial experiments involving preparation of AgNPs in suspension with sodium borohydride and ascorbic acid produced uniform NPs, but the NPs were quite difficult to pin on the paper surface. The overall silver content of these papers was quite low, only 0.06 mg Ag per g of paper. Another AgNP deposition method was needed, and a few authors were exploring the formation of silver nanoparticles through *in situ* reduction on cellulosic fibers [1, 2]. Those studies triggered many experiments in determining how best to simply and quickly reduce silver salts directly on the paper fibers to silver nanoparticles. Our further contribution to the field of AgNP formation in cellulose is: an original green chemistry procedure using microwave synthesis and demonstration of NCC films as another substrate for AgNPs.

The microwave synthesis expanded on the use of glucose as a reducing agent to make this reaction faster and less toxic than other methods. Due to their smooth surfaces and translucent quality, the AgNP NCC films serve as an excellent model material for studying the behavior of AgNPs in cellulosic materials.

Because of our focus on water purification, we needed to design a new test protocol to evaluate the bactericidal effectiveness of the AgNP paper. Our method used a modified version of the membrane filter method, which is commonly used for bacteria enumeration in water quality tests. The membrane filter method traps bacteria on the 0.45 μm pore sized membrane as the water sample passes through, the filter is then placed on an agar plate containing nutrient media, and from the bacteria growth on the agar plates, their concentration can be determined [3]. Because the blotting papers have a greater pore size than the membrane filters, bacteria pass through the paper, instead of being captured on the filter surface. For subsequent bacteria viability analysis in our method, the bacteria are collected from the effluent water and then added to the agar nutrient plates. This larger pore size is key to allowing the bacteria to come into contact with the biocide, yet pass through the paper without the need for vacuum suction.

One of the important factors of water purification through the AgNP paper is an adequate flow rate, which in turn depends on the wettability of the paper surface. Our contact angle measurements show that the AgNP paper is close to the base paper in its wettability [4]. The hydrophilic and porous nature of the substrate facilitate the passage of bacteria through the sheet.

We explored the use of the AgNP paper for microbiological water purification in more realistic settings with some model dissolved substances, including natural organic matter, salts, and proteins, in the feed water. Natural organic matter showed no detrimental effects on the bactericidal properties of the AgNP paper. In contrast, this work showed significant variations in the bactericidal effectiveness with respect to

proteins dissolved in the influent water. This suggests that certain applications could be problematic to achieving optimal bacterial inactivation.

Lastly, we showed the possibility of studying aggregation behavior of AgNPs on a nanocomposite material, rather than in suspension, as more typical [5, 6]. Largely, in applications, AgNPs are embedded in or coated on a material, and a greater understanding of the stability of nanoparticles in materials can lead to better materials design.

6.2 Suggestions for Further Research

There are several different directions further research could take from this point. Briefly, they can be divided into four different areas: chemical studies, filter engineering, microbiological assessment, and field tests.

One of the big questions for silver nanoparticle toxicity is what the biocidal mechanism is. We have not directly targeted this question, but others much more skilled in biochemistry and cell biology have been actively addressing this question for some time.

One of the potentially limiting aspects of using this bactericidal paper in proposed water purification applications is the rate of silver release. We have detected a very low concentration of silver leachate in the effluent water under pristine laboratory conditions, but if sodium chloride or proteins are added to the influent water, this significantly increases the silver leachate. Silver leaching may be mitigated by a pre-filter that absorbs proteins in the the influent stream. The silver release kinetics from the AgNP paper needs to be better understood. A way to evaluate for whether silver ions or nanoparticles are present in the effluent involves removing AgNPs using a centrifugation ultrafiltration device with a membrane filter with a pore size limit of 1-2 nm

(Amicon by Millipore) and further atomic absorption analysis to provide the concentration of each form of silver [6].

For simplicity and reproducibly of results, we have only used one filter design in the lab. There are several variables that need to be optimized. These include pore size and thickness of the paper (which influences the flow rate), bactericidal capacity, and the time necessary for microorganism inactivation. Following the optimization process, a prototype can be designed. Perhaps, a starting point would be designing an attachment to a water bottle for an emergency/disaster relief model.

Further microbiological assessment is underway with collaborators at the University of Guelph from Mansel Griffiths' research group. This group is examining the bactericidal effectiveness of our AgNP papers with a set of common waterborne pathogenic bacteria, including *E. col*i O157:H7, *Salmonella typhi, Campylobacter jejuni, Legionella,* and *Aeromonas hydrophila.* This selection is highly relevant and of emerging concern for water purification. If these tests prove to be successful, then a wider range of microorganisms, such as viruses, bacterial spores, and protozoa, would need to be evaluated.

Following prototype development, the water filter should be tested with water samples from real water sources, such as lakes, streams, etc. The microbiological variety will present new challenges, as compared to the mono-cultures of bacteria investigated so far in the lab. Additionally, there is a possibility that silver may interact with other dissolved substances in the water, such as sulfur or halogens, which have a high affinity to form insoluble compounds that may negatively impact the antimicrobial performance. If necessary, the design could be modified to incorporate a filter material that would absorb these compounds.

6.3 References

1. J.H. He, T. Kunitake, and A. Nakao, *Facile in situ synthesis of noble metal nanoparticles in porous cellulose fibers.* Chem Mater, 2003. **15**(23): p. 4401-4406.
2. T. Maneerung, S. Tokura, and R. Rujiravanit, *Impregnation of silver nanoparticles into bacterial cellulose for antimicrobial wound dressing.* Carb Polym, 2008. **72**(1): p. 43-51.
3. L.S. Clesceri, A.E. Greenberg, and A.D. Eaton, eds. *Standard methods for the examination of water and wastewater*. 20th ed., American Water Works Association, Water Pollution Control Federation, Water Environment Federation, 1998, American Public Health Association: Washington, D.C.
4. T.A. Dankovich and D.G. Gray, *Bactericidal paper impregnated with silver nanoparticles for point-of-use water treatment.* Environ Sci Technol, 2011. **45**(5): p. 1992-1998.
5. R.I. MacCuspie, *Colloidal stability of silver nanoparticles in biologically relevant conditions.* Journal of Nanoparticle Research, 2011. **13**(7): p. 2893-2908.
6. J. Liu and R.H. Hurt, *Ion release kinetics and particle persistence in aqueous nano-silver colloids.* Environ Sci Technol, 2010. **44**(6): p. 2169-2175.